AD_____

Award Number: W81XWH-11-1-0237

TITLE: Old Receptors, New Treatment Strategies for Breast Cancer

PRINCIPAL INVESTIGATOR: Wei Xu, Ph.D.

CONTRACTING ORGANIZATION: University of Wisconsin, Madison
Madison, WI 53715

REPORT DATE: April 2012

TYPE OF REPORT: Annual

PREPARED FOR: U.S. Army Medical Research and Materiel Command
Fort Detrick, Maryland 21702-5012

DISTRIBUTION STATEMENT: Approved for Public Release;
Distribution Unlimited

REPORT DOCUMENTATION PAGE

Form Approved
OMB No. 0704-0188

1. REPORT DATE	2. REPORT TYPE	3. DATES COVERED
April 2012	Annual	1 April 2011 – 31 March 2012

4. TITLE AND SUBTITLE

Old Receptors, New Treatment Strategies for Breast Cancer

5a. CONTRACT NUMBER

5b. GRANT NUMBER
W81XWH-11-1-0237

5c. PROGRAM ELEMENT NUMBER

6. AUTHOR(S)

Wei Xu

E-Mail: wxu@oncology.wisc.edu

5d. PROJECT NUMBER

5e. TASK NUMBER

5f. WORK UNIT NUMBER

7. PERFORMING ORGANIZATION NAME(S) AND ADDRESS(ES)

University of Wisconsin, Madison
Madison, WI 53715

8. PERFORMING ORGANIZATION REPORT NUMBER

9. SPONSORING / MONITORING AGENCY NAME(S) AND ADDRESS(ES)
U.S. Army Medical Research and Materiel Command
Fort Detrick, Maryland 21702-5012

10. SPONSOR/MONITOR'S ACRONYM(S)

11. SPONSOR/MONITOR'S REPORT NUMBER(S)

12. DISTRIBUTION / AVAILABILITY STATEMENT
Approved for Public Release; Distribution Unlimited

13. SUPPLEMENTARY NOTES

14. ABSTRACT

We have made considerable progress towards each project proposed in the original grant. For Aim 1, we have developed TR-FRET assays that can be adapted for high throughput screening to identify chemical activator of CARM1 for breast cancer differentiation therapy. For Aim 2, we have developed isogenic MDA-mb-468 cell line inducibly express either ERα or ERβ. These cell lines have been validated to form xenograft tumors in nude mice. We have begun to assess whether 18Fluoro-17β-estradiol could detect ERβ-positive breast tumors in vivo and thus suitable for in vivo PET imaging. We have optimized conditions to use a commercial ERβ antibody for immunohistochemistry. Using Tissue Microarray (TMA), we demonstrated that ~25% of triple negative breast tumors express significant amount of ERβ. Using MDA-mb-468-ERβ cell line, we performed RNA-sequencing and identified ERβ target genes. These target genes will be tested in tumor samples from clinical trial to determine whether estrogen treatment activated ERβ in patients. For Aim 3, we have determined pharmacokinetics of one of the ERα/β heterodimer-selective phytoestrogens, cosmosiin, in ACI rat model and showed that serum concentration of cosmosiin could reach μM that is sufficient to induce ERα/β heterodimer in vivo.

15. SUBJECT TERMS
Establishment of cell-based assay to screen CARM1 activator; identification of ERβ target genes as biomarker; development of cell line for in vivo imaging of ERβ+ tumor

16. SECURITY CLASSIFICATION OF:			17. LIMITATION OF ABSTRACT	18. NUMBER OF PAGES	19a. NAME OF RESPONSIBLE PERSON
a. REPORT	b. ABSTRACT	c. THIS PAGE			USAMRMC
U	U	U	UU		19b. TELEPHONE NUMBER *(include area code)*

Table of contents:

Introduction:

Background: Estrogen is essential for normal growth and differentiation of the mammary gland. It also supports growth of 70% of primary breast cancers. The biological effects of estrogen are mediated by two estrogen receptors, ERα and ERβ. Both are transcription factors regulating target gene expression by formation of dimers at the genomic sites. While ERα is the prominent target in breast cancer therapy, and its expression strongly predicts response to endocrine therapy, ERβ is neither a prognostic marker nor a therapeutic target. Expression of ERβ partially overlaps with that of ERα in breast cancer cells. Among ERα-positive breast cancer, 60% of cells co-express ERβ. ERβ also uniquely expresses in 50-80% of triple-negative breast cancer (TNBC), which do not express ERα, progesterone receptor and Her2. TNBCs have a worse prognosis, and targeted therapies are desperately needed for this group of women. Our idea is that novel treatment strategies should be developed based on the function of different ER dimers in context of breast cancer subtypes. Although dimerization of ERs is a prerequisite to transcriptional activation, the biology of ER homo- and hetero-dimers (i.e. ERα/α, ERβ/β, ERα/β) in physiological and pathological processes are poorly understood. In order to probe for ER dimer function, we developed Bioluminescence Resonance Energy Transfer (BRET) assays to monitor ER dimerization in living cells and identified compounds selectively induce ERα/α, ERβ/β homodimers and ERα/β-heterodimers. Dimer-selective estrogen receptor modulators will be explored for breast cancer prevention and treatment.

Objective/Hypothesis: We hypothesize that ER homo- and hetero-dimers are targets for different subtypes of breast cancer. Three hypotheses were proposed: 1) For ERα-positive breast cancer which failed conventional treatment, we propose to target CARM1, a histone arginine methyltransferase which is an emerging epigenetic target for differentiation therapy; 2) We have found that activating ERβ activity (agonism) provides anti-cancer effects. Therefore, we hypothesize that drugs that activate ERβ will be effective for treating TNBC; 3) Using ERα/β-heterodimer selective, natural estrogenic compounds as tools, we reveal that ERα/β is anti-proliferative in cell-based models. We hypothesize that ERα/β heterodimers may be targeted in 60% of ERα-positive tumors which co-express ERβ, as well as served as cancer preventive targets for women who take natural products enriched in ERα/β heterodimer inducing activities. Our overall objectives are to target ERα+ tumors for differentiation in patients who failed conventional treatment, to target ERβ for treatment of TNBC, and to explore the biology of ERα/β, the most mysterious dimers in cancer prevention and treatment.

PROGRESS SINCE LAST REPORT:

We have made considerable progress towards each project proposed in the original grant.

AIM1: To explore CARM1 as epigenetic target for differentiation therapy in ERα-positive breast cancer. We propose to develop assays for identification of CARM1 methyltransferase activators, which may be developed as tumor differentiation drugs.

We have demonstrated that overexpressing CARM1 or activating CARM1 could lead to differentiation of ERα-positive breast cancer cells. In collaboration with scientists at Life Technology, Madison, WI, we have developed time-resolved fluorescence resonance energy transfer (TR-FRET) assays that can be adapted for high throughput screening to identify chemical activator of CARM1 for breast cancer differentiation therapy. This assay is based on methylation of poly(A) binding protein 1 (PABP1), a known CARM1 substrate, by cellular CARM1. We have shown that PABP1 methylation level is proportional to CARM1 level and activity. We are collaborating with Dr. Hoffmann, director of UW Small Molecule Screen and Synthesis Facility, to optimize the assay for high throughput screening. A manuscript describing the assay characterization is in preparation for publication.

a) We have demonstrated that CARM1 is a unique coactivator of ERα and over-expressing CARM1 induces cell differentiation in ERα-positive breast cancer cells (Al-Dhaheri, M., et al. (2011) CARM1 Is an Important Determinant of ERα-Dependent Breast Cancer Cell Differentiation and Proliferation in Breast Cancer Cells. Cancer Res., 71: 2118-2128). At the mechanism level, we have identified PAF1 complex as "effector" protein to be recruited to H3R17me2 mark modified by CARM1 (Wu, J., (2012), Histone H3R17me2a mark recruits human PAF complex to activate transcription. Proc. Natl. Acad. Sci. USA, 109: 5675-80).

b) TR-FRET assay have been established for identification of allosteric activator of CARM1 for breast cancer differentiation therapy. A manuscript describing the assay is under preparation (Zeng H., Bi, K., Hoffmann M., Xu, W. Establishment of assays to monitor cellular activity of a histone arginine methyltransferase CARM1).

AIM2: To target ERβ for treatment of triple-negative breast cancer. We will evaluate ERβ-selective agonists as imaging tools and for TNBC treatment and identify ERβ target genes as ancillary biomarker for ongoing TNBC trial. We will use xenograft mouse model to develop ^{18}Fluoro-ERβ agonists as imaging agents for PET imaging of ERβ+ human tumors. Genomic approaches will be taken to identify direct ERβ target genes. These effectors will be tested to determine if they are responsible for the anti-cancer effect of activating ERβ. Also, these target genes will be tested in tumor samples from clinical trial to determine whether estrogen treatment activated ERβ in patients, and whether TNBC response to estrogen correlate with ERβ expression in the phase II clinical trial.

We have developed isogenic MDA-mb-468 cell line inducibly express either ERα or ERβ. These cell lines have been validated to form xenograft tumors in nude mice. We have begun to assess whether ^{18}Fluoro-17β-estradiol (FES) could detect ERβ-positive breast tumors *in vivo* and thus suitable for *in vivo* PET imaging to identify ERβ-expressing breast tumors. We have optimized conditions to use a commercial ERβ antibody for immunohistochemistry (IHC). Using Tissue Microarray (TMA), we demonstrated that ~25% of triple negative breast tumors express significant amount of ERβ. Using MDA-mb-468-ERβ cell line, we performed RNA-sequencing and identified novel ERβ target genes. Expression of these target genes will be tested in tumor samples from clinical trial to determine whether estrogen treatment activated ERβ in patients. The phase II clinical trial is ongoing. Ten patients have enrolled in the clinical trial. One patient showed regression of liver metastasis after 6-week treatment of high dose of E2. This result proves the principle that triple-negative breast cancer patient could have response to endocrine therapy.
We have established two isogenic cell lines for screening ERβ-selective ligands (Shanle E., Hawse J., Xu, W. (2012), Biochemical Pharmacology, 82:1940-1949).

AIM3: To delineate the biological function of ERα/β heterodimer in cultured cells and *in vivo*. We plan to examine whether two phytoestrogens identified to be ERα/β heterodimer selective could prevent estrogen-induced breast cancer in an ACI rat model through collaboration with Jim Shull's laboratory. We will also identify genes regulated by ERα/β heterodimers in normal mammary epithelial cell lines and epithelial cells isolated from rat mammary gland.

The previously established BRET assays identified two naturally occurring phytoestrogens that induce ERα/β heterodimer formation in cell-based assay. We hypothesize that compounds inducing ERα/β heterodimer formation *in vivo* could have preventive and therapeutic effects for breast cancer. In collaboration with Dr. Jim Shull in my department, we have learned to implant one of the ERα/β heterodimer-selective phytoestrogens, cosmosiin, as pellet in the back of ACI female rat. We have determined pharmacokinetics of cosmosiin in ACI rat model and showed that serum concentration of cosmosiin could reach μM that is sufficient to induce ERα/β heterodimer *in vivo* after 2-wks cosmosiin implant. We have begun to do a longer time pharmacokinetics experiment to optimize conditions for breast cancer prevention experiment. Meanwhile, we are modifying BRET assays to BRET^3 for *in vivo*

application as compounds exhibiting heterodimer specificity in cell-based assays may not maintain heterodimer-specificity in vivo.

Using BRET assays, we identified two naturally occurring phytoestrogens, cosmosiin and angolensin, which induce ERα/β heterodimer formation in cells (Powell, E. et. Al. (2012) Plos One, 7(2):e30993).

Key Research Accomplishments:

1) We have demonstrated that CARM1 is a unique coactivator of ERα and over-expressing CARM1 induces cell differentiation in ERα-positive breast cancer cells (Al-Dhaheri, M., et al. (2011) CARM1 Is an Important Determinant of ERα-Dependent Breast Cancer Cell Differentiation and Proliferation in Breast Cancer Cells. Cancer Res., 71: 2118-2128). At the mechanism level, we have identified PAF1 complex as "effector" protein to be recruited to H3R17me2 mark modified by CARM1 (Wu, J., (2012), Histone H3R17me2a mark recruits human PAF complex to activate transcription. Proc. Natl. Acad. Sci. USA, 109: 5675-80).

2) TR-FRET assay have been established for identification of allosteric activator of CARM1 for breast cancer differentiation therapy. A manuscript describing the assay is under preparation (Zeng H., Bi, K., Hoffmann M., Xu, W. Establishment of assays to monitor cellular activity of a histone arginine methyltransferase CARM1).

3) We have established two isogenic cell lines for screening ERβ-selective ligands (Shanle E., Hawse J., Xu, W. (2012), Biochemical Pharmacology, 82:1940-1949).

4) Using BRET assays, we identified two naturally occurring phytoestrogens, cosmosiin and angolensin, which induce ERα/β heterodimer formation in cells (Powell, E. et. Al. (2012) Plos One, 7(2):e30993).

Reportable outcomes:

See Appendix Materials for published research. We have developed isogenic ERα or ERβ expressing Hs578T and MDA-mb-468 cell lines. We have developed cell-based BRET assay for high throughput screening of naturally occurring estrogenic compounds.

Presentations:

Department of Human Oncology, University of Wisconsin-Madison, March 15, 2012. Title: Epigenetic control of breast cancer.
Oregon Health & Science University, March 20, 2012. Title: Regulation of estrogen signaling in breast cancer.
World Cancer Congress, Beijing, May 18-21, 2012. Title: Targeting estrogen receptor coactivator for breast cancer treatment.
National Cheng Kung University, Taiwan, June 7-9, 2012. Title: Transcriptional control of estrogen signaling in breast cancer.

Recent Funding Applications:

NIH, submitted 6/2012: Please add “Cell-based HTS for Allosteric Activators of the CARM1 Arginine Methyltransferase”.
We propose to develop and optimize a cell-based high throughput screening assay to identify small molecule activators of CARM-1, using a time-resolved fluorescence method to quantify the CARM1 methylation of specific arginines on poly A binding protein 1 (PABP1). We hope these screens will lead to more facile and rigorous approaches to understanding the roles of CARM1 activity in cancer cells *in vitro* and *in vivo*, as well as provide leads for anticancer drugs with a novel mechanism of action. We will use a library of ~50,000 compounds available at the UW-Madison Small Molecule Screening & Synthesis Facility. The best compound(s) identified from these assays will be used to interrogate the global effects of CARM1 activation on re-programming the epigenome through RNA-seq and chromatin immunoprecipitation approaches. Successful completion of the this proposal will provide 1) a new HTS assay for an important molecular target in epigenetic regulation that can be implemented at many other academic or NIH screening centers, 2) an assay strategy that could be adopted for HTS with other protein methylases, and 3) molecular probes for testing hypotheses about CARM1 in human disease, including the hypothesis that small molecules enhancing CARM1 activity may be useful as “epigenetic” drugs for ERα+ breast cancers that fail conventional endocrine therapy.

Conclusions:

We have demonstrated that CARM1 is a valid epigenetic target for breast cancer differentiation therapy. TR-FRET assay has been established to screen for small molecule activators of CARM1 to be developed as epi-drugs. To our knowledge, assays for screening “activators” of epigenetic enzymes do not exist and epigenetic therapy for breast cancer is not yet widely applicable. We have provided solid evidence suggesting that ERβ should be activated in triple-negative breast cancer, both *in vitro* and in the ongoing clinical trial. Using our highly optimized isogenic ERα or ERβ expressing cell lines, animal models have been developed to validate FES for *in vivo* PET imaging to screen patients whose tumors express ERβ. Finally, two ERα/β heterodimer inducing phytoestrogens have been identified. One compound cosmosiin has been shown to reach μM serum concentration in the ACI rat model in a pharmacokinetics experiment. This is proof of principle that cosmosiin might have chemo-preventative effects *in vivo*.

References:

Al-Dhaheri, M., Wu, J., Skliris, G. P., Li, J., Higashimato, K., Wang, Y., White, K. P., Lambert, P., Zhu, Y., Murphy, L., and **Xu, W.** (2011) CARM1 Is an Important Determinant of ERα-Dependent Breast Cancer Cell Differentiation and Proliferation in Breast Cancer Cells. Cancer Res., 71: 2118-2128.

Shanle E., Hawse J., **Xu, W**. (2011) Generation of stable reporter breast cancer cell lines for the identification of ER subtype selective ligands. Biochemical Pharmacology, 82:1940-1949.

Powell, E., Shanle, E., Brinkman, A., Li J., Keles, S., Wisinski K.B., Huang, W., **Xu, W.** (2012) Identification of estrogen receptor α/β heterodimer selective ligands reveals growth-inhibitory effects on cells co-expressing ERα and ERβ. Plos One, 7(2):e30993.

Wu, J. and **Xu, W.** (2012) Histone H3R17me2a mark recruits human PAF complex to activate transcription. Proc. Natl. Acad. Sci. USA, 109: 5675-80.

Published OnlineFirst January 31, 2011; DOI:10.1158/0008-5472.CAN-10-2426

Cancer Research

CARM1 Is an Important Determinant of ERα-Dependent Breast Cancer Cell Differentiation and Proliferation in Breast Cancer Cells

Mariam Al-Dhaheri, Jiacai Wu, Georgios P. Skliris, et al.

Cancer Res 2011;71:2118-2128. Published OnlineFirst January 31, 2011.

Published OnlineFirst January 31, 2011; DOI:10.1158/0008-5472.CAN-10-2426

Cancer Research

CARM1 Is an Important Determinant of ERα-Dependent Breast Cancer Cell Differentiation and Proliferation in Breast Cancer Cells

Mariam Al-Dhaheri[1], Jiacai Wu[1], Georgios P. Skliris[3], Jun Li[1], Ken Higashimato[1], Yidan Wang[1], Kevin P. White[4], Paul Lambert[1], Yuerong Zhu[2], Leigh Murphy[3], and Wei Xu[1]

Abstract

Breast cancers with estrogen receptor α (ERα) expression are often more differentiated histologically than ERα-negative tumors, but the reasons for this difference are poorly understood. One possible explanation is that transcriptional cofactors associated with ERα determine the expression of genes which promote a more differentiated phenotype. In this study, we identify one such cofactor as coactivator-associated arginine methyltransferase 1 (CARM1), a unique coactivator of ERα that can simultaneously block cell proliferation and induce differentiation through global regulation of ERα-regulated genes. CARM1 was evidenced as an ERα coactivator in cell-based assays, gene expression microarrays, and mouse xenograft models. In human breast tumors, CARM1 expression positively correlated with ERα levels in ER-positive tumors but was inversely correlated with tumor grade. Our findings suggest that coexpression of CARM1 and ERα may provide a better biomarker of well-differentiated breast cancer. Furthermore, our findings define an important functional role of this histone arginine methyltransferase in reprogramming ERα-regulated cellular processes, implicating CARM1 as a putative epigenetic target in ER-positive breast cancers. *Cancer Res; 71(6); 2118–28. ©2011 AACR.*

Introduction

In normal breast tissue, estrogen receptor α (ERα) regulates growth and development of the mammary gland by regulating the balance between cell proliferation and differentiation. This balance is deregulated in cancer. Enhanced ERα proliferative action contributes to the initiation and progression of breast cancer (1) by promoting cell-cycle progression, in particular S-phase entry (2, 3). Microarray analyses using breast cancer cell lines have revealed that a majority of ERα target genes are involved in metabolism and cell-cycle regulation (4–6). ERα is expressed in nearly 70% of breast cancers. Interestingly, ERα-positive tumors are more histologically well-differentiated (7). ERα decreases in high-grade tumors (8), and its presence serves as a hallmark of differentiation and predictor of low aggressiveness and favorable disease-free survival (9, 10). The protective effect of ERα raises the possibility that ERα functions to regulate both proliferation and differentiation in breast cancer cells, albeit with the balance tilted toward proliferation. Cell proliferation and differentiation are 2 mutually exclusive processes. Forced differentiation of primary tumors with therapeutic compounds can inhibit proliferation (11). Differentiation therapy such as all-*trans* retinoic acid was successfully used in treating acute promyelocytic leukemia. However, this strategy is not widely applied to breast carcinomas because breast tumors are more heterogeneous. Moreover, how ERα regulates the balance of proliferation and differentiation is not well understood.

ERα regulates transcription through recruitment of multiple cofactors (12). Although ERα coactivators share the common feature of activating ERα in transcriptional assays, to date, no ERα coactivator has been reported to promote differentiation in breast cancer cells. Coactivator-associated arginine methyltransferase 1 (CARM1) was originally identified as a steroid receptor coactivator which activates transcription of ERα target genes (13, 14). Furthermore, loss of CARM1 in the mouse embryo leads to abrogation of the estrogen response and reduced expression of some ER target genes (15), highlighting the significance of CARM1 in ER-regulated processes. CARM1 is a multifunctional protein engaged in a variety of cellular processes including gene expression (16), coupling of transcription and mRNA processing (17), regulating protein stability (18), and tissue development (15). However, the function of CARM1 in regulating cell differentiation or proliferation is contradictory and seems to be context dependent. CARM1 is required for differentiation of adipocytes (19), myocytes (20),

Authors' Affiliations: [1]McArdle Laboratory for Cancer Research, University of Wisconsin; [2]BioInfoRx Inc., Madison, Wisconsin; [3]Manitoba Institute of Cell Biology, University of Manitoba, Winnipeg, Canada; and [4]Department of Human Genetics, University of Chicago, Cummings Life Science Center, Chicago, Illinois

Note: Supplementary data for this article are available at Cancer Research Online (http://cancerres.aacrjournals.org/).

Note: M. Al-Dhaheri and J. Wu contributed equally to this work.

Corresponding Author: Wei Xu, McArdle Laboratory for Cancer Research, 1400 University Ave., Madison, WI 53706. Phone: 608-265-5540; Fax: 608-262-2824; E-mail: wxu@oncology.wisc.edu

doi: 10.1158/0008-5472.CAN-10-2426

Published OnlineFirst January 31, 2011; DOI:10.1158/0008-5472.CAN-10-2426

pulmonary epithelial cells (21), and early thymocyte progenitor cells (22). In contrast, CARM1 was implicated in cancer cell proliferation and was shown to regulate the expression of E2F1 and cyclin E1, factors promoting cell-cycle progression (16, 23). Thus, functions of CARM1 in ERα-dependent breast cancer require further elucidation.

Here we report an extensive study of the biological function of CARM1 in ERα-regulated processes in breast cancer cells, using both gain-of-function and loss-of-function approaches.

Materials and Methods

Cell culture maintenance and construction

All cell lines were purchased from American Type Culture Collection (ATCC) and used within 6 months. MCF7-Tet-on-shCARM1 was generated by 2 steps: First, we synthesized shRNA-encoding oligo DNA "CGGCGAGATCCAGCGGCAC" targeting human CARM1 and cloned the sequence into pLVTHM plasmid (24). MCF7 cells (ATCC HTB-22) were sequentially infected with the lenti-KRAB and pLVTHM-CARM1 shRNA vectors, followed by selection of single clones by Western blotting. MCF7-Tet-on-CARM1 was generated by cotransfecting pTRE-tight CARM1 plasmid with pBabe-puromycin vectors at a ratio of 10:1 into MCF7-Tet-on cells (Clontech cat #630918, generous gift of Elaine Alarid), followed by selection with puromycin. MCF7-CARM1 has been described previously (25). MDA-MB-231 (ATCC HTB-26) or ZR-75 (ATCC CRL-1500) cells were infected with retrovirus derived from pLNCX (Clontech), pLNCX-CARM1, and pSIREN-Q-shCARM1 vectors to obtain pooled clones. The shRNA-encoding oligo DNA "CAGCGTCCTCATCCAGTTC" targeting human CARM1 was cloned into pSIREN-Q (Clontech) vector. All cells were maintained in DMEM containing 10% FBS and seeded in phenol red–free media with 5% of stripped FBS for experiments.

Immunohistochemistry and tissue microarrays of human breast tumors

All primary invasive breast tumors used in this study were obtained from the Manitoba Breast Tumor Bank [MBTB; Cancer Care Manitoba and University of Manitoba (http://www.umanitoba.ca/institutes/manitoba_institute_cell_biology/MBTB/Index4.htm)]. The MBTB operates with approval from the Research Ethics Board of the Faculty of Medicine, University of Manitoba. Tissue collection and selection of samples for constructing tissue microarrays (TMA) have been reported before (26, 27). Although 450 cases were represented on the original ER-positive TMAs, due to exhaustion of tumor cores from previous use of the TMAs, or incomplete data for some cases, the number (n) of tumors analyzed for some of the markers was less than 450. Immunohistochemistry scores (IHC scores) derive from assessment of both staining intensity (scale: 0, 1, 2, 3) and percentage of positive cancer cells (0%–100%). These 2 scores were multiplied to generate an IHC or H-score with a range of 0 to 300 as previously described (27). Only nuclear staining was scored. Briefly, serial sections (5 μm) of the TMAs were stained with anti-CARM1 antibodies, using an automated tissue immunostainer (Discovery Staining Module; Ventana Medical Systems). The dilution of the primary CARM1 antibody (Ab) applied initially to the slides was 1:150, incubated for 1 hour at 42°C on the Ventana Discovery Staining module, using CC1 buffer and the Mild and Standard protocols for Antigen Retrieval (AR). The VIEW DAB kit and reagents from Ventana Medical Systems were used. Slides were viewed and scored using standard light microscopy.

Additional assays and methods

Cell growth assays, quantitative real-time PCR (qRT-PCR), cell-cycle profiling, CARM1 Ab characterization, mouse xenograft experiments, and microarray gene expression analyses are described in Supplementary Methods and Materials. The microarray GEO numbers are GSE26454 and GSE26259.

Statistical analysis

One-way ANOVA and ANOVA single-factor analysis was applied and a value of $P < 0.05$ was regarded as statistically significant.

Results

Overexpression of CARM1 in MCF7 breast cancer cell line inhibits estrogen-dependent cell proliferation and anchorage-independent growth and stimulates the expression of CDK inhibitors $p21^{cip1}$ and $p27^{kip1}$

MCF7 breast cancer cells stably overexpressing CARM1, MCF7-CARM1, were generated (25). MCF7-CARM1 grows at a slower rate than parental cells carrying empty vector (MCF7-vector) as measured by MTT assays (Fig. 1A). The altered growth rate was not due to the superphysiologic amounts of CARM1 in MCF7-CARM1, because compared with MCF7-vector controls, MCF7-CARM1 cells have only a 2-fold increase in CARM1 expression (Fig. 1B). Consistent with the growth phenotype, the expression of the CDK inhibitors $p21^{cip1}$ and $p27^{kip1}$ was elevated in MCF7-CARM1 treated with 17beta-estradiol (E2) (Fig. 1B). Also the expression of $p21^{cip1}$ and $p27^{kip1}$ was stimulated by E2 in a time-dependent manner in MCF7-CARM1 cells (Supplementary Fig. 1) but not in parental MCF7 cells, suggesting that ERα and CARM1 are involved in regulating their expression. The effect of CARM1 on anchorage-independent cell growth was determined using soft-agar assays. E2 stimulates colony formation of MCF7-vector cells; in contrast, no colonies were formed in soft agar with MCF7-CARM1 (Fig. 1C). This result suggests that overexpressing CARM1 in MCF7 may inhibit anchorage-independent growth. In contrast to MCF7, no growth effects were detected by overexpressing or knocking down CARM1 in MDA-MB-231, an ERα-negative breast cancer cell line (Fig. 1D and E). Consistent with it being ERα negative, the growth rate of MDA-MB-231 was E2 independent (Fig. 1D). Similarly, overexpressing CARM1 exhibits no growth effect on MDA-MB-468, another ERα-negative breast cancer cell line (Supplementary Fig. 2), supporting the notion that the growth inhibitory effect of CARM1 in MCF7 is ERα dependent. The growth inhibitory effect of CARM1 was further validated in another ERα-positive breast cancer cell line ZR-75 (Supplementary Fig. 3). $p21^{cip1}$ has been reported to induce both cell cycle arrest and cell

Published OnlineFirst January 31, 2011; DOI:10.1158/0008-5472.CAN-10-2426

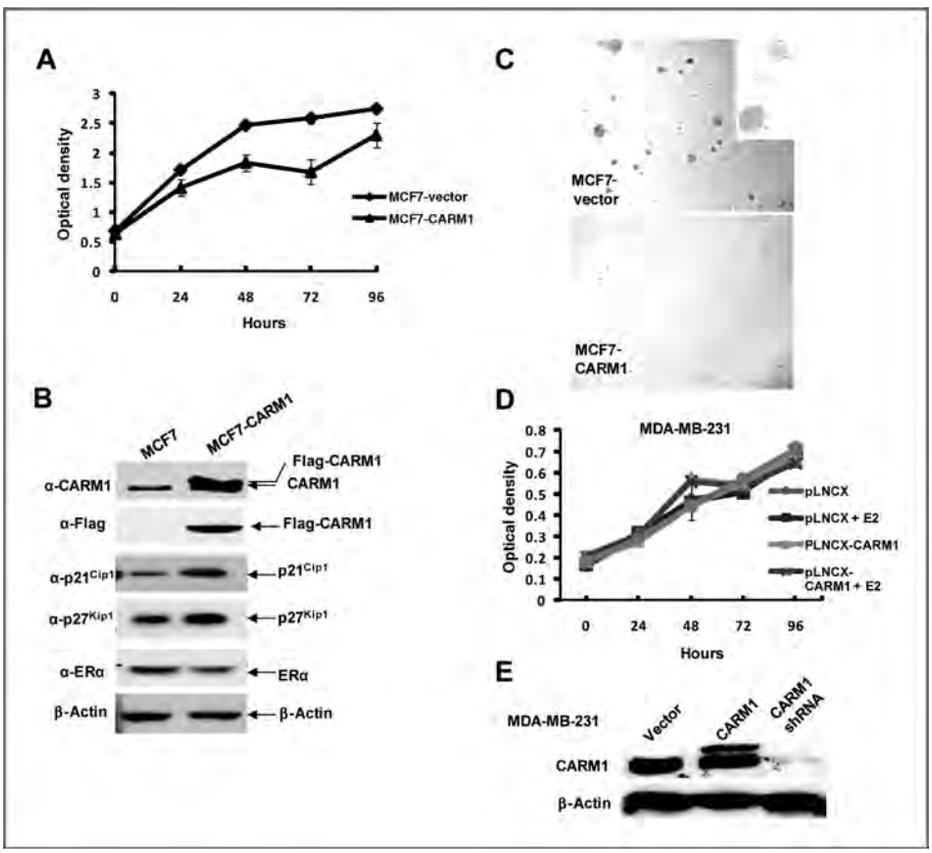

Figure 1. Overexpression of CARM1 inhibits growth and colony formation of MCF7 while exhibiting no effect on MDA-MB-231. A, the CARM1-overexpressing MCF7 cell line MCF7-CARM1 grew at a slower rate than the MCF7-vector control as measured by MTT. Error bars, SD ($n = 3$). B, $p21^{cip1}$ and $p27^{kip1}$ were expressed at higher levels in MCF7-CARM1 than in MCF7-vector cells in the presence of 10 nmol/L E2. C, overexpression of CARM1 inhibited colony formation of MCF7-CARM1 in soft agar in the presence of 10 nmol/L E2. The inset shows colonies under higher amplification in MCF7-vector cells. D, neither overexpressing nor knocking down CARM1 has growth effects on MDA-MB-231. Each assay was conducted in triplicate and the error bars represent SD. E, Western blotting showed that CARM1 was overexpressed in MDA-MB-231-CARM1 and knocked down in MDA-MB-231-shCARM1 cells.

differentiation in various carcinomas (28, 29). The findings that $p21^{cip1}$ expression is increased by E2 in the presence of exogenous CARM1 (Supplementary Fig. 1) raises the possibility that CARM1 may inhibit breast cancer growth by modulating key ERα target genes involved in cell-cycle control and differentiation.

CARM1 decreases estrogen-dependent breast cancer cell growth and S-phase entry

To eliminate the possibility that the growth effects of CARM1 in MCF7-CARM1 cells could be attributed to additional changes during retroviral integration events, we generated 2 inducible MCF7 stable cell lines: one overexpresses CARM1 (MCF7-Tet-on-CARM1) and the other expresses CARM1 shRNA (MCF7-Tet-on-shCARM1) under the control of a tetracycline-inducible promoter. These stable cell lines serve as gain-of-function and loss-of-function cell culture models for studying the effects of CARM1 in estrogen-dependent breast cancer growth. Cells were preincubated with doxycycline (Dox) for 4 days to induce or knockdown CARM1 expression, followed by E2 treatment for 24 hours. With either cell line, E2 alone has no significant effect on CARM1 expression at both mRNA and protein levels (Fig. 2A and B). Dox could increase CARM1 expression in MCF7-Tet-on-CARM1 cells by 2-fold (Fig. 2A) and reduce CARM1 to greater than 90% in MCF7-Tet-on-shCARM1 cells (Fig. 2B). E2 has no additional effect on CARM1 expression compared with Dox alone when both are present. The 2 cell lines were employed to measure cell growth by MTT assays under 4 treatment conditions: vehicle, E2, Dox, or combination of Dox and E2 for 4 time points (24, 48, 72, and 96 hours). As expected, E2 treatment significantly increases MCF7 cell growth starting from day 2 (P value <0.001; Fig. 2C). Overexpression of CARM1 by Dox treatment alone decreased MCF7 cell growth (Fig. 2C). Statistical analysis of 3 independent experiments suggested that overexpression of CARM1 by Dox treatment significantly repressed E2-induced cell growth in 2 individual clones, clone 7 (Fig. 2C) and clone 13 (Supplementary Fig. 4). This is in contrast to the nonstatistically significant effect of Dox upon E2-induced cell growth in MCF7-Tet-on-shCARM1 cells ($P > 0.05$; Fig. 2D) and a CARM1 stable knockdown MCF7 (MCF7-shCARM1) cell line expressing shRNA targeting a different sequence of human CARM1 (Supplementary Fig. 5, $P = 0.04$).

The main proliferative action of E2 in breast cancer is to promote cell-cycle progression during G_1/S transition (3). Since CARM1 can induce expression of $p21^{cip1}$ and $p27^{Kip1}$, which are negative regulators of the cell cycle, and inhibit E2-dependent growth, we determined whether CARM1 would interfere with E2-induced cell cycle progression. MCF7-Tet-on-CARM1 cells were preincubated with Dox for 4 days, followed by E2 treatment for 24 hours. Fluorescence-activated cell-sorting analysis of MCF7-tet-on-CARM1, using propidium iodide labeling, showed that E2-induced S-phase entry was inhibited by overexpressing CARM1 (Fig. 2E). This result was

Published OnlineFirst January 31, 2011; DOI:10.1158/0008-5472.CAN-10-2426

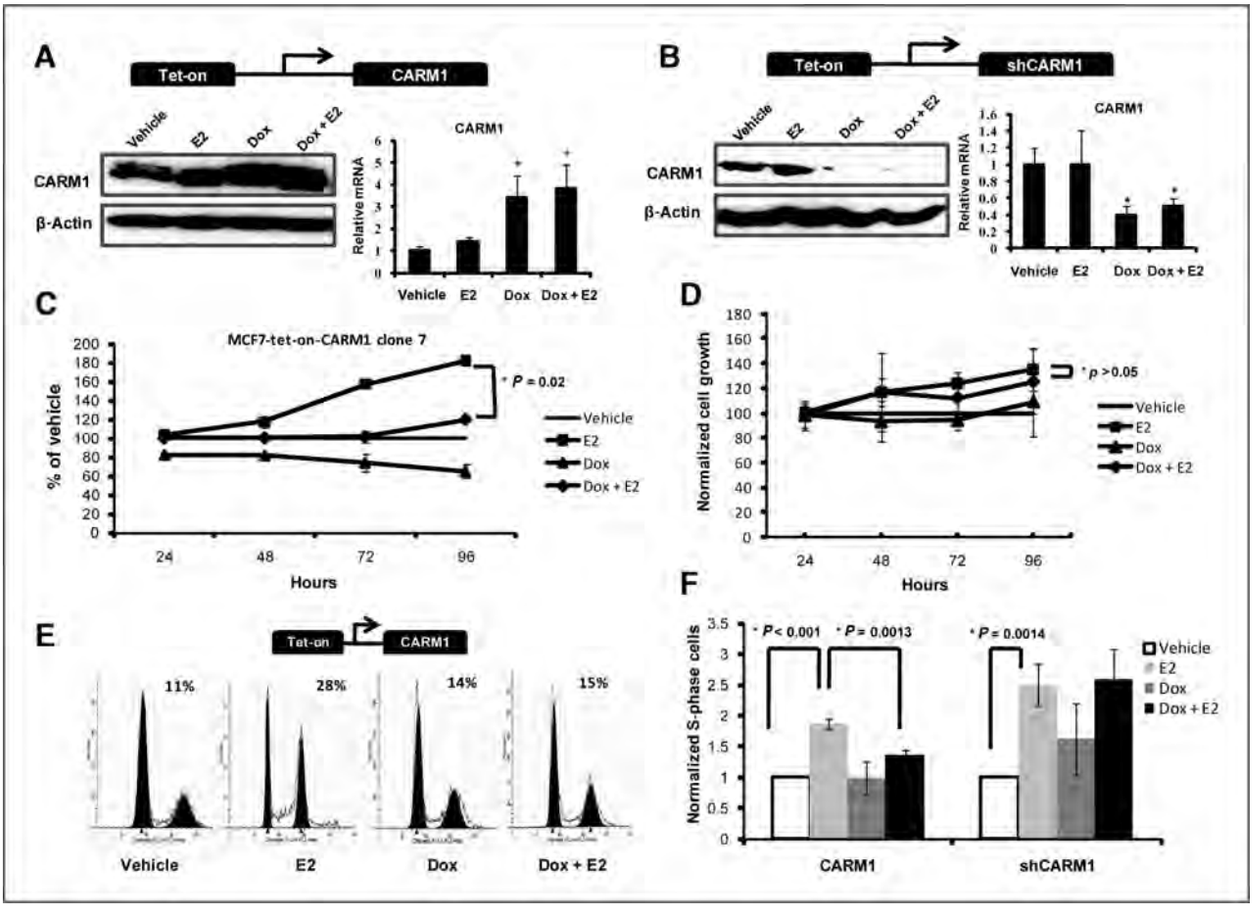

Figure 2. CARM1 inhibits E2-dependent MCF7 cell growth and S-phase entry. MCF7-Tet-on-CARM1 (A) and MCF7-Tet-on-shCARM1 (B) tetracycline-inducible cell lines were constructed as gain-of-function and loss-of-function cell-based models to modulate the endogenous level of CARM1. CARM1 was detected by Western blotting and mRNA was determined by qRT-PCR. *, statistically significant *P* value. C, inhibition of E2-dependent cell growth by overexpressing CARM1 (+Dox) in MCF7-Tet-on-CARM1. Bars, SD ($n = 9$). D, knocking down CARM1 in MCF7-Tet-on-shCARM1 (+Dox) did not affect the basal and E2-dependent growth of MCF7 cells in MTT assays. Bars, SD ($n = 9$). E, E2 increased the S-phase entry, an event inhibited by CARM1 overexpression in MCF7-Tet-on-CARM1 cells. F, the effects of CARM1 overexpression or knockdown on E2-dependent S-phase entry ($P > 0.05$) measured by BrdU labeling. Error bars, SD ($n = 3$).

validated by bromodeoxyuridine (BrdU) labeling (Fig. 2F). Although E2 and E2 + Dox both increased S-phase entry as compared with that of the vehicle (*P* value <0.001 and 0.0015, respectively), results from 3 independent experiments showed that the percentage of S-phase entry induced by Dox + E2 was significantly decreased compared with E2 treatment alone ($P = 0.0013$), indicating that overexpression of CARM1 decreased E2 induction of S-phase entry. In contrast, in MCF7-Tet-on-shCARM1, Dox + E2 treatment displayed no difference in S-phase entry compared with E2 alone and both treatment groups induced S-phase entry compared with the vehicle treatment ($P = 0.0014$). In either MCF7-Tet-on-CARM1 or MCF7-Tet-on-shCARM1 cells, Dox alone had no significant effect on S-phase entry (Fig. 2F). These data suggest that overexpression of CARM1 can inhibit E2-stimulated cell growth through modulating cell cycle, while loss of CARM1 could not further accelerate E2-stimulated growth within 4 days of treatment.

Changes of cell morphology and differentiation marker expression by increasing CARM1 level in MCF7 cells

In addition to the growth inhibitory effects of CARM1, we noticed that MCF7 cells stably overexpressing CARM1 displayed a distinct cell morphology from that of MCF7-vector cells (Fig. 3A) and exhibited increased cell adhesion (requires longer trypsin treatment time). Next we investigated desmoplakin 1 (DSP1) expression, a known differentiation marker of epithelial cells that plays an essential role in maintaining cell adhesion and differentiation (30, 31), and a CARM1 target gene identified in this study. Three independent experiments showed that E2 significantly decreased DSP1 mRNA, which was reversed by overexpressing CARM1 in MCF7-Tet-on-CARM1 cells (Fig. 3B). In addition, induction of 2 additional differentiation markers, GATA-3 and E-cadherin, by overexpressing CARM1 was observed in MCF7-Tet-on-CARM1 (Fig. 3C) by Western blotting. These data suggested that growth inhibitory

Published OnlineFirst January 31, 2011; DOI:10.1158/0008-5472.CAN-10-2426

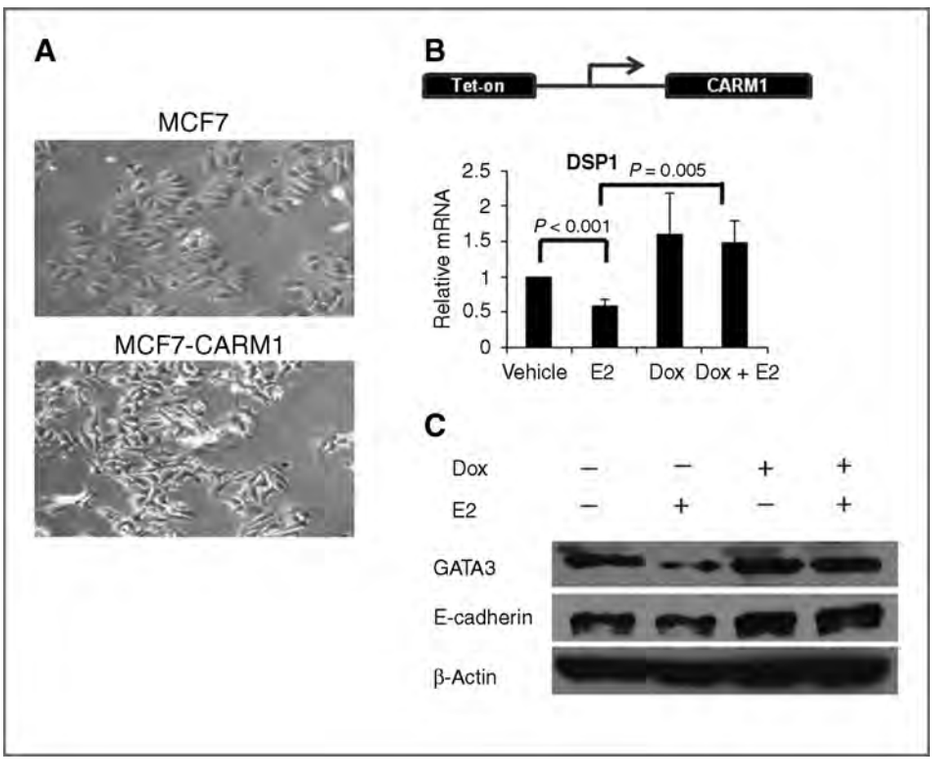

Figure 3. Overexpression of CARM1 induces morphologic changes in MCF7 characteristic of a differentiated phenotype. A, MCF7-CARM1 and MCF7-vector cells exhibit different morphology. B, DSP1 mRNA level was significantly repressed by E2 treatment and overexpression of CARM1 could reverse E2-mediated DSP1 repression. Error bars, SD from triplicate experiments. C, Western blotting showed that overexpression of CARM1 restored protein levels of E2-repressed E-cadherin and GATA-3 at 12 hours after E2 treatment.

function of CARM1 may be accompanied by the induction of cell differentiation.

CARM1 levels in MCF7 cells modulate the ERα gene signature

Since CARM1 inhibits E2-dependent growth of MCF7 cells and induces a morphology change, we determined the global effect of CARM1 on E2-dependent ERα gene signature by microarray analyses of CARM1 gain-of-function and loss-of-function cell lines treated with vehicle or E2. MCF7-inducible cells were treated under 4 conditions: DMSO, Dox, E2, and E2 plus Dox. The gene signature as calculated by fold change was normalized to vehicle control (Fig. 4A). Microarray analysis of MCF7-Tet-on-CARM1 reveals that E2 upregulated expression of 313 genes and downregulated 157 genes ($P < 0.05$, fold change $\geq$1.6). Overexpression of CARM1 drastically altered E2-regulated gene signatures. Approximately 16% of E2-induced genes including cell-cycle regulators (e.g., c-Myc; Fig. 4B) were inhibited. The most profound effect of CARM1 overexpression on E2-dependent signature was to relieve the repression of approximately 56% of E2-repressed genes (Fig. 4C; $P < 0.05$, fold change $\leq$0.6 compared with vehicle). To our knowledge, CARM1 is the only coactivator which affects global expression of E2-repressed genes. Interestingly, gene ontology (GO) of the affected genes suggested that most E2-repressed, CARM1-activated genes are involved in cell differentiation and development (Fig. 4C). The ability of CARM1 both to inhibit E2-dependent growth and S-phase entry and to modulate E2-dependent genes involved in cell-cycle progression, cell differentiation, and development supports a role of CARM1 in modulating the programming of E2-dependent cellular processes (i.e., regulating the balance between cell differentiation and proliferation).

Since CARM1 has putative effects on ERα-dependent proliferation and differentiation, we applied qRT-PCR to validate the effect of CARM1 overexpression on 6 differentially expressed genes identified by microarray. $p21^{cip1}$ and $p27^{kip1}$ are known to inhibit breast cancer growth (32). Cyclin G2 is an ERα target gene and a negative regulator of cell cycle (33). Among genes involved in cell differentiation, GATA-3 is an ERα target gene and prodifferentiation marker of breast cancer (8, 34). MAZ is a transcriptional factor (35), and KRTAP10.12 is a potential prodifferentiation marker. As shown in Figure 4D, E2 alone significantly decreased cyclin G2 and KRTAP10.12 mRNA but not $p21^{cip}$, $p27^{kip1}$, MAZ, and GATA-3 mRNA after 4-hour treatment. However, overexpression of CARM1 relieved E2 repression of cyclin G2 and KRTAP10.12 and significantly induced $p21^{cip1}$, $p27^{kip1}$, MAZ, and GATA-3 regardless of E2 (Fig. 4D) at mRNA level. Consistently, the protein levels of GATA-3, E-cadherin (Fig. 3C), and $p21^{cip1}$ and $p27^{kip1}$ (Fig. 1B) were also increased by CARM1 overexpression and E2 treatment. These results validate our microarray data and reinforce the hypothesis that CARM1 may antagonize the proliferative action of estrogen in breast cancer cells by activating multiple cell-cycle–negative regulators and prodifferentiation genes. It is worth noting that $p21^{cip1}$ induction requires both CARM1 overexpression and E2 treatment. In contrast, overexpressing CARM1 alone is sufficient to induce genes such as $p27^{kip1}$,

Published OnlineFirst January 31, 2011; DOI:10.1158/0008-5472.CAN-10-2426

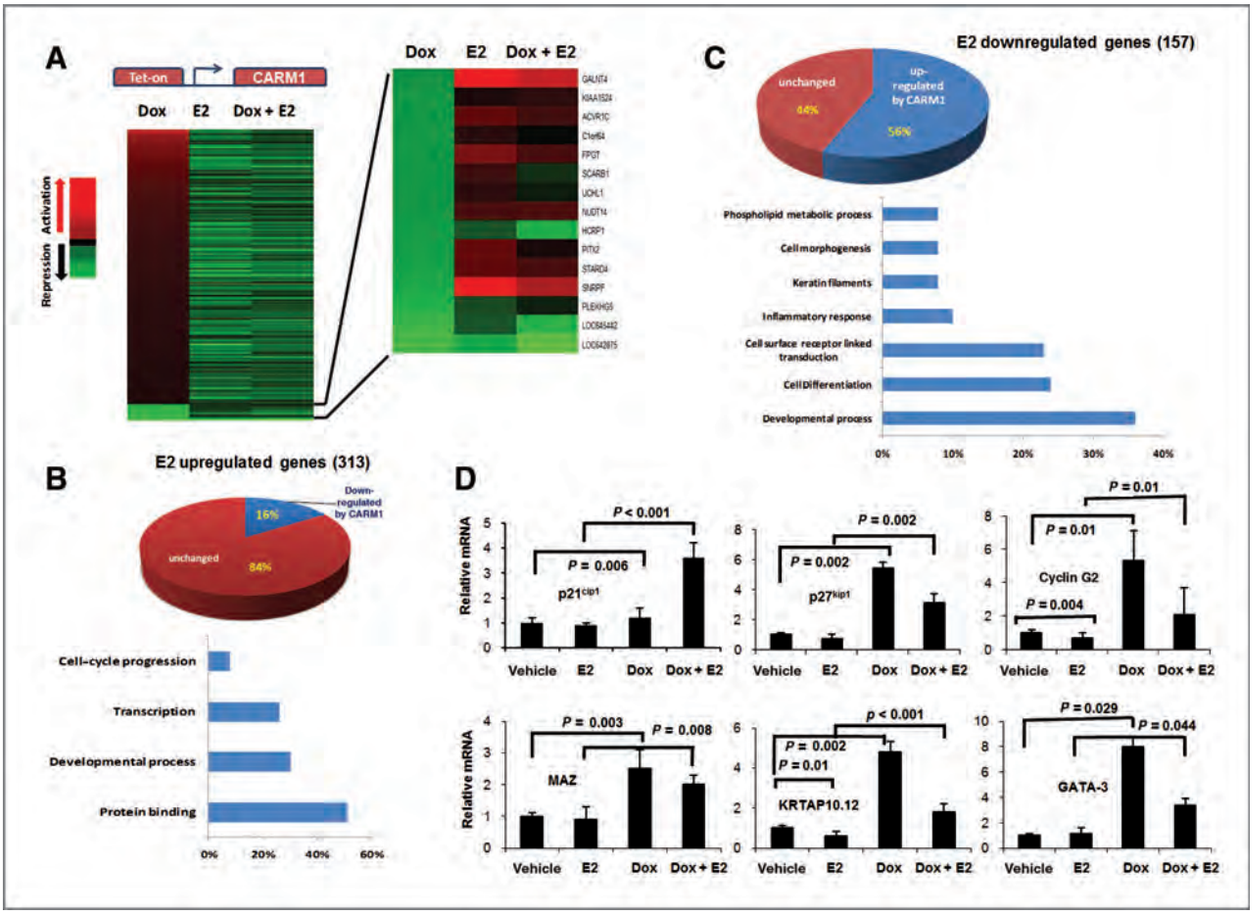

Figure 4. Overexpression of CARM1 modulates E2-dependent gene signature. A, the ratios of normalized intensities for Dox, E2, or Dox + E2-treated samples versus that of samples treated with control vehicle (Dox vs. DMSO, E2 vs. DMSO, and DOX + E2 vs. DMSO) were used to show the activation or repression. Heat map of gene expression calculated as fold changes compared with vehicle indicated that CARM1-induced genes (+Dox) are largely nonoverlapping with E2-activated genes. Among CARM1-repressed genes, many are activated by E2 (see blowup of the heat map), indicating that overexpressing CARM1 can inhibit some E2-activated genes. B, pie graph shows that among all E2-upregulated genes, 16% of them are downregulated by CARM1 overexpression. The bottom of chart shows, among all CARM1-downregulated, E2-upregulated genes, the percentage of genes in each molecular function category. GO of the affected genes was determined by GOStat tool online (http://gostat.wehi.edu.au/cgi-bin/goStat.pl),"goa_human" database, where % represent the percentage of the affected genes that belong to each represented category. C, pie graph shows that among all E2-downregulated genes, 56% of them are upregulated by CARM1 overexpression. The bottom chart shows, among all CARM1-upregulated, E2-downregulated genes, the percentage of genes in each molecular function category. D, Q-RT PCR analyses of $p21^{cip1}$, $p27^{kip1}$, cyclin G2, MAZ, KRTAP10.12, and GATA-3 expression in MCF7-Tet-on-CARM1. Error bars, SD from 3 independent experiments.

suggesting that CARM1 may regulate some genes in hormone-deprived conditions.

The global effects of CARM1 on ER target genes were next examined in the loss-of-function model, MCF7-Tet-on-shCARM1 under aforementioned conditions. The heat map of the fold-change gene signature relative to vehicle control is shown in Figure 5A and additional description can be found in Supplementary Methods. Using Agilent array platform herein, CARM1 shRNA expression upregulated 62 genes and downregulated 2,122 genes ($P < 0.05$, fold change ≥ 1.6 and ≤ 0.6 compared with vehicle, respectively). E2 treatment upregulated 780 genes and downregulated 5,099 genes ($P < 0.05$, fold change ≥ 1.6). Interestingly, the genes affected by loss-of-CARM1 largely overlapped with those affected by E2 in wild-type cells. Further microarray analysis showed that 65% of genes activated by knocking down CARM1 are also activated by E2 (Fig. 5B) and 75% of genes repressed by CARM1 knockdown are also repressed by E2 (Fig. 5C). GO of genes affected by Dox and E2 treatment also overlap (Fig. 5B and C). Among these genes, a majority are involved in metabolism, development, protein binding, and gene expression (Fig. 5B and C). These data further support the notions that CARM1 is a global regulator of E2-responsive genes in breast cancer cells and profoundly affects estrogen-mediated processes. We also validated the effect of loss of CARM1 on $p21^{cip1}$, $p27^{kip1}$, cyclin G2, MAZ, GATA-3, and KRTAP10.12 mRNA expression. Loss of CARM1 significantly repressed $p21^{cip1}$, $p27^{kip1}$, cyclin G2, MAZ, GATA-3, KRTAP10.12, and DSP1 at mRNA levels, similar to the effect of E2 in MCF7-Tet-on-shCARM1 (Fig. 5D and Supplementary

Published OnlineFirst January 31, 2011; DOI:10.1158/0008-5472.CAN-10-2426

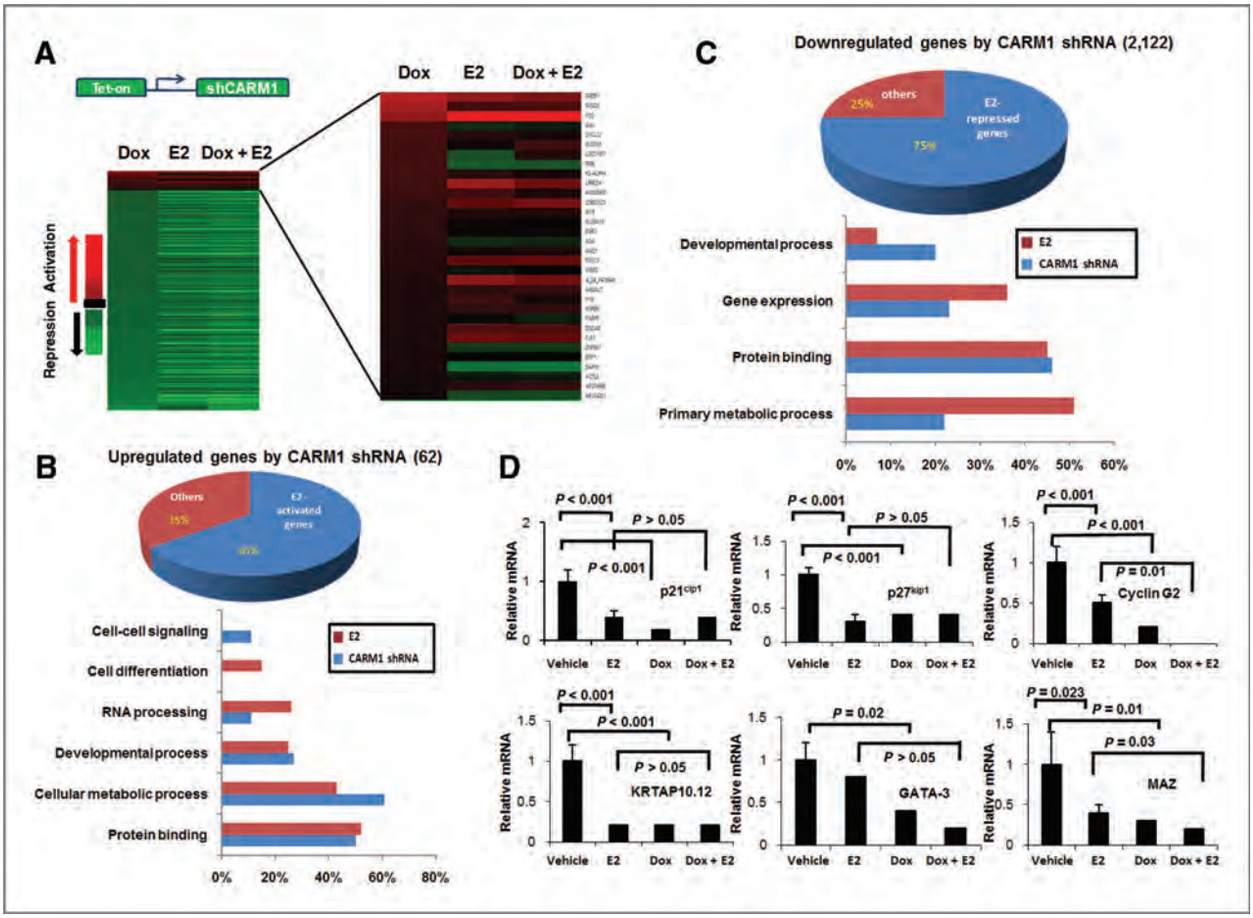

Figure 5. Knocking down CARM1 shared common gene signatures with that of E2 treatment in MCF7-Tet-on-shCARM1. A, heat map showed that CARM1 shRNA (+Dox)-activated and -repressed genes were largely overlapping with those regulated by E2. A blowup of the heat map illustrated that many Dox-activated genes (knocking down CARM1) were also activated by E2. B, pie graph shows that approximately 65% of CARM1 shRNA–activated genes were also activated by E2; approximately 35% of knocking down CARM1-activated genes was E2-nonresponsive (labeled as others). Gene ontology illustrated the top affected gene categories by expressing CARM1 shRNA or E2 treatment. C, pie graph shows that among all downregulated genes by CARM1 knockdown, 75% of them are E2-repressed genes and 25% of them are E2-nonresponsive (labeled as others). The bottom chart shows, among all downregulated genes by E2 treatment or CARM1 knockdown, the percentage of genes in each molecular function category. D, qRT-PCR analyses of ER target genes in MCF7-Tet-on-shCARM1. Error bars, SD.

Fig. 6A). In agreement with the mRNA results, cyclin G2, GATA-3, and E-cadherin (Supplementary Fig. 6B) were decreased at protein levels with the loss of CARM1. Since both cyclin G2 (33) and GATA-3 (36) are ERα target genes, CARM1 may antagonize E2 action via ERα during reprogramming of ERα-dependent differentiation and proliferation processes. Fold changes of key cell-cycle regulators and genes involved in cell differentiation in MCF7-Tet-on-shCARM1 are listed in Supplementary Table S1. Overall, our data suggest that loss of CARM1 induces gene signatures resembling those affected by E2 and CARM1 is a regulator of E2-dependent, key cell cycle progression, and differentiation genes. Collectively, the microarray analyses using CARM1 gain-of-function and loss-of-function cell models reveal that CARM1 is a unique ER coactivator that profoundly affects the balance of genes involved in cellular differentiation and proliferation (i.e., inhibit cell growth and promote cell differentiation).

Knocking down of CARM1 increased E2-dependent tumor growth in an MCF7 xenograft mouse model

To examine the effects of CARM1 *in vivo*, we transplanted MCF7-Tet-on-CARM1 shRNA cells in nude mice. The design of the xenograft experiment is shown in Figure 6A, representing one of triplicate experiments. We first validated that the growth of xenografted tumors was E2-dependent because no growth or only tiny tumors developed in the negative control group not receiving estrogen. Tumors collected from mice engrafted with MCF7-Tet-on-shCARM1 cells and receiving Dox showed a reduction of CARM1 expression at the mRNA and protein levels (Fig. 6B). Knocking down CARM1 increased the size of E2-induced tumors (Fig. 6C) and was associated with a modest increase in BrdU labeling. The differential rate of BrdU labeling for xenografted tumors was further increased in mice receiving a higher dose of E2 and that was associated with higher mitotic index (Fig. 6D and E). All the data suggest that knocking down CARM1 enhances

Published OnlineFirst January 31, 2011; DOI:10.1158/0008-5472.CAN-10-2426

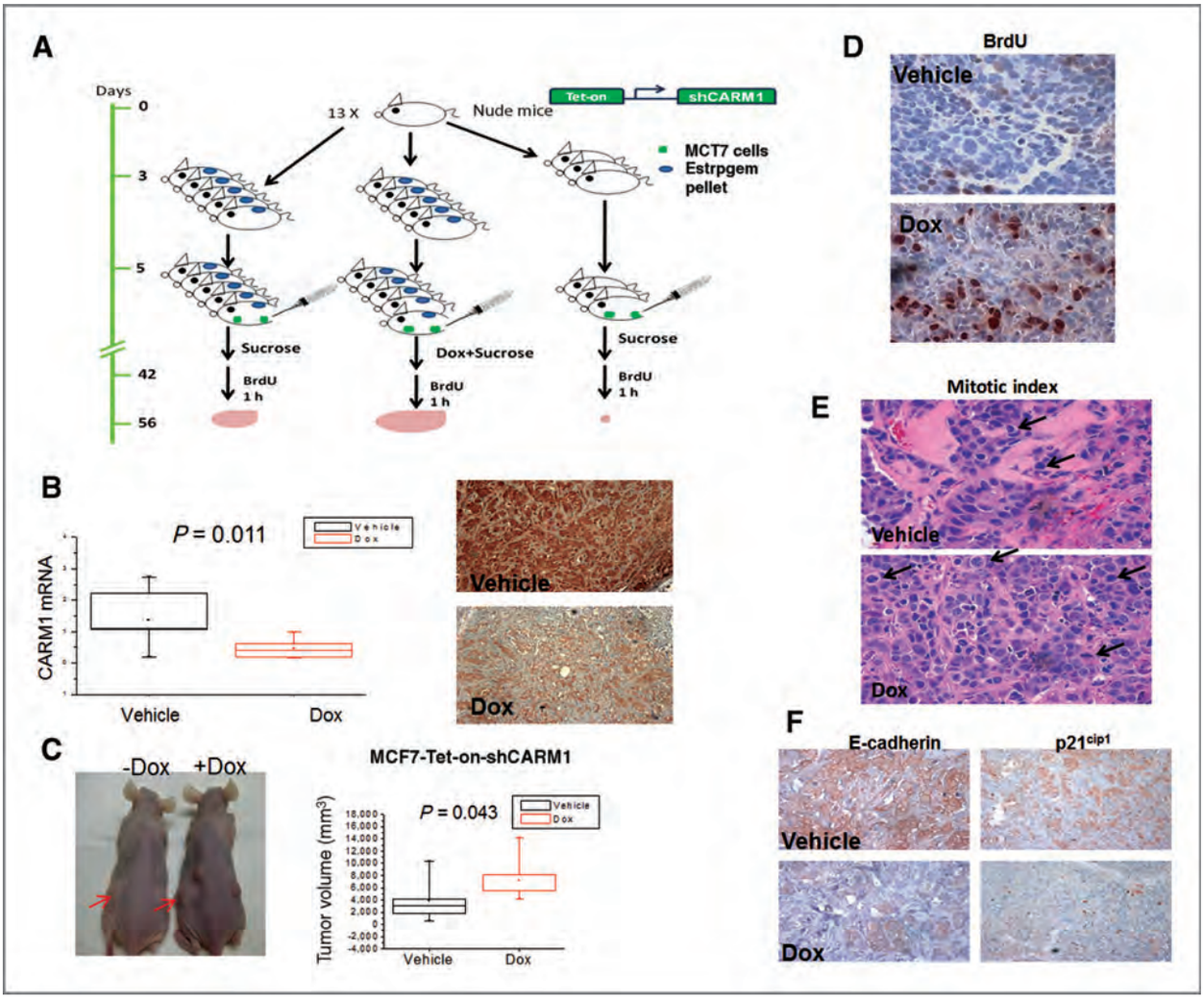

Figure 6. Knocking down CARM1 increased E2-dependent tumor growth in xenografted mice. A, schematic design of the xenograft study using MCF7-Tet-on-shCARM1 cell line. B, CARM1 mRNA and protein levels were decreased in tumors from Dox recipient mice. CARM1 mRNA in tumors was quantified using qRT-PCR (vehicle: $n = 7$; Dox: $n = 10$); protein was visualized by IHC. C, increased tumor volume in CARM1 knocked down mice. A representative experiment showed a higher tumor volume with knocking down CARM1 ($n = 10$) than E2-alone–induced tumors ($n = 8$). The red arrows point to tumors in 2 representative mice. D, BrdU and hematoxylin and eosin staining of representative tumor samples from vehicle and Dox-treated mice. E, mitotic index of representative tumor samples from vehicle and Dox-treated mice implanted with a high-dose E2 pellets. F, correlation of $p21^{cip1}$ and E-cadherin protein level by IHC.

E2-dependent proliferation of breast cancer cells *in vivo*. Since CARM1 inhibits E2-dependent growth by modulating negative cell-cycle regulators $p21^{cip1}$, $p27^{kip1}$, and cyclin G2 and pro-differentiation genes, we examined the relationship between $p21^{cip1}$ and E-cadherin, a differentiation marker, in E2-induced xenografted tumors. A direct correlation was observed between $p21^{cip1}$ and E-cadherin expression in tumors derived from xenografts (Fig. 6F), suggesting inhibition of cell growth and induction of differentiation are coherent processes in ERα-positive tumors.

CARM1 expression in human breast tumor biopsy samples

Our rabbit polyclonal CARM1 Ab was determined to be specific because it detects both nuclear and cytoplasmic CARM1 in normal breast tissues and breast tumors while exhibiting no activity toward mouse embryonic fibroblasts derived from CARM1 knockout mice ($MEF^{-/-}$; Supplementary Fig. 7). CARM1 expression was determined by IHC in ER^{+} breast tumor TMAs available in the MBTB (26, 37). Statistically significant correlations between ERα expression as determined by IHC ($n = 310$, Spearman $r = 0.324$, $P < 0.0001$) and tumor grade ($n = 328$, Spearman $r = -0.159$, $P = 0.004$) were found. Significantly higher CARM1 expression as determined by IHC score was found in tumors with higher ERα expression than in those with lower ERα expression (Fig. 7A). Significantly higher CARM1 expression was found in lower-grade (3, 4) tumors as well (Fig. 7B and C). In addition, CARM1 expression was positively correlated with ERα levels in ER-positive, node-negative human breast tumors ($P < 0.0001$;

Published OnlineFirst January 31, 2011; DOI:10.1158/0008-5472.CAN-10-2426

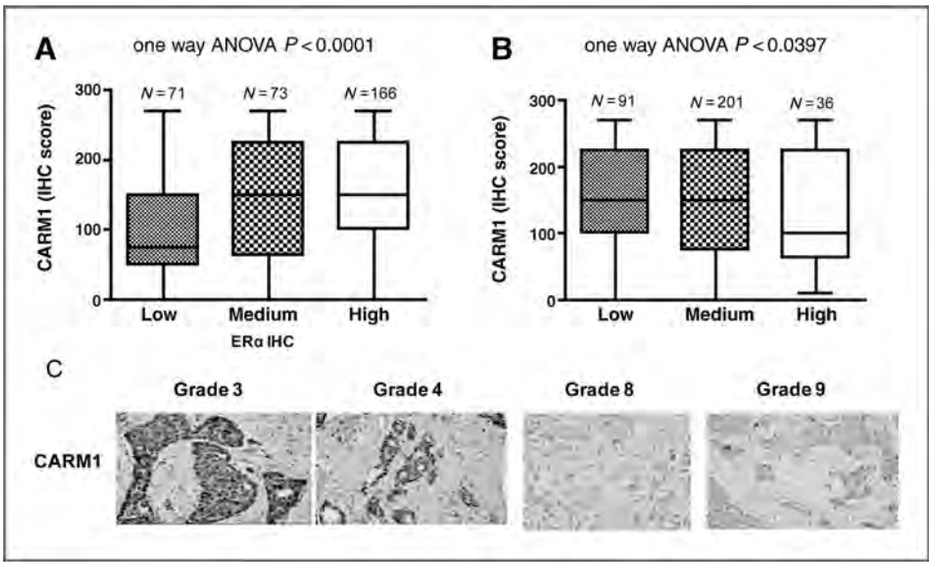

Figure 7. The expression level of CARM1 positively correlates with ERα level and inversely correlates with tumor grade in ER-positive breast tumors. A, CARM1 expression level is directly correlated with ERα expression level in more than 300 human breast tumor samples, using TMAs. B and C, CARM1 expression level is higher in ER-positive, low-grade tumors than in high-grade tumors, supporting a potential link between CARM1 and the differentiation status of ERα-dependent breast tumors. ERα+ve, grade 3, 4 (low), IHC score 270, magnification × 500; ERα+ve, grade 8, 9 (HIGH), IHC score 0, magnification × 500.

Supplementary Fig. 8A). We also found an inverse correlation between CARM1 expression and tumor grade in ER-positive, node-negative human breast tumors ($P < 0.0398$; Supplementary Fig. 8B). Collectively, the findings from clinical samples support a role of CARM1 in regulating ERα-dependent differentiation in ERα-positive tumors.

Discussion

In most cases, proliferation and differentiation are inversely coupled: repression of proliferation is a prerequisite for initiation of differentiation (11). In many cell types, however, cell-cycle arrest is necessary but not sufficient for differentiation. CARM1 seems to be a unique ER coactivator regulating both processes. Overexpression of CARM1 in MCF7 cells results in inhibition of E2-dependent growth through inhibition of the G_0/G_1 transition to S phase. This is in part due to upregulation of key negative cell-cycle regulators such as $p21^{cip1}$, $p27^{kip1}$, and cyclin G2. Inhibition of E2-dependent cell growth by CARM1 is accompanied by morphologic changes characteristic of a more differentiated phenotype and induction of multiple differentiation markers such as GATA-3 and MAZ. This finding is supported by previous reports that CARM1 can promote cell differentiation in other systems (19–21). Nonetheless, regulation of cell differentiation by CARM1 seems to be cell-type and context dependent. In mouse embryo and embryonic stem cells, CARM1 was shown to elevate expression of key pluripotency genes and delay their response to differentiation signals (38).

In contrast to growth inhibition by CARM1 overexpression, knocking down CARM1 in MCF7 did not alter E2-dependent cell growth in cell culture, nor did it affect E2-induced S-phase entry. This observation contradicts the conclusion by Frietze and colleagues that CARM1 increases growth of MCF7 cells. The discrepancies may be due to the transient transfection of CARM1 siRNA throughout the cell-cycle study by Frietze and colleagues (16). Moreover, the authors measured the percentage of cells in $S + G_2 + M$ phase without distinguishing the percentage of cells in S phase. Also, in consistent with the observation of O'Brien and colleagues (21), we did not observe change of E2F1 with CARM1 knockdown in contrast to Frietze and colleagues (16). Interestingly, and in contrast to cells grown in culture, knocking down CARM1 enhanced E2-induced xenograft tumors. This may be due to increased breast cancer cell interaction with the microenvironment which plays essential roles in promoting tumor growth in animals.

The growth inhibitory effect of CARM1 is unique from that of SRCs. Knocking down SRC2 and SRC3 but not SRC1 inhibits growth of MCF7 cells and decreases cyclin D1 expression (39). Overexpression of SRC3 also increases breast cancer cell proliferation and invasiveness. Similarly, SRC-1 promotes breast tumor metastasis and inhibits tumor cell differentiation (40). Thus, the ERα-dependent, growth inhibitory effect of CARM1 is unlikely to be mediated through SRC1, 2, and 3.

Cell-cycle genes that are regulated by E2 or loss of CARM1 include cyclin D1, c-Myc, cyclin G2, cyclin L1, cyclin T2, $p21^{cip1}$, $p27^{kip1}$, p130, and Rb (Supplementary Table S1). E2 treatment alone significantly represses cyclin G2 (33), which is reversed by overexpressing CARM1. Cyclin D1 is a well-known, E2-induced ERα target gene; however, its expression is not affected by overexpression of CARM1 in the presence of E2, yet knocking down CARM1 upregulates cyclin D1 in MCF7 cells (Supplementary Table S1). c-Myc is upregulated by E2 alone or loss of CARM1 (Supplementary Table S1) but is not affected by depletion of any of the p160 coactivators in MCF7 cells (39). Thus, the mechanism of CARM1 regulation of cell-cycle regulators is complex and only partially depends on the p160 coactivators.

Microarray gene expression analyses reveal that approximately 16% of E2-activated genes were repressed by CARM1, consistent with the repressive effects of CARM1 on some ER target genes (41). The mechanism of CARM1-mediated repression is unclear. The major effect of CARM1 overexpression was

to relieve E2-repressed genes. CARM1 methyltransferase activity may be responsible for the activation because we observed increased H3R17Me2 mark on $p21^{cip1}$ promoter upon CARM1 induction in MCF7-Tet-on-CARM1 (data not shown), consistent with a recent publication that CARM1 is recruited to $p21^{cip1}$ promoter (42). Whether CARM1 regulates ERα target genes via an epigenetic mechanism remains to be determined. Nonetheless, global ERα transcriptional regulation by CARM1 leads to the induction of many E2-repressed genes associated with differentiation.

Consistent with this finding, knocking down CARM1 shares more than 65% of the E2 gene signature. Most CARM1- and E2-regulated genes are involved in gene expression, metabolism, cell cycle, and differentiation. Knocking down CARM1 leads to upregulation of positive cell-cycle regulators (e.g., c-Myc) and downregulation of negative cell-cycle regulators (e.g., cyclin G2). This result suggests that loss of CARM1 function may lead to the acquisition of a proliferative phenotype resembling estrogen stimulation of breast cancer. Furthermore, knocking down CARM1 also modulates genes involved in cell differentiation. For example, combination of CARM1 shRNA and E2 treatment significantly reduced the level of PPARγ, which induces terminal differentiation of breast cancer (43). Loss of CARM1 also significantly decreases *KRTAP10.12*, an E2-repressed gene involved in keratin filament formation and potentially in cell differentiation processes (44, 45). Collectively, either loss of CARM1 or E2 treatment significantly inhibits expression of various differentiation markers (Supplementary Table S1). Overall, the gene expression data from CARM1 gain-of-function and loss-of-function models suggest that CARM1 plays an important role in regulating ERα target genes in differentiation and proliferation.

Evidence for a functional interplay of ERα and CARM1 was explored in human breast cancer specimens. A direct correlation was observed between CARM1 and ERα in ER-positive tumors. Higher ERα expression is associated with less aggressive and more differentiated tumors, and ER status is known to inversely correlate with histologic grade (46). Our observation contradicts an earlier report that CARM1 is overexpressed in grade III breast tumors (23). The difference could result from analysis of RNA versus protein and the sample size. In the study by El Messaoudi and colleagues, CARM1 was analyzed only at the RNA level in 81 human breast tumors whereas we analyzed CARM1 protein level in more than 300 human breast tumors.

Histologic grade using the Nottingham method integrates scores from glandular differentiation, nuclear morphology, and mitotic counts (47, 48), and higher grade is significantly associated with poor outcome and survival. The inverse correlation of CARM1 expression and tumor grade found in ER-positive breast cancer cases, together with enhanced tumor volume in CARM1 knockdown breast cancer xenografts in animal models, supports an association of low levels of CARM1 with less well-differentiated, high-grade breast cancers and is consistent with the hypothesis that CARM1 inhibits breast cancer progression in ERα-positive tumors. Our results suggest that coexpression of ERα and CARM1 together may serve as a better biomarker of well-differentiated breast cancers.

ERα is believed to regulate growth and differentiation through balanced interaction with cofactors. This study reports an unexpected biological function of the ER coactivator CARM1 in breast cancer. The hallmark of CARM1 action might be due to global modulation of E2-regulated genes, leading to reprogramming of cell proliferation and differentiation. To our knowledge, CARM1 is the only ER coactivator that is able to simultaneously block cell proliferation and induce differentiation. Since CARM1 has histone modification activity, inducing differentiation of breast cancer cells by upregulating CARM1 activity may be therapeutically effective in breast cancer.

Disclosure of Potential Conflicts of Interest

No potential conflicts of interest were disclosed.

Acknowledgments

We thank Elaine Alarid for providing MCF7-Tet-on cells. We thank Sanghyuk Chung, Amy Cole, Ruth Sullivan, and Yunhong Zan for the technical help, and Sujun Hua (University of Chicago) and flow cytometry and histology lab facility for assistance. We also thank Lin-Feng Chen for comments and Erin Shanle for editing. We acknowledge the strong support of the Cancer Care Manitoba Foundation (CCMF) for facilities at MICB.

Grant Support

This work is supported by NCI grant CA125387 and Shaw Scientist Award from Greater Milwaukee Foundation to W. Xu and in part by grants to LCM from the Canadian Institutes of Health Research (CIHR) and the Canadian Breast Cancer Research Alliance (CBCRA). K. Higashimato is supported by Uehara Memorial Foundation.

Received July 2, 2010; revised December 20, 2010; accepted January 18, 2011; published OnlineFirst January 31, 2011.

References

1. Ikeda K, Inoue S. Estrogen receptors and their downstream targets in cancer. Arch Histol Cytol 2004;67:435–42.
2. Foster JS, Henley DC, Bukovsky A, Seth P, Wimalasena J. Multifaceted regulation of cell cycle progression by estrogen: regulation of Cdk inhibitors and Cdc25A independent of cyclin D1-Cdk4 function. Mol Cell Biol 2001;21:794–810.
3. Doisneau-Sixou SF, Sergio CM, Carroll JS, Hui R, Musgrove EA, Sutherland RL. Estrogen and antiestrogen regulation of cell cycle progression in breast cancer cells. Endocr Relat Cancer 2003;10:179–86.
4. Creighton CJ, Cordero KE, Larios JM, Miller RS, Johnson MD, Chinnaiyan AM, et al. Genes regulated by estrogen in breast tumor cells *in vitro* are similarly regulated *in vivo* in tumor xenografts and human breast tumors. Genome Biol 2006;7:R28.
5. Frasor J, Danes JM, Komm B, Chang KC, Lyttle CR, Katzenellenbogen BS. Profiling of estrogen up- and down-regulated gene expression in human breast cancer cells: insights into gene networks and pathways underlying estrogenic control of proliferation and cell phenotype. Endocrinology 2003;144:4562–74.
6. Vendrell JA, Magnino F, Danis E, Duchesne MJ, Pinloche S, Pons M, et al. Estrogen regulation in human breast cancer cells of new downstream gene targets involved in estrogen metabolism, cell proliferation and cell transformation. J Mol Endocrinol 2004;32:397–414.

Published OnlineFirst January 31, 2011; DOI:10.1158/0008-5472.CAN-10-2426

7. McGuire WL, Chamness GC, Fuqua SA. Estrogen receptor variants in clinical breast cancer. Mol Endocrinol 1991;5:1571–7.
8. Badve S, Nakshatri H. Oestrogen-receptor-positive breast cancer: towards bridging histopathological and molecular classifications. J Clin Pathol 2009;62:6–12.
9. Clark GM, Osborne CK, McGuire WL. Correlations between estrogen receptor, progesterone receptor, and patient characteristics in human breast cancer. J Clin Oncol 1984;2:1102–9.
10. Osborne CK, Yochmowitz MG, Knight WA III, McGuire WL. The value of estrogen and progesterone receptors in the treatment of breast cancer. Cancer 1980;46:2884–8.
11. Stein JL, van Wijnen AJ, Lian JB, Stein GS. Control of cell cycle regulated histone genes during proliferation and differentiation. Int J Obes Relat Metab Disord 1996;20 Suppl 3:S84–90.
12. Xu W. Nuclear receptor coactivators: the key to unlock chromatin. Biochem Cell Biol 2005;83:418–28.
13. Chen D, Ma H, Hong H, Koh SS, Huang SM, Schurter BT, et al. Regulation of transcription by a protein methyltransferase. Science 1999;284:2174–7.
14. Bauer UM, Daujat S, Nielsen SJ, Nightingale K, Kouzarides T. Methylation at arginine 17 of histone H3 is linked to gene activation. EMBO Rep 2002;3:39–44.
15. Yadav N, Lee J, Kim J, Shen J, Hu MC, Aldaz CM, et al. Specific protein methylation defects and gene expression perturbations in coactivator-associated arginine methyltransferase 1-deficient mice. Proc Natl Acad Sci U S A 2003;100:6464–8.
16. Frietze S, Lupien M, Silver PA, Brown M. CARM1 regulates estrogen-stimulated breast cancer growth through up-regulation of E2F1. Cancer Res 2008;68:301–6.
17. Cheng D, Cote J, Shaaban S, Bedford MT. The arginine methyltransferase CARM1 regulates the coupling of transcription and mRNA processing. Mol Cell 2007;25:71–83.
18. Feng Q, Yi P, Wong J, O'Malley BW. Signaling within a coactivator complex: methylation of SRC-3/AIB1 is a molecular switch for complex disassembly. Mol Cell Biol 2006;26:7846–57.
19. Yadav N, Cheng D, Richard S, Morel M, Iyer VR, Aldaz CM, et al. CARM1 promotes adipocyte differentiation by coactivating PPARgamma. EMBO Rep 2008;9:193–8.
20. Chen SL, Loffler KA, Chen D, Stallcup MR, Muscat GE. The coactivator-associated arginine methyltransferase is necessary for muscle differentiation: CARM1 coactivates myocyte enhancer factor-2. J Biol Chem 2002;277:4324–33.
21. O'Brien KB, Alberich-Jorda M, Yadav N, Kocher O, Diruscio A, Ebralidze A, et al. CARM1 is required for proper control of proliferation and differentiation of pulmonary epithelial cells. Development 2010;137:2147–56.
22. Kim J, Lee J, Yadav N, Wu Q, Carter C, Richard S, et al. Loss of CARM1 results in hypomethylation of thymocyte cyclic AMP-regulated phosphoprotein and deregulated early T cell development. J Biol Chem 2004;279:25339–44.
23. El Messaoudi S, Fabbrizio E, Rodriguez C, Chuchana P, Fauquier L, Cheng D, et al. Coactivator-associated arginine methyltransferase 1 (CARM1) is a positive regulator of the Cyclin E1 gene. Proc Natl Acad Sci U S A 2006;103:13351–6.
24. Wiznerowicz M, Trono D. Conditional suppression of cellular genes: lentivirus vector-mediated drug-inducible RNA interference. J Virol 2003;77:8957–61.
25. Xu W, Cho H, Kadam S, Banayo EM, Anderson S, Yates JR III, et al. A methylation-mediator complex in hormone signaling. Genes Dev 2004;18:144–56.
26. Snell L, Watson PH. Breast tissue banking: collection, handling, storage, and release of tissue for breast cancer research. Methods Mol Med 2006;120:3–24.
27. Skliris GP, Leygue E, Curtis-Snell L, Watson PH, Murphy LC. Expression of oestrogen receptor-beta in oestrogen receptor-alpha negative human breast tumours. Br J Cancer 2006;95:616–26.
28. de Jong JS, van Diest PJ, Michalides RJ, Baak JP. Concerted overexpression of the genes encoding p21 and cyclin D1 is associated with growth inhibition and differentiation in various carcinomas. Mol Pathol 1999;52:78–83.
29. Wainwright LJ, Lasorella A, Iavarone A. Distinct mechanisms of cell cycle arrest control the decision between differentiation and senescence in human neuroblastoma cells. Proc Natl Acad Sci U S A 2001;98:9396–400.
30. Pang H, Rowan BG, Al-Dhaheri M, Faber LE. Epidermal growth factor suppresses induction by progestin of the adhesion protein desmoplakin in T47D breast cancer cells. Breast Cancer Res 2004;6:R239–45.
31. Sommers CL, Byers SW, Thompson EW, Torri JA, Gelmann EP. Differentiation state and invasiveness of human breast cancer cell lines. Breast Cancer Res Treat 1994;31:325–35.
32. Skildum AJ, Mukherjee S, Conrad SE. The cyclin-dependent kinase inhibitor p21WAF1/Cip1 is an antiestrogen-regulated inhibitor of Cdk4 in human breast cancer cells. J Biol Chem 2002;277:5145–52.
33. Stossi F, Likhite VS, Katzenellenbogen JA, Katzenellenbogen BS. Estrogen-occupied estrogen receptor represses cyclin G2 gene expression and recruits a repressor complex at the cyclin G2 promoter. J Biol Chem 2006;281:16272–8.
34. Kouros-Mehr H, Bechis SK, Slorach EM, Littlepage LE, Egeblad M, Ewald AJ, et al. GATA-3 links tumor differentiation and dissemination in a luminal breast cancer model. Cancer Cell 2008;13:141–52.
35. Zaytseva YY, Wang X, Southard RC, Wallis NK, Kilgore MW. Down-regulation of PPARgamma1 suppresses cell growth and induces apoptosis in MCF-7 breast cancer cells. Mol Cancer 2008;7:90.
36. Deblois G, Hall JA, Perry MC, Laganière J, Ghahremani M, Park M, et al. Genome-wide identification of direct target genes implicates estrogen-related receptor alpha as a determinant of breast cancer heterogeneity. Cancer Res 2009;69:6149–57.
37. Watson PH, Snell L, Parisien M. The NCIC-Manitoba Breast Tumor Bank: a resource for applied cancer research. Can Med Assoc J 1996;155:281–3.
38. Wu Q, Bruce AW, Jedrusik A, Ellis PD, Andrews RM, Langford CF, et al. CARM1 is required in ES cells to maintain pluripotency and resist differentiation. Stem Cells 2009;27:2637–45.
39. Karmakar S, Foster EA, Smith CL. Unique roles of p160 coactivators for regulation of breast cancer cell proliferation and estrogen receptor-alpha transcriptional activity. Endocrinology 2009;150:1588–96.
40. Wang S, Yuan Y, Liao L, Kuang SQ, Tien JC, O'Malley BW, et al. Disruption of the SRC-1 gene in mice suppresses breast cancer metastasis without affecting primary tumor formation. Proc Natl Acad Sci U S A 2009;106:151–6.
41. Lupien M, Eeckhoute J, Meyer CA, Krum SA, Rhodes DR, Liu XS, et al. Coactivator function defines the active estrogen receptor alpha cistrome. Mol Cell Biol 2009;29:3413–23.
42. Kim YR, Lee BK, Park RY, Nguyen NT, Bae JA, Kwon DD, et al. Differential CARM1 expression in prostate and colorectal cancers. BMC Cancer 2010;10:197.
43. Mueller E, Sarraf P, Tontonoz P, Evans RM, Martin KJ, Zhang M, et al. Terminal differentiation of human breast cancer through PPAR gamma. Mol Cell 1998;1:465–70.
44. Kuhn F, Lassing C, Range A, Mueller M, Hunziker T, Ziemiecki A, et al. Pmg-1 and pmg-2 constitute a novel family of KAP genes differentially expressed during skin and mammary gland development. Mech Dev 1999;86:193–6.
45. Eckert RL, Crish JF, Robinson NA. The epidermal keratinocyte as a model for the study of gene regulation and cell differentiation. Physiol Rev 1997;77:397–424.
46. Parl FF, Schmidt BP, Dupont WD, Wagner RK. Prognostic significance of estrogen receptor status in breast cancer in relation to tumor stage, axillary node metastasis, and histopathologic grading. Cancer 1984;54:2237–42.
47. Elston CW, Ellis IO. Pathological prognostic factors in breast cancer. I. The value of histological grade in breast cancer: experience from a large study with long-term follow-up.Histopathology 1991;19:403–10.
48. Page DL, Gray R, Allred DC, Dressler LG, Hatfield AK, Martino S, et al. Prediction of node-negative breast cancer outcome by histologic grading and S-phase analysis by flow cytometry: an Eastern Cooperative Oncology Group Study (2192). Am J Clin Oncol 2001;24:10–8.

Biochemical Pharmacology 82 (2011) 1940–1949

Contents lists available at SciVerse ScienceDirect

Biochemical Pharmacology

journal homepage: www.elsevier.com/locate/biochempharm

Generation of stable reporter breast cancer cell lines for the identification of ER subtype selective ligands

Erin K. Shanle [a,b], John R. Hawse [c], Wei Xu [a,b,*]

[a] McArdle Laboratory for Cancer Research, University of Wisconsin, Madison, WI, USA
[b] Molecular and Environmental Toxicology Center, University of Wisconsin, Madison, WI, USA
[c] Department of Biochemistry and Molecular Biology, Mayo Clinic, Rochester, MN, USA

ARTICLE INFO

Article history:
Received 22 June 2011
Accepted 29 August 2011
Available online 6 September 2011

Keywords:
Estrogen receptors
Subtype selectivity
Phytoestrogens
Breast cancer

ABSTRACT

Estrogen signaling is mediated by two estrogen receptors (ERs), ERα and ERβ, which have unique roles in the regulation of breast cancer cell proliferation. ERα induces proliferation in response to estrogen and ERβ inhibits proliferation in breast cancer cells, suggesting that ERβ selective ligands may be beneficial for promoting the anti-proliferative action of ERβ. Subtype selective ligands can be identified using transcriptional assays, but cell lines in which ERα or ERβ are independently expressed are required. Of the available reporter cell lines, none have been generated in breast cancer cells to identify subtype selective ligands. Here we describe the generation of two isogenic breast cancer cell lines, Hs578T-ERαLuc and Hs578T-ERβLuc, with stable integration of an estrogen responsive luciferase reporter gene. Hs578T-ERαLuc and Hs578T-ERβLuc cell lines are highly sensitive to estrogenic chemicals and ER subtype selective ligands, providing a tool to characterize the transcriptional potency and subtype selectivity of estrogenic ligands in the context of breast cancer cells. In addition to measuring reporter activity, ERβ target gene expression and growth inhibitory effects of ERβ selective ligands can be determined as biological endpoints. The finding that activation of ERβ by estrogen or ERβ selective natural phytoestrogens inhibits the growth of Hs578T-ERβ cells implies therapeutic potential for ERβ selective ligands in breast cancer cells that express ERβ.

1. Introduction

Estrogens regulate mammary gland growth and differentiation, ovary and uterus maturation, and bone homeostasis [1]. The physiological effects of estrogens are primarily mediated by two estrogen receptors (ERs), ERα and ERβ. Because of the broad range of ER target tissues and the ligand dependent activity of the receptors, synthetic and natural estrogens hold therapeutic promise in selectively targeting ERs. Therapies aimed at preventing ERα transcriptional activation are currently used for breast cancer treatment and osteoporosis prevention [2]. Though ERβ is not currently a therapeutic target, accumulating evidence suggests an anti-proliferative role for ERβ in breast cancer [3]. In the mammary gland, ERα and ERβ play opposing roles in regulating growth and differentiation in response to estrogens; ERα promotes proliferation while ERβ inhibits ERα-mediated proliferation [4–6]. Because the anti-proliferative action of ERβ may be enhanced by ligand-dependent activation, the paradigm of ER targeted therapies is expanding towards the development of ER subtype selective ligands [7].

Though ERα and ERβ share many structural and transcriptional features, ligands can display subtype selectivity. In classical ligand dependent transcriptional activation, the receptors dimerize upon ligand binding and undergo conformational changes to allow cofactor recruitment. The receptors directly bind DNA most often at estrogen response elements (EREs), consisting of a consensus GGTCAnnnTGACC sequence. ERα and ERβ have 97% identity within the DNA binding domains, and the receptors bind similar DNA sequences with high affinity. Genome wide binding studies in MCF7 breast cancer cells expressing ERα or ERβ independently have shown that ERα and ERβ bind similar sites in response to 17β-estradiol (E2); ~60% of ER binding sites contain full EREs and ~25% contain half EREs [8].

The ligand binding pockets of ERα and ERβ are relatively large, and the receptors bind a wide array of chemicals. The ligand binding domains of ERα and ERβ have 59% identity, and the receptors bind E2 with similar affinities. Despite similarities

Abbreviations: BRET, bioluminescence resonance energy transfer; Cos, cosmosiin; Dox, doxycycline; DPN, diarylpropionitrile; E2, 17β-estradiol; ER, estrogen receptor; PPT, propyl pyrazole triol; ERE, estrogen response element; ICI, ICI 182,780; Liq, liquiritigenin.

* Corresponding author at: McArdle Laboratory for Cancer Research, 1400 University Ave, Madison, WI 53706, USA. Tel.: +1 608 265 5540; fax: +1 608 262 2824.
E-mail address: wxu@oncology.wisc.edu (W. Xu).

0006-2952/$ – see front matter © 2011 Elsevier Inc. All rights reserved.
doi:10.1016/j.bcp.2011.08.026

in their ligand binding domains, several ligands have modest selectivity for ERα or ERβ [9], and some synthetic ligands maintain high selectivity. For example, propyl pyrazole triol (PPT) is an ERα selective agonist that displays a 400-fold higher binding affinity for ERα compared to ERβ [10]. Estrogenic chemicals produced in plants, known as phytoestrogens, often display subtype selectivity for ERβ. For example, liquiritigenin is a flavanone derived from *Glycyrrhizae uralensis* that has been shown to have 20-fold higher binding affinity for ERβ and even greater selectivity in transcriptional assays [11]. Compounds such as liquiritigenin often show low binding affinities relative to E2, and ERβ selective ligands with higher affinity and greater selectivity are needed to fully elucidate the anti-proliferative role of ERβ in breast cancer.

Mammalian cell lines have been developed to enable screening for subtype selective ligands. HeLa cervical carcinoma cells have been used to create HELN-ERα and HELN-ERβ, two cell lines in which ERα or ERβ, respectively, are constitutively expressed with stable integration of a luciferase reporter downstream of an ERE [12]. Human embryonic kidney cells, HEK293, have also been created using a similar strategy in which ERα or ERβ are constitutively expressed and human placental alkaline phosphatase downstream of the vitellogenin ERE is stably integrated [13]. The only available breast cancer reporter cell line is T47D-KBLuc in which three tandem EREs upstream of a luciferase reporter have been stably integrated [14]. However, identification of subtype selective ligands is prohibited because T47D cells express both ERα and ERβ.

Here, we describe the generation of two isogenic reporter cell lines, Hs578T-ERαLuc and Hs578T-ERβLuc, that provide a tool to characterize the transcriptional potencies and subtype selectivity of estrogenic compounds in the context of breast cancer cells. These cell lines are highly sensitive to estrogenic ligands and can be used to validate ER transcriptional activation by analysis of endpoints such as endogenous target gene regulation. Further, ERβ selective ligands induce ERβ-mediated reporter gene expression, endogenous gene regulation, and growth inhibition, suggesting that Hs578T-ERβLuc cells may be used to isolate ERβ selective ligands with desired biological effects.

2. Materials and methods

2.1. Cell lines and reagents

Cosmosiin (apigenin 7-glucoside), dimethyl sulfoxide (DMSO), E2, and diethylstilbestrol (DES) were obtained from Sigma (St. Louis, MO); DPN, PPT, and ICI 182,780 were obtained from Tocris (Ellinsville, MO); liquiritigenin was obtained from Chromadex (Irvine, CA). Doxycycline (Dox) was obtained from Clontech. Hygromycin B, blasticidin S, zeocin, NaCl, sodium dodecyl sulfate (SDS), and dithiothreitol (DTT) were obtained from Research Products International (Mount Prospect, IL). Triton X-100 was obtained from Fisher (Fair Lawn, NJ); protease inhibitors were obtained from Roche Scientific (Basel, Switzerland); benzonase was obtained from Novagen (San Diego, CA). All other chemicals were obtained from Sigma (St. Louis, MO).

Cell culture media were obtained from Invitrogen (Carlsbad, CA). MCF7 and HEK293 cells were cultured in DMEM + 10% fetal bovine serum (FBS; Gemini Bio Products, West Sacramento, CA) at 37 °C and 5% CO_2. Hs578T-ERα and Hs578T-ERβ were previously created by Secreto and coworkers [15]. These cells were cultured at 37 °C and 5% CO_2 in DMEM/F12 supplemented with L-glutamine, 10% Tet-system approved FBS (Clontech Mountain View, CA), 500 mg/L zeocin and 5 mg/L blasticidin S.

2.2. Generation of Hs578T-ERαLuc and Hs578T-ERβLuc reporter cell lines

Stable reporter cell lines were created using a modified pGL4.32 reporter (Promega, Madison, WI) which contains the *luc2P* reporter and hygromycin resistance. The pGL4.32 vector was digested with *Nhe*I and *Hind*III (New England Biolabs, Ipswich, MA) and three consensus EREs spaced by three nucleotides were cloned upstream of *luc2P* using the following oligonucleotides: 5′-CTA GCG GTC ACA GTG ACC TGC GAG GTC ACA GTG ACC TGC GAG GTC ACA GTG ACC TGC GA-3′ and 5′-AGC TTC GCA GGT CAC TGT GAC CTC GCA GGT CAC TGT GAC CTC GCA GGT CAC TGT GAC CG-3′. Successful cloning was verified by complete sequencing and the vector was designated pGL4.3xERE. Estrogen responsiveness was validated by batch transfecting HEK293 cells with 2 ng of CMX-ERα or CMX-ERβ, 45 ng pGL4.3xERE vector, and 40 ng CMX-β-galactosidase per well of a 48 well plate. Cells were incubated 24 hr to allow protein expression before the addition of the indicated ligands. After 24 hr of ligand treatment, cells were lysed, firefly luciferase substrate (Promega) was added, and luminescence was measured on a Victor X5 microplate reader (Perkin Elmer, Waltham, MA) using luminescence detection and a 700 nm filter. To normalize data for transfection efficiency, β-galactosidase expression was analyzed using the Tropix β-galactosidase detection kit (Applied Biosystems, Foster City, CA). Luciferase counts were normalized to β-gal counts in each well.

After characterizing the pGL4.3xERE stable reporter vector, Hs578T-ERα and Hs578T-ERβ cells were transfected with 10 μg of the vector and selected in 125 μg/mL hygromycin B for 4 weeks. Individual colonies were selected using 3 mm cloning discs, expanded, and screened for estrogen induced luciferase expression. One clone from each cell line was selected for further characterization, referred to here as Hs578T-ERαLuc and Hs578T-ERβLuc.

2.3. Quantitative western blots and ligand binding assays

For quantitative western blots, cells were split in phenol red free DMEM/F12 + 5% SFS and treated with 50 ng/mL Dox or vehicle (water) 24 hr later. After 48 hr treatment, cells were collected by trypsinization, washed with Dulbecco's phosphate buffer saline (Invitrogen), and lysed by suspension in lysis buffer (50 mM Tris pH 8.0, 400 mM NaCl, 10% glycerol, 0.5% triton X-100, protease inhibitors, and benzonase). After centrifugation, total protein was quantified using BioRad Protein Assay (BioRad), and 40 μg of protein was resolved using SDS–PAGE and 8% polyacrylamide gels. Proteins were transferred to a nitrocellulose membrane for 1.5 hr at 0.35 A. Membranes were blocked with 5% nonfat milk and incubated overnight with 1:1000 anti-FLAG-M2 antibody (Sigma) or 1:5000 anti-β-Actin (Sigma) at 4 °C. Membranes were then incubated with IRDye 800CW goat-anti-mouse IgG secondary antibody (Licor Biosciences, Lincoln, NE) for 1 hr at room temperature and visualized on a Licor Odyssey near-infrared gel reader (Licor Biosciences).

For ligand binding assays, Hs578T-ERαLuc and Hs578T-ERβLuc cells were cultured in phenol red free DMEM/F12 + 10% 6× charcoal stripped FBS (SFS) for 3 days prior to the assay to remove residual estrogens from the cells. At 90% confluence, cells were collected, resuspended in phenol red free DMEM/F12 + 5% SFS, and plated at a density of 10^5 cells/well on a 24 well plate in the presence or absence of 50 ng/mL Dox. After 24 hr, cells were labeled in triplicate with 20 nM [^{3}H]-E2 (89.2 Ci/mmol specific activity, Perkin Elmer) in the presence or absence of 450 μM DES cold competitor for 2 hr at 37 °C and 5% CO_2. Labeled cells were washed 3 times with cold PBS + 0.1% BSA and lysed with 500 μL SDS lysis buffer (0.5% SDS, 0.05 M Tris–HCl pH 8.0, and 1 mM DTT). Total cell lysate (400 μL) was mixed with 5 mL liquid scintillation

cocktail and [^{3}H] bound radioactivity was liquid scintillation counted for 5 min. Two additional wells of each condition were used to count the cell number and determine the total protein using RC DC protein assay (BioRad, Hercules, CA).

2.4. Luciferase assays

Hs578T-ERαLuc and Hs578T-ERβLuc cells were cultured in phenol red free DMEM/F12 + 10% SFS for 3 days prior to the assay to remove residual estrogens from the cells. Cells were seeded in triplicate at a density of 10^4 cells/well on white 96 well tissue culture plates (Fisher) in phenol red free DMEM/F12 + 5% SFS treated with 50 ng/mL Dox. After 24 hr of Dox treatment, media were replaced with treated media containing vehicle (0.15% DMSO) or a range of serially diluted ligands. All treatments were conducted in the presence and absence of 100 nM ICI 182,780. After treatment for 24 hr, cells were washed with PBS and lysed with 35 μL lysis buffer (100 mM K_2HPO_4, 0.2% Triton X-100, pH 7.8). Lysate (30 μL) was mixed 1:1 with luciferase substrate (Promega) and luminescence was measured on a Victor X5 microplate reader (Perkin Elmer, Waltham, MA) using luminescence detection and a 700 nm filter. Total protein (5 μL) was quantified using BioRad Protein Assay (BioRad). EC_{50} values were calculated using GraphPad Prism Software (Version 5.04, GraphPad Software Inc., San Diego, CA) and a three parameter log versus response nonlinear regression. Two tailed *t*-tests performed with GraphPad Prism Software were used to determine statistically significant differences from control treatments.

2.5. Gene expression analysis

For analysis of reporter induction by cosmosiin, Hs578T-ERαLuc and Hs578T-ERβLuc cells were split in phenol red free DMEM/F12 + 5% SFS and treated with 50 ng/mL Dox for 48 hr followed by treatment with DMSO (0.1%), 1 nM E2, or 1 μM cosmosiin for 4 or 24 hr. Total RNA was extracted using RNEasy Plus Kit according to manufacturer protocol (Qiagen, Valencia, CA). RNA (2 μg) was reverse transcribed using Superscript II RT according to manufacturer protocol (Invitrogen), and firefly luciferase (FLuc) expression was determined by reverse-transcription polymerase chain reaction using primers shown in Table 1.

For quantitative real-time PCR analysis of endogenous target gene expression, Hs578T-ERα and Hs578T-ERβ cells were cultured in phenol red free DMEM/F12 + 10% SFS for 3 days prior to the assay to remove residual estrogens from the cells. Cells were split in phenol red free DMEM/F12 + 5% SFS and treated with 50 ng/mL Dox for 48 hr prior to ligand treatment. Cells were treated with Dox and ligands or vehicle (0.1% DMSO) for 24 hr, and total RNA was extracted using RNEasy Plus Kit according to manufacturer protocol (Qiagen). RNA (2 μg) was reverse transcribed as above, and quantitative PCR was performed using TaqMan Prime Time custom designed assays (IDT, Coralville, IA), FastStart Universal Probe Master Mix (Roche Scientific), and a CFX96 instrument (BioRad). Primer and probe sequences are shown in Table 1. Data were analyzed using the ΔΔCq method calculated by the CFX Manager Software (BioRad). Two tailed *t*-tests performed with GraphPad Prism Software were used to determine statistically significant differences from control treatments using data from three biological replicates.

Table 1
Primer and probe sequences.

RPL13A	Primer 1	5′-TGT TTG ACG GCA TCC CAC-3′
	Primer 2	5′-CTG TCA CTG CCT GGT ACT TC-3′
	Probe	5′-CTT CAG ACG CAC GAC CTT GAG GG-3′
C3	Primer 1	5′-AAC TAC ATC ACA GAG CTG CG-3′
	Primer 2	5′-AAG TCC TCA ACG TTC CAC AG-3′
	Probe	5′-CGT TTC CCG AAG TGA GTT CCC AGA-3′
JAG1	Primer 1	5′-GGA CTA TGA GGG CAA GAA CTG-3′
	Primer 2	5′-AAA TAT ACC GCA CCC CTT CAG-3′
	Probe	5′-TCA CAC CTG AAA GAC CAC TGC CG-3′
ITGA6	Primer 1	5′-ACC CGA GAA GGA AAT CAA GAC-3′
	Primer 2	5′-CGC CAT CTT TTG TGG GAT TC-3′
	Probe	5′-TGG GTT GGA AGG GCT GTT TGT CA-3′
FLuc	Primer 1	5′-GGC TGA ATA CAA ACC ATC GG-3′
	Primer 2	5′-CTT TCT TGC TCA CGA ATA CGA-3′

2.6. Cell counting assays

Hs578T-ERα and Hs578T-ERβ cells were cultured in phenol red free DMEM/F12 + 10% SFS for 3 days prior to the assay to remove residual estrogens from the cells. Cells were seeded at a density of 15,000 cells/well in phenol red free DMEM/F12 + 5% SFS in triplicate in 6 well tissue culture dishes in the presence or absence of 50 ng/mL Dox. After 24 hr, the cells were treated with DMSO (0.1%) or compound in the presence or absence of 50 ng/mL Dox. Media were refreshed every 48 hr, and cells were counted after trypan blue exclusion using an automated cell counter (BioRad) according to manufacturer protocol.

3. Results

3.1. Generation of Hs578T-ERαLuc and Hs578T-ERβLuc reporter cell lines

In order to generate stable reporter breast cancer cell lines, we first cloned a construct encoding a selection marker and a luciferase reporter linked to EREs. The pGL4.32 vector (Promega) contains the *luc2P* gene and was modified to contain 3 tandem consensus EREs upstream of the minimal promoter (pGL4.3xERE, Fig. 1A). Upon complete sequencing, the estrogen responsiveness of the vector was validated in ER-negative HEK293 cells transfected with full length ERα (Fig. 1B) or ERβ (Fig. 1C). The pGL4.3xERE reporter showed extremely low background with a 65-fold induction in cells transfected with ERα. The ER antagonist ICI 182,780 abolished estrogen induced expression, reducing the luciferase signal to that of vehicle treated cells. Cells transfected with ERβ showed a 15-fold induction of luciferase upon E2 treatment; ICI 182,780 inhibited luciferase expression in both vehicle and estrogen treated cells. The minimal background luciferase expression and the selection marker conferred by the pGL4.3xERE vector made the vector suitable for creating stable reporter cells lines for the identification and characterization of ER selective agonists.

In order to create stable ER reporter breast cancer cell lines, an ER negative breast cancer cell line engineered to express either ERα or ERβ was necessary. Previously, Secreto and coworkers created such lines using Hs578T cells [15], a triple negative breast cancer cell line with a basal-like gene expression profile [16]. Hs578T cells lack expression of ERα and ERβ providing a clean background in which to express ERα or ERβ. Using the tetracycline inducible system, two cell lines were created in which ERα or ERβ are inducibly expressed (Hs578T-ERα and Hs578T-ERβ cells, respectively) [15]. Hs578T-ERα and Hs578T-ERβ cells were transfected with the pGL4.3xERE vector, and individual clones were isolated after hygromycin selection. Over 20 clones were screened for estrogen induced luciferase expression (data not shown). One clone from each cell line was selected for further characterization, referred to here as Hs578T-ERαLuc and Hs578T-ERβLuc. Additional ERα and ERβ reporter clones were used to verify reporter data obtained from Hs578T-ERαLuc and Hs578T-ERβLuc cells.

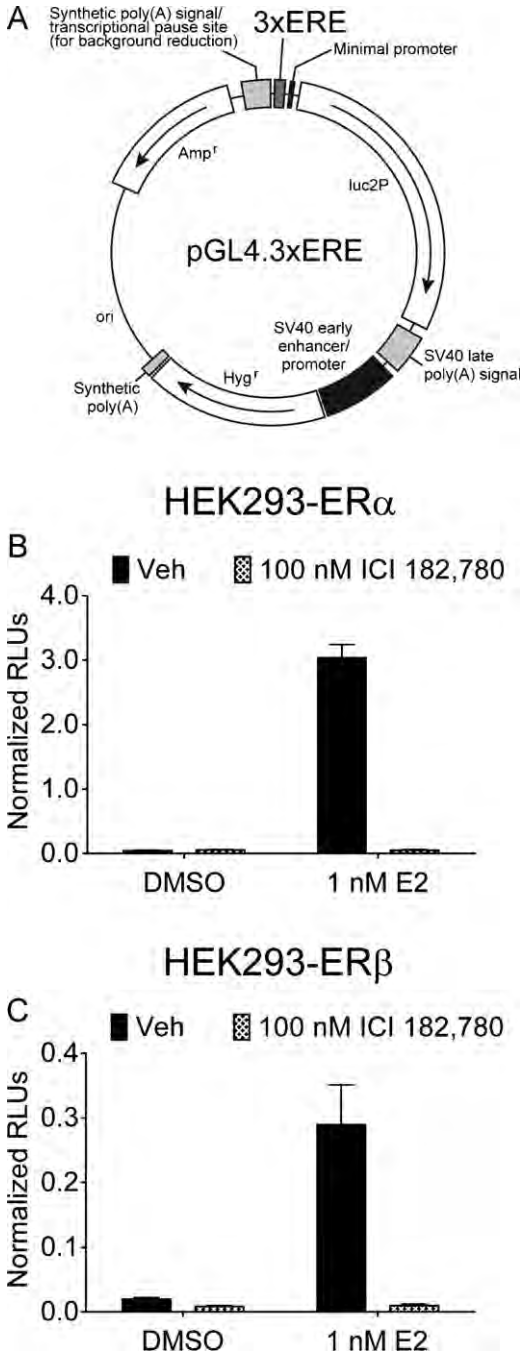

Fig. 1. The pGL4.3xERE reporter construct is estrogen responsive. (A) Three tandem EREs were inserted upstream of the *luc2P* gene in the pGL4.32 luciferase reporter construct. HEK293 cells were batch transfected with the pGL4.3xERE reporter construct, a β-galactosidase construct, and full length ERα (B) or ERβ (C). After allowing 24 hr for protein expression, cells were treated in triplicate with vehicle (DMSO) or 1 nM E2 and vehicle or 100 nM ICI 182,780 (0.15% final DMSO concentration) for an additional 24 hr. Raw luciferase units (RLUs) were normalized to β-galactosidase to normalize for transfection efficiency. Error bars represent standard deviations.

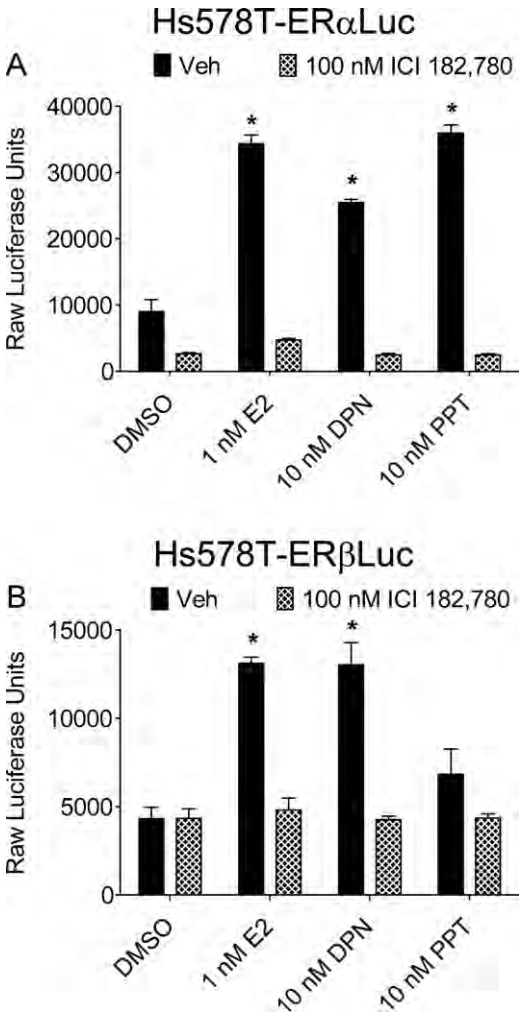

Fig. 2. ER subtype selective ligands selectively induce luciferase in Hs578T-ERαLuc and Hs578T-ERβLuc cells. Hs578T-ERαLuc (A) and Hs578T-ERβLuc (B) cells were seeded in triplicate on 96 well plates in the presence of 50 ng/mL Dox to induce ER expression. After 24 hr, cells were treated with vehicle (DMSO), 1 nM E2, 10 nM DPN, or 10 nM PPT in the presence or absence of 100 nM ICI 182,780 (0.15% final DMSO concentration). Cells were lysed 24 hr after ligand treatment and raw luciferase units were counted. Error bars represent standard deviations. $^{*}p$ values < 0.05.

Hs578T-ERαLuc and Hs578T-ERβLuc cells were first characterized by assessing luciferase induction by ER ligands in the presence or absence of the full antagonist ICI 182,780 (Fig. 2). Cells were treated with vehicle, 1 nM E2, 10 nM DPN (a reported ERβ selective agonist), or 10 nM PPT (a reported ERα selective agonist). PPT selectively activated luciferase expression in Hs578T-ERαLuc, but DPN activated the reporter in both Hs578T-ERαLuc and Hs578T-ERβLuc cells, though to a lesser extent in Hs578T-ERαLuc cells. Co-treatment with ICI 182,780 blocked luciferase induction in both cell lines (Fig. 2), and luciferase was not induced in the absence of Dox treatment (data not shown).

Basal and E2-induced luciferase signals were much higher in Hs578T-ERαLuc cells when compared to Hs578T-ERβLuc cells, a trend observed in all luciferase assays. On average, Hs578T-ERβLuc cells expressed 630 luciferase units per mg protein and Hs578T-ERαLuc expressed 2900 luciferase units per mg protein at saturating E2 concentrations (0.1 nM or greater). A range of luciferase signals was observed among the clones screened (data not shown), suggesting the accessibility of the reporter in the chromatin may be responsible for differences in luciferase expression. In order to verify Hs578T-ERαLuc and Hs578T-ERβLuc cells had similar ER expression levels at the Dox concentration used throughout the study (50 ng/mL), quantitative western blots were used to compare ER expression in the parent cell lines and reporter cell lines (Fig. 3A). Western blots with FLAG antibody demonstrated similar ER expression in Hs578T-ERαLuc and Hs578T-ERβLuc cells and also confirmed expression levels similar to the parent cell lines. In addition, whole cell ligand binding assays were used to quantify the active receptor in each cell line (Fig. 3B).

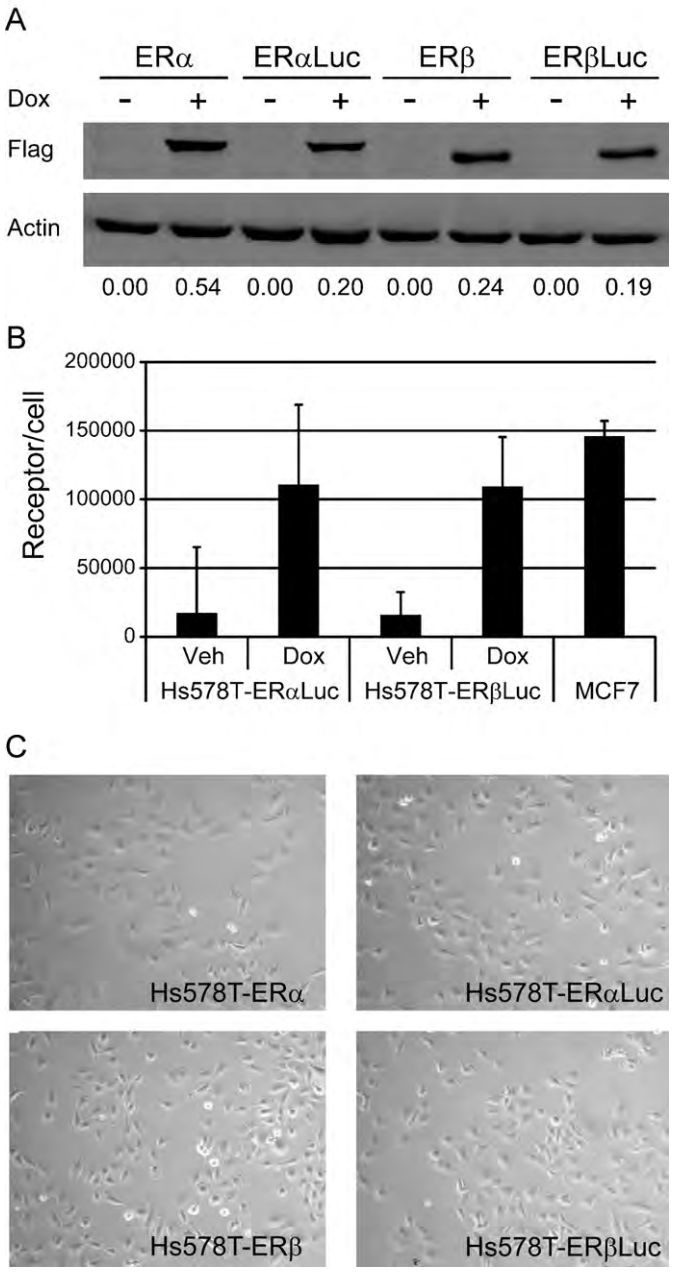

Fig. 3. Hs578T-ERαLuc and Hs578T-ERβLuc cells express similar levels of ER. (A) Quantitative western blot with Hs578T-ERα (ERα), Hs578T-ERαLuc (ERαLuc), Hs578T-ERβ (ERβ), and Hs578T-ERβLuc (ERβLuc) treated with vehicle (−Dox) or 50 ng/mL Dox (+Dox). ER expression was detected using FLAG antibody and quantified by normalizing to beta-actin using the Licor Odyssey near-infrared gel reader. The normalized integrated intensity for the FLAG signal is shown below the images. (B) Ligand binding assays confirmed the quantitative western blots. Hs578T-ERαLuc and Hs578T-ERβLuc cells were seeded in triplicate and treated with vehicle or 50 ng/mL Dox for 24 hr. Cells were labeled with 20 nM [^{3}H]-E2 in the presence or absence of cold competitor for 2 hr, washed, and total cell lysate was assessed for bound radioactivity as described in Section 2. MCF7 cells were included for comparison. Two additional wells of each cell line and condition were used to determine the cell number and the numbers of receptors per cell were calculated based on a 1:1 molar ratio of ligand to receptor. The average and standard deviation of three independent experiments are shown. (C) The morphology of Hs578T-ERαLuc and Hs578T-ERβLuc was similar to that of the parent Hs578T-ERα and Hs578T-ERβ cell lines. Representative phase-contrast microscopy images of each cell line (100× magnification).

ERα positive MCF7 breast cancer cells expressed ~150,000 receptors/cell which was very similar to reported values [17]. Both Hs578T-ERαLuc and Hs578T-ERβLuc cells expressed ~120,000 receptors/cell after 50 ng/mL Dox treatment. The comparable number of ERs per cell suggests that differences in ER expression do not account for the higher luciferase signal observed Hs578T-ERαLuc cells. Higher luciferase expression in Hs578T-ERαLuc cells may be due to the accessibility of the reporter in the chromatin or the enhanced transcriptional activity of ERα, in agreement with previous findings that the transcriptional activity of ERα is greater than that of ERβ on ERE-containing reporters [18]. Finally, the reporter cell lines did not have an altered morphological phenotype compared to the parent cell lines (Fig. 3C), and no other phenotypic changes due to the integration of the luciferase reporter were observed in Hs578T-ERαLuc and Hs578T-ERβLuc cells.

3.2. Ligand selectivity of Hs578T-ERαLuc and Hs578T-ERβLuc reporter cell lines

We next assessed ligand subtype selectivity using these isogenic reporter cell lines. All luciferase data were normalized to the luciferase signal induced by a saturating concentration of E2 (0.1 nM) and expressed as the percent transactivation relative to 0.1 nM E2. Dose–response curves were obtained for E2, DPN, and PPT to characterize the sensitivity of the reporter cells to ER ligands (Fig. 4). Cells were treated with 10-fold dilutions of ligands and approximate EC_{50} concentrations for each ligand were calculated from 3 independent experiments (Table 2). The ratios of EC_{50} values obtained from Hs578T-ERαLuc cells and Hs578T-ERβLuc cells are also presented in Table 2 and provide a measure of the selectivity of the ligands. Higher α/β ratios indicate selectivity for ERβ.

Both cell lines were highly sensitive to estrogen (Fig. 4A). Hs578T-ERαLuc cells showed EC_{50} values near 1 pM; four additional Hs578T-ERαLuc clones showed similar sensitivities (data not shown). Hs578T-ERβLuc cells also showed EC_{50} values for estrogen in the pM range, though the average EC_{50} was 6.5-fold higher than that of Hs578T-ERαLuc cells. Similar differences in estrogen sensitivities have been observed in other ERE-luciferase reporter cell lines expressing ERα or ERβ [12–14], suggesting the difference in E2 sensitivity between Hs578T-ERαLuc and Hs578T-ERβLuc cells is due to differences in the transactivation of ERα and ERβ.

Next, dose responses to two highly selective ERα and ERβ agonists, PPT and DPN respectively, were analyzed using Hs578T-ERαLuc and Hs578T-ERβLuc cells. PPT showed nearly 1000-fold selectivity for ERα (Fig. 4B). Surprisingly, PPT could activate reporter expression in Hs578T-ERβLuc cells at concentrations greater than 100 nM, although it could not induce luciferase expression to the same extent as E2. It has been reported that PPT was unable to induce an estrogen responsive reporter in HEC-1 cells transfected with ERβ [10] or in HELN-ERα cells [12]. DPN was not as selective as PPT and could maximally activate luciferase expression Hs578T-ERαLuc cells at 100 nM (Fig. 4C). DPN fully activated ERβ at 10 nM. Though DPN has been shown to have a 50 to 70-fold higher binding affinity for ERβ [12,19], comparison of EC_{50} values showed approximately 30-fold selectivity for ERβ in these reporter assays.

Next, the subtype selectivity of two natural phytoestrogens, liquiritigenin and cosmosiin, were analyzed using Hs578T-ERαLuc and Hs578T-ERβLuc cells (Fig. 5). Liquiritigenin is a phytoestrogen derived from *Glycyrrhizae uralensis* and is the most active estrogenic component of MF101, an herbal supplement with therapeutic potential [11]. In the initial characterization of liquiritigenin, Mersereau and coworkers found liquiritigenin showed minimal activation of ERα at concentrations up to 2.5 μM in transcriptional assays in U2OS, HeLa, or WAR5 prostate cancer cells transfected with ERα [11]. Binding assays demonstrated that liquiritigenin had a 20-fold higher affinity for ERβ and

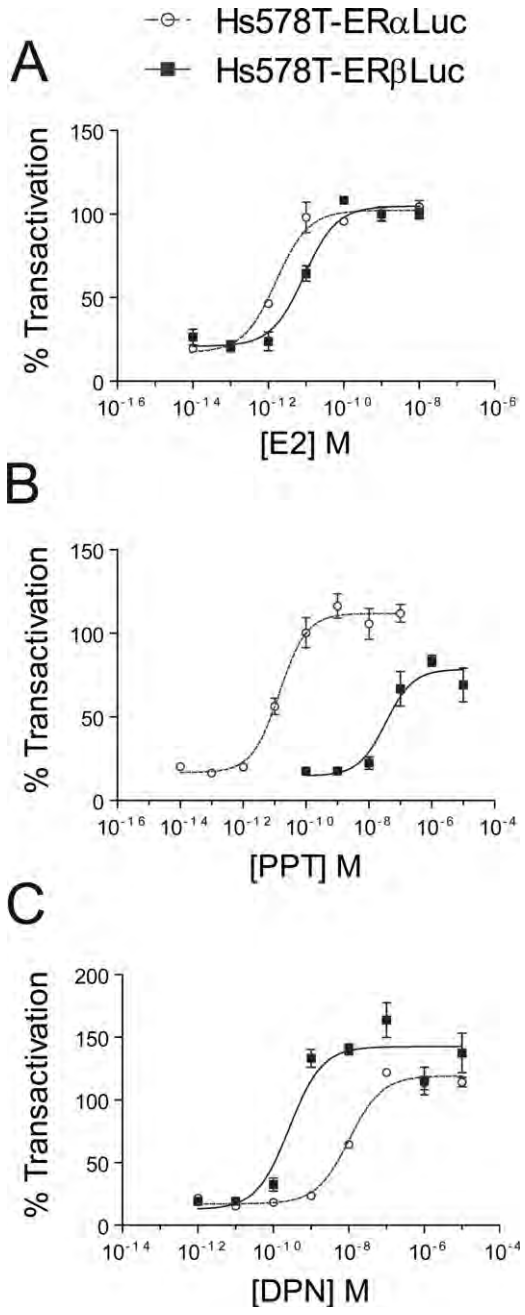

Fig. 4. Hs578T-ERαLuc and Hs578T-ERβLuc show subtype selective activation. Dose response curves of E2 (A), PPT (B), and DPN (C). Hs578T-ERαLuc and Hs578T-ERβLuc were seeded in triplicate and treated with 50 ng/mL Dox for 24 hr. Cells were then treated with a range of ligand concentrations (0.15% final DMSO concentration) for 24 hr. Each plate contained DMSO, 0.1 nM E2, and 100 nM ICI 182,780 for controls. Luciferase signal was normalized to total protein in each well and expressed as a percent transactivation relative to signal obtained from saturating E2 treatment (0.1 nM). Each dose response experiment was conducted at least 3 times; data shown are from one representative experiment. EC_{50} values are shown in Table 2.

Table 2
Average EC_{50} values for ER ligands ($M \times 10^{-9}$).

	Hs578T-ERαLuc	Hs578T-ERβLuc	α/β
E2	0.001 (0.0005)	0.0065 (0.008)	0.15
DPN	8.5 (3)	0.26 (0.02)	33
PPT	0.016 (0.001)	26 (21)	0.001
Liquiritigenin	100 (40)	28 (2)	3.6

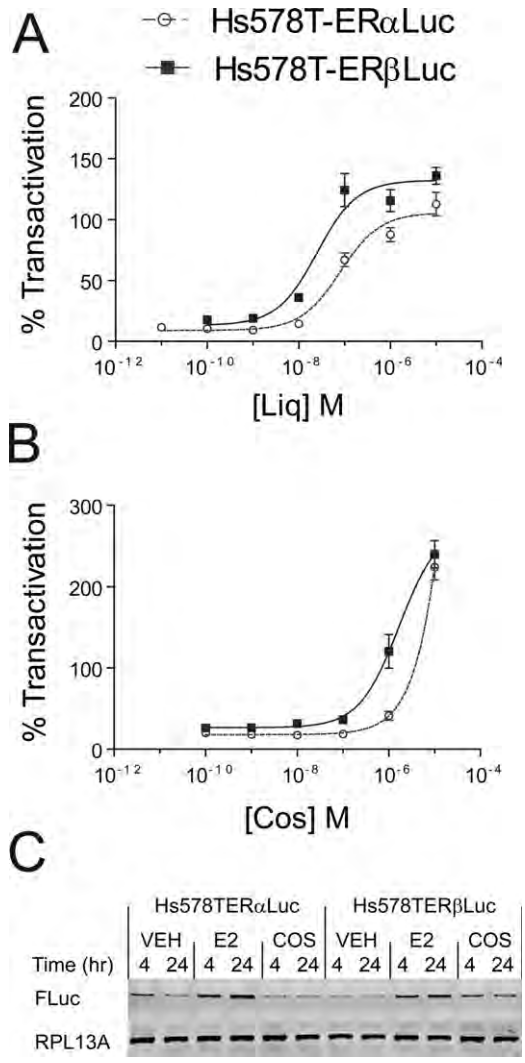

Fig. 5. Liquiritigenin (Liq) and cosmosiin (Cos) induce reporter expression in Hs578T-ERαLuc and Hs578T-ERβLuc. Dose response curves of liquiritigenin (A) and cosmosiin (B). Hs578T-ERαLuc and Hs578T-ERβLuc were seeded in triplicate and treated with 50 ng/mL Dox for 24 hr. Cells were then treated with a range of ligand concentrations (0.15% final DMSO concentration) for 24 hr. Each plate contained DMSO, 0.1 nM E2, and 100 nM ICI 182,780 for controls. Luciferase signal was normalized to total protein in each well and expressed as a percent transactivation relative to signal obtained from saturating E2 treatment (0.1 nM). Each dose response experiment was conducted at least 3 times; data shown are from one representative experiment. EC_{50} values are shown in Table 2. EC_{50} values for cosmosiin could not be determined because of supramaximal reporter induction. The supramaximal induction by cosmosiin was not due to supramaximal transcription of the luciferase reporter (C). Hs578T-ERαLuc and Hs578T-ERβLuc cells were treated with 50 ng/mL Dox for 48 hr followed by treatment with DMSO (0.1%), 1 nM E2, or 1 μM cosmosiin for 4 or 24 hr. Firefly luciferase (FLuc) expression was determined by RT-PCR. RPL13A expression was used to ensure equal loading.

selectivity was proposed to be due to selective recruitment of co-activators to ERβ, namely SRC-2 [11]. Comparison of EC_{50} values showed liquiritigenin had a 3.6-fold selectivity for ERβ, and maximal reporter induction was obtained by 100 nM liquiritigenin in Hs578T-ERβLuc cells and 1 μM in Hs578T-ERαLuc (Fig. 5A and Table 2).

Cosmosiin, or apigenin 7-glucoside, is a flavone found in chamomile [20] that was identified as an ER agonist that selectively induces ERα/β and ERβ/β dimers as measured by bioluminescence resonance energy transfer (BRET) assays (unpublished data). It has a 3-fold higher binding affinity for ERβ as measured by competitive ligand binding assays (IC_{50} ERα 15.9 μM, IC_{50} ERβ 3.3 μM,

unpublished data). Interestingly, cosmosiin induced luciferase expression to a much greater extent than E2, an effect described as supramaximal induction [21]. Even at concentrations upto 10 μM, cosmosiin did not saturate the luciferase output, and EC_{50} values could not be reasonably calculated (Fig. 5B). Another Hs578T-ERβLuc clone treated with cosmosiin also showed supramaximal induction (data not shown). Cosmosiin did not induce luciferase expression in Dox-treated cells co-treated with ICI 182,780 or cells not treated with Dox (data not shown), suggesting the supramaximal induction was due to ERβ activation. To determine if the supramaximal induction truly represented enhanced transcriptional activation, the transcript levels of luciferase were assessed after 4 and 24 hr treatments of E2 and cosmosiin (Fig. 5C). Cosmosiin did not induce luciferase expression to a greater extent than E2 in either Hs578T-ERαLuc or Hs578T-ERβLuc cells, indicating alternative mechanisms are responsible for the supramaximal effect.

3.3. Selective regulation of ERα and ERβ target genes by ERβ selective ligands

We next sought to validate the subtype selectivity of DPN, PPT, liquiritigenin, and cosmosiin by assessing regulation of endogenous ER target genes. Estrogen responsive target genes of ERα and ERβ were previously identified in Hs578T-ERα and Hs578T-ERβ cells [15], and two ERβ target genes and one ERα target gene were selected for analysis. Cells were treated with 50 ng/mL Dox for 48 hr to induce expression of the receptors and further treated with the corresponding ligands for 24 hr. Complement component 3 (*C3*, NM_000064) was up-regulated in Hs578T-ERβ cells upon E2 treatment (Fig. 6A). DPN and liquiritigenin were capable of inducing *C3* expression to a comparable level as E2 at concentrations that fully activate ERβ with minimal ERα activation, as measured by reporter assays (Fig. 6A). Cosmosiin induced *C3* expression at 1 μM, but not to the same extent as E2, demonstrating cosmosiin does not fully activate the receptor at this concentration. PPT slightly induced *C3* expression compared to DMSO in Hs578T-ERβ cells, although PPT induced expression of *C3* to a much lesser degree compared to E2. Repression of the ERβ target gene Jagged 1 (*JAG1*, NM_000214) occurred to a similar degree by E2, DPN, liquiritigenin, and cosmosiin, although 100 nM liquiritigenin and 1 μM cosmosiin do not fully repress *JAG1* expression compared to E2, DPN, or 1 μM liquiritigenin (Fig. 6B). Although the ERα selective agonist PPT slightly induced *C3* expression in Hs578T-ERβ cells, it had no effect on *JAG1* repression, demonstrating incomplete ERβ activation by PPT. To further validate the subtype selectivity observed in reporter assays, expression of the ERα target gene alpha-6 integrin (*ITGA6*, NM_000210) was determined after treatment of Hs578T-ERα cells with E2, DPN, PPT, liquiritigenin, and cosmosiin. As shown in Fig. 6C, *ITGA6* was up-regulated by E2 and PPT treatment, but DPN and liquiritigenin did not fully activate its expression at concentrations that showed selectivity in reporter assays (10 nM and 100 nM, respectively). At 1 μM, liquiritigenin and cosmosiin were capable of activating ERα, and *ITGA6* expression was induced in Hs578T-ERα cells. Therefore, the subtype selectivity of DPN and liquiritigenin observed in reporter cell lines was validated by subtype selective regulation of endogenous target genes. Cosmosiin, however, activated expression of an Hs578T-ERα endogenous gene target at concentrations that only slightly activated luciferase reporter expression in Hs578T-ERαLuc cells.

3.4. Growth inhibition of Hs578T-ERβ cells by liquiritigenin and cosmosiin

We next characterized the growth effects of liquiritigenin and cosmosiin in Hs578T-ERα and Hs578T-ERβ cells. It was previously

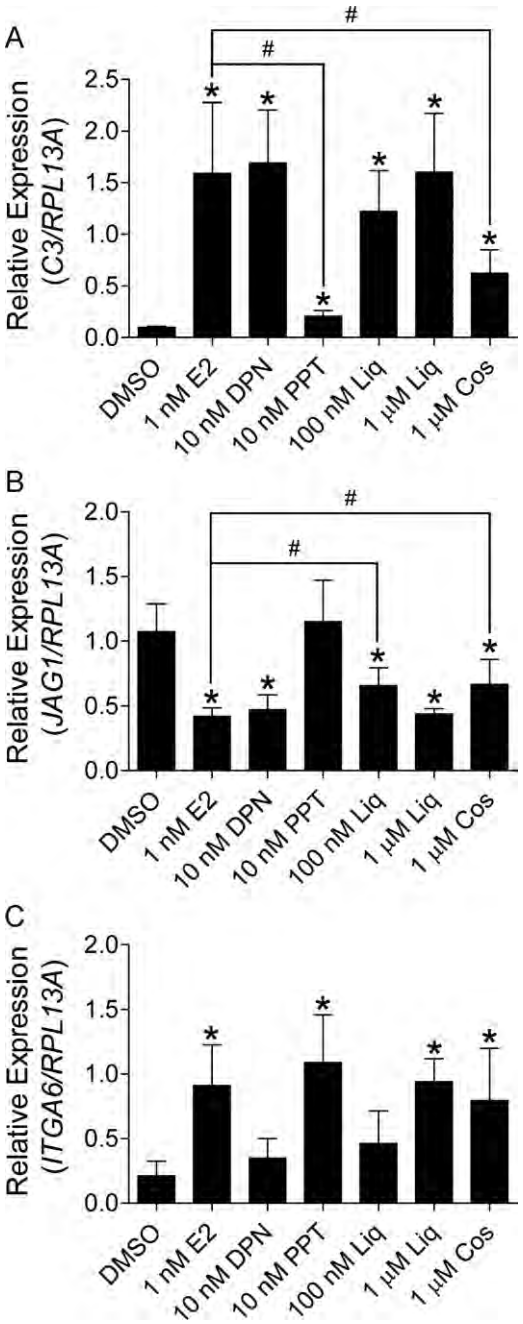

Fig. 6. ERβ selective ligands selectively regulate ER target genes. Hs578T-ERα and Hs578T-ERβ cells were treated with 50 ng/mL Dox for 48 hr to induce ER expression followed by treatment with the corresponding ligands for 24 hr. Total RNA was assayed for expression of the ERβ target genes *C3* and *JAG1* in Hs578T-ERβ cells (A and B, respectively) and the ERα target gene *ITGA6* in Hs578T-ERα (C) cells by quantitative reverse-transcription polymerase chain reaction. Target gene expression was calculated using the ΔΔCq method by normalizing to the ribosomal protein *RPL13A*. Data represent the average and standard deviation of three biological replicates. *p values < 0.05 compared to DMSO control; #p values < 0.05 compared to E2 treatment.

shown that E2 inhibits the growth of Hs578T-ERβ cells [15], supporting the notion that the anti-proliferative action of ERβ may be activated by estrogenic ligands. We tested whether 100 nM liquiritigenin, a concentration at which ERβ was selectively activated, and 1 μM cosmosiin could also inhibit the growth of Hs578T-ERβ cells. Hs578T-ERα and Hs578T-ERβ cells were treated with vehicle (DMSO), 1 nM E2, 100 nM liquiritigenin or 1 μM cosmosiin in the presence or absence of 50 ng/mL Dox (with

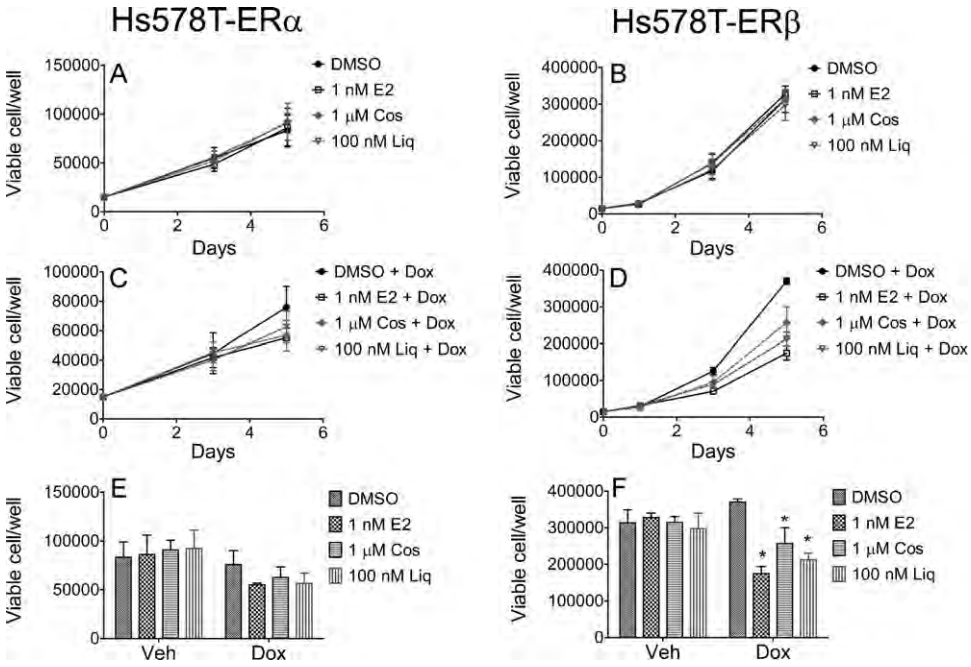

Fig. 7. Cosmosiin (Cos) and liquiritigenin (Liq) inhibit the growth of Hs578T-ERβ cells. Hs578T-ERα (A, C, and E) and Hs578T-ERβ cells (B, D, F) were seeded in 6-well plates and treated with vehicle (A and B) or 50 ng/mL Dox (C and D). After 24 hr, the cells were treated with vehicle (0.1% DMSO) or the indicated ligands, and treatments were refreshed every 48 hr. Cells were counted at the times indicated using trypan blue exclusion. Comparisons of the cell number on day 5 are represented in panels E (Hs578T-ERα) and F (Hs578T-ERβ). Data represent two independent experiments. $^{*}p$ values < 0.05.

or without ER, respectively) for a total of 5 days. When ERα and ERβ were not expressed (−Dox), the compounds had no effect on the growth of the cells (Fig. 7A and B). In contrast, E2, liquiritigenin, and cosmosiin inhibited the growth of Hs578T-ERβ cells when ERβ was expressed (+Dox, Fig. 7D), and there was an approximately 50% reduction in the number of cells after 5 days of treatment with all three compounds (Fig. 7F). Hs578T-ERα cells showed slight inhibition with E2 and liquiritigenin treatment when ERα was expressed (Fig. 7C), but there was not a statistically significant effect after 5 days of treatment as measured by 2 independent experiments (Fig. 7E). However, ERα expression in ER negative cells often leads to growth inhibition [22,23], and it is likely that activation of ERα inhibits the growth of Hs578T-ERα cells. This suggests that 100 nM liquiritigenin partially activates ERα despite minimal regulation of *ITGA6* at this concentration.

4. Discussion

ERα is an established therapeutic target for breast cancer treatment, but the development of subtype selective estrogenic ligands has gained interest with the identification of ERβ [1]. ERβ opposes the actions of ERα suggesting that it may be a potential therapeutic target. Exogenous ERβ expression in ERα positive breast cancer cells impaired E2 stimulated proliferation [24] and tumor growth in xenografts [25]. In support of the anti-proliferative role of ERβ, MCF7 cells were more proliferative when ERβ was knocked down [6]. Activation of ERβ by subtype selective ligands may enhance ERβ growth repression without stimulating proliferation through ERα; indeed ERβ selective ligands inhibited growth of HC11 mouse mammary cells [5]. Here, we have also shown that ERβ ligands can inhibit the growth of breast cancer cells when ERβ is expressed. In breast cancer, however, ERβ expression is thought to decline during progression [26–28] so ligands aimed at targeting ERβ must be highly selective and used only in patients that lack ERα or those with low ERα:ERβ ratios of expression. The rate of ERβ positivity in breast cancer has been reported to range from 13% to 83% [29–32]. In order to effectively target ERβ for cancer treatment, there is an imminent need to: (a) identify ERβ selective ligands with minimal side effects and better *in vivo* efficacy and selectivity, and (b) design clinical trials to recruit patients with low ERα:ERβ ratios in earlier stages of disease progression.

Although ERβ selective ligands have not yet been used for cancer treatment, the therapeutic value of ERβ has been assessed in other diseases. Two of the most promising ERβ selective therapies are the ERβ selective ligand ERB-041 and the herbal extract MF-101 [33]. Clinical trials have been completed to determine the efficacy of ERB-041 for treatment of Crohn's disease, endometriosis, interstitial cystitis, and rheumatoid arthritis. Although results have not been published for most of the clinical trials, results of the rheumatoid arthritis trial showed ERB-041was well tolerated but did not improve arthritis symptoms [34]. MF-101 also showed a relatively safe profile and reduced the frequency of hot flashes in a phase II clinical trial for treatment of post-menopausal symptoms [35]. Liquiritigenin is the most active estrogenic component of MF-101 [11], suggesting ERβ selective ligands may prove useful for treating post-menopausal symptoms.

Strategies to identify ER subtype selective ligands include competitive ligand binding, dimerization, transcriptional reporter, and proliferation assays [21,36]. Competitive ligand binding assays provide insight into binding affinities and are useful for high throughput small molecule screening [37], but they are limited because ligands can act as agonists or antagonists and binding affinity does not often reflect transcriptional potency. Subtype selective ligands have been identified using BRET assays that measure receptor dimerization [38], but dimerization assays cannot differentiate between agonists or antagonists [39]. Agonists can be characterized using MCF7 cell proliferation assays, which are highly sensitive and provide a biologically relevant endpoint in the context of estrogen-sensitive cells [40]. However, these assays are limited by a lack of specificity, as non-estrogenic mitogens can stimulate proliferation, and cannot be used to detect subtype selective agonists.

Transcriptional assays can differentiate between agonists and antagonists, overcoming limitations of binding and dimerization assays. Mammalian reporter cell lines useful for identifying subtype selective ligands have been created from HeLa cervical carcinoma cells [12] and HEK293 kidney cells [13]. HELN-ERα and HELN-ERβ were generated from HeLa cells in two steps: (1) stable integration of ERE-luciferase to generate HELN cells, (2) stable expression of ERα or ERβ to generate HELN-ERα and HELN-ERβ [12]. 293/hERα and 293/hERβ cells were generated by a similar strategy. Only one breast cancer reporter cell line, T47D-KBLuc, is available to characterize agonists in the context of breast cancer cells [14], but both ERα and ERβ are expressed, preventing identification of subtype selective ligands.

In this report, we described the development of a new set of breast cancer reporter cell lines to characterize subtype selective estrogenic ligands. Hs578T-ERαLuc and Hs578T-ERβLuc cells were highly sensitive to E2 with EC_{50} values of 1 pM and 6.5 pM, respectively (Fig. 4A). Similar E2 sensitivity was observed in T47D-KBLuc cells, which showed an approximate EC_{50} of 3 pM [14]. Hs578T-ERαLuc and Hs578T-ERβLuc cells were more sensitive to E2 than HELN-ER and 293/ER reporter cells, but all reporter cell lines showed greater E2 sensitivity in ERα expressing cells. HELN-ERα cells were approximately 3 times more sensitive to E2 than HELN-ERβ cells (EC_{50} of 0.017 nM and 0.068 nM, respectively) [12] and 293/hERα cells were approximately 4 times more sensitive to E2 than cells expressing ERβ (EC_{50} of 50 pM and 200 pM, respectively) [13]. Although Hs578T-ERαLuc and Hs578T-ERβLuc cells were not created using the same strategy as HELN-ER or 293/hER reporter cells and likely have unique genomic integration of the reporter, similar sensitivities observed in all reporter cell lines suggest that this does not inhibit comparison of subtype selectivity.

Reporter assays with two ER subtype selective ligands confirmed that Hs578T-ERαLuc and Hs578T-ERβLuc cells could be used to differentiate between ERα and ERβ selective ligands. The ERβ selective agonist DPN maintained 33-fold selectivity in Hs578T-ERLuc cells (EC_{50} of 0.26 nM for ERβ and 8.5 nM for ERα, Table 2). Dose response assays with the ERα selective agonist PPT revealed the sensitivity of Hs578T-ERβLuc cells (Fig. 4B). Although PPT was unable to activate reporter expression in HEC-1 cells transfected with ERβ [12], PPT did activate reporter expression in Hs578T-ERβLuc cells at high concentrations, although not to the full extent induced by E2. PPT reporter activation was blocked by ICI 182,780 co-treatment (Fig. 2A) and did not occur in the absence of Dox treatment (data not shown), verifying reporter activation was mediated by ERβ. Despite activation of ERβ at high concentrations, PPT could not fully activate reporter expression in Hs578T-ERβLuc cells and maintained 1000-fold selectivity for ERα.

Subtype selectivity of two natural phytoestrogens, cosmosiin and liquiritigenin, was also assessed in Hs578T-ERαLuc and Hs578T-ERβLuc cells. Liquiritigenin maintained selectivity for ERβ but to a lesser extent than expected, as it has been shown to minimally activate ERα in other cell lines [11]. The discrepancy in the selectivity of liquiritigenin may be due to the enhanced sensitivity of Hs578T-ERαLuc cells, differences in cofactor expression in Hs578T cells, or purity of the compound (our studies utilized commercially available liquiritigenin and Mersereau and coworkers [11] used extract from *G. uralensis*). The selectivity of cosmosiin could not be assessed using luciferase assays due to supramaximal induction (Fig. 5B). Supramaximal activation of estrogen responsive reporters have been described in many systems [21]. Here, we showed that supramaximal induction by cosmosiin was not due to enhanced transcriptional activation of the reporter (Fig. 5C). Despite limitations of the reporter system, the subtype selectivity of cosmosiin could be characterized by assessing target gene regulation in Hs578T-ERα and Hs578T-ERβ cells. While DPN and liquiritigenin maintained similar extents of selectivity as measured by reporter assays, cosmosiin activated both ERα and ERβ as measured by endogenous gene regulation (Fig. 6). Cosmosiin and liquiritigenin induced similar growth inhibitory effects as E2 in Hs578T-ERβ cells, indicating the phytoestrogens could elicit ERβ activation to a similar extent as E2 (Fig. 7).

Hs578T-ERαLuc and Hs578T-ERβLuc cells have several advantages for identifying ERβ selective agonists in comparison to available mammalian reporter cell lines. First, the Hs578T reporter cell lines have inducible expression of ERα and ERβ, allowing determination of off-target reporter activation by assessing reporter expression in the absence of Dox. Second, Hs578T-ERαLuc and Hs578T-ERβLuc cells are highly sensitive to estrogenic ligands. Third, endogenous gene regulation can be used to validate subtype selectivity. Finally, growth inhibition assays using Hs578T-ERβ cells in the presence and absence of Dox can be used to determine the biological endpoint of ERβ activation and validate specificity of ligands to ensure they do not have off-target cytotoxic effects. High throughput screening may be possible using Hs578T-ERαLuc and Hs578T-ERβLuc cells, and luciferase assay optimization using Hs578T-ERβLuc cells has shown a Z factor of 0.5 (data not shown), an acceptable range for high throughput screening [41]. Therefore, Hs578T-ERαLuc and Hs578T-ERβLuc cells are useful for the identification and characterization of ER subtype selective ligands that may hold therapeutic promise.

Acknowledgements

This work was supported by the National Institute of Environmental Health and Safety (Grant T32 ES007015), the National Institutes of Health (Grants R01CA125387, R03MH089442) the Shaw Scientist Award from the Greater Milwaukee Foundation, the Department of Defense Breast Cancer Research Program (Grants BC100252, Era of Hope Scholar Award), and the UWCCC (Multi-IT Grant). We gratefully acknowledge Linda Schuler, Nancy Thompson, and Serife Ayaz-Guner for critical review of the manuscript.

References

[1] Nilsson S, Gustafsson JA. Estrogen receptors: therapies targeted to receptor subtypes. Clin Pharmacol Ther 2011;89:44–55.
[2] Swaby R, Sharma C, Jordan V. SERMs for the treatment and prevention of breast cancer. Rev Endocr Metab Disord 2007;8:229–39.
[3] Hartman J, Ström A, Gustafsson JA. Estrogen receptor beta in breast cancer—diagnostic and therapeutic implications. Steroids 2009;74:635–41.
[4] Chang EC, Frasor J, Komm B, Katzenellenbogen BS. Impact of estrogen receptor beta on gene networks regulated by estrogen receptor alpha in breast cancer cells. Endocrinology 2006;147:4831–42.
[5] Helguero LA, Faulds MH, Gustafsson JA, Haldosen LA. Estrogen receptors alpha (ERα) and beta (ERβ) differentially regulate proliferation and apoptosis of the normal murine mammary epithelial cell line HC11. Oncogene 2005;24:6605–16.
[6] Treeck O, Lattrich C, Springwald A, Ortmann O. Estrogen receptor beta exerts growth-inhibitory effects on human mammary epithelial cells. Breast Cancer Res Treat 2010;120:557–65.
[7] Minutolo F, Macchia M, Katzenellenbogen BS, Katzenellenbogen JA. Estrogen receptor β ligands: recent advances and biomedical applications. Med Res Rev 2011;31:364–442.
[8] Charn TH, Liu ET-B, Chang EC, Lee YK, Katzenellenbogen JA, Katzenellenbogen BS. Genome-wide dynamics of chromatin binding of estrogen receptors {alpha} and {beta}: mutual restriction and competitive site selection. Mol Endocrinol 2010;24:47–59.
[9] Kuiper GG, Carlsson B, Grandien K, Enmark E, Haggblad J, Nilsson S, et al. Comparison of the ligand binding specificity and transcript tissue distribution of estrogen receptors alpha and beta. Endocrinology 1997;138:863–70.
[10] Stauffer SR, Coletta CJ, Tedesco R, Nishiguchi G, Carlson K, Sun J, et al. Pyrazole ligands: structure–affinity/activity relationships and estrogen receptor-β-selective agonists. J Med Chem 2000;43:4934–47.
[11] Mersereau JE, Levy N, Staub RE, Baggett S, Zogric T, Chow S, et al. Liquiritigenin is a plant-derived highly selective estrogen receptor beta agonist. Mol Cell Endocrinol 2008;283:49–57.
[12] Escande A, Pillon A, Servant N, Cravedi J-P, Larrea F, Muhn P, et al. Evaluation of ligand selectivity using reporter cell lines stably expressing estrogen receptor alpha or beta. Biochem Pharmacol 2006;71:1459.

[13] Barkhem T, Carlsson B, Nilsson Y, Enmark E, Gustafsson J-Å, Nilsson S. Differential response of estrogen receptor α and estrogen receptor β to partial estrogen agonists/antagonists. Mol Pharmacol 1998;54:105–12.
[14] Wilson VS, Bobseine K, Gray Jr LE. Development and characterization of a cell line that stably expresses an estrogen-responsive luciferase reporter for the detection of estrogen receptor agonist and antagonists. Toxicol Sci 2004;81:69–77.
[15] Secreto FJ, Monroe DG, Dutta S, Ingle JN, Spelsberg TC. Estrogen receptor alpha/beta isoforms, but not betacx, modulate unique patterns of gene expression and cell proliferation in Hs578T cells. J Cell Biochem 2007;101:1125–47.
[16] Kao J, Salari K, Bocanegra M, Choi YL, Girard L, Gandhi J, et al. Molecular profiling of breast cancer cell lines defines relevant tumor models and provides a resource for cancer gene discovery. PLoS One 2009;4:e6146.
[17] Brünner N, Boulay V, Fojo A, Freter CE, Lippman ME, Clarke R. Acquisition of hormone-independent growth in MCF-7 cells is accompanied by increased expression of estrogen-regulated genes but without detectable DNA amplifications. Cancer Res 1993;53:283–90.
[18] Cowley SM, Parker MG. A comparison of transcriptional activation by ERα and ERβ. J Steroid Biochem Mol Biol 1999;69:165–75.
[19] Meyers MJ, Sun J, Carlson KE, Marriner GA, Katzenellenbogen BS, Katzenellenbogen JA. Estrogen receptor-β potency-selective ligands: structure–activity relationship studies of diarylpropionitriles and their acetylene and polar analogues. J Med Chem 2001;44:4230–51.
[20] Srivastava JK, Gupta S. Antiproliferative and apoptotic effects of chamomile extract in various human cancer cells. J Agric Food Chem 2007;55:9470–8.
[21] Montaño M, Bakker EJ, Murk AJ. Meta-analysis of supramaximal effects in in vitro estrogenicity assays. Toxicol Sci 2010;115:462–74.
[22] Garcia M, Derocq D, Freiss G, Rochefort H. Activation of estrogen receptor transfected into a receptor-negative breast cancer cell line decreases the metastatic and invasive potential of the cells. Proc Natl Acad Sci USA 1992; 89:11538–42.
[23] Wang W, Smith R, Burghardt R, Safe SH. 17 Beta-estradiol-mediated growth inhibition of MDA-MB-468 cells stably transfected with the estrogen receptor: cell cycle effects. Mol Cell Endocrinol 1997;133:49–62.
[24] Hodges-Gallagher L, Valentine C, Bader S, Kushner P. Estrogen receptor beta increases the efficacy of antiestrogens by effects on apoptosis and cell cycling in breast cancer cells. Breast Cancer Res Treat 2008;109:241–50.
[25] Ström A, Hartman J, Foster JS, Kietz S, Wimalasena J, Gustafsson JA. Estrogen receptor β inhibits 17β-estradiol-stimulated proliferation of the breast cancer cell line T47D. Proc Natl Acad Sci USA 2004;101:1566–71.
[26] Bardin A, Boulle N, Lazennec G, Vignon F, Pujol P. Loss of ER{beta} expression as a common step in estrogen-dependent tumor progression. Endocr Relat Cancer 2004;11:537–51.
[27] Shaw JA, Udokang K, Mosquera JM, Chauhan H, Jones JL, Walker RA. Oestrogen receptors alpha and beta differ in normal human breast and breast carcinomas. J Pathol 2002;198:450–7.
[28] Skliris GP, Munot K, Bell SM, Carder PJ, Lane S, Horgan K, et al. Reduced expression of oestrogen receptor beta in invasive breast cancer and its re-expression using DNA methyl transferase inhibitors in a cell line model. J Pathol 2003;201:213–20.
[29] Marotti JD, Collins LC, Hu R, Tamimi RM. Estrogen receptor-[beta] expression in invasive breast cancer in relation to molecular phenotype: results from the Nurses' Health Study. Mod Pathol 2009;23:197.
[30] Honma N, Horii R, Iwase T, Saji S, Younes M, Takubo K, et al. Clinical importance of estrogen receptor-beta evaluation in breast cancer patients treated with adjuvant tamoxifen therapy. J Clin Oncol 2008;26:3727–34.
[31] O'Neill PA, Davies MP, Shaaban AM, Innes H, Torevell A, Sibson DR, et al. Wild-type oestrogen receptor beta (ERbeta1) mRNA and protein expression in tamoxifen-treated post-menopausal breast cancers. Br J Cancer 2004;91: 1694–702.
[32] Mann S, Laucirica R, Carlson N, Younes PS, Ali N, Younes A, et al. Estrogen receptor beta expression in invasive breast cancer. Hum Pathol 2001;32: 113–8.
[33] Mohler ML, Narayanan R, Coss CC, Hu K, He Y, Wu Z, et al. Estrogen receptor β selective nonsteroidal estrogens: seeking clinical indications. Expert Opin Ther Pat 2010;20:507–34.
[34] Roman-Blas JA, Castañeda S, Cutolo M, Herrero-Beaumont G. Efficacy and safety of a selective estrogen receptor β agonist, ERB-041, in patients with rheumatoid arthritis: a 12-week, randomized, placebo-controlled, phase II study. Arthritis Care Res (Hoboken) 2010;62:1588–93.
[35] Grady D, Sawaya GF, Johnson KC, Koltun W, Hess R, Vittinghoff E, et al. MF101, a selective estrogen receptor beta modulator for the treatment of menopausal hot flushes: a phase II clinical trial. Menopause 2009;16:458–65.
[36] Shanle EK, Xu W. Endocrine disrupting chemicals targeting estrogen receptor signaling: identification and mechanisms of action. Chem Res Toxicol 2010; 24:6–19.
[37] Bolger R, Wiese TE, Ervin K, Nestich S, Checovich W. Rapid screening of environmental chemicals for estrogen receptor binding capacity. Environ Health Perspect 1998;106:551–7.
[38] Powell E, Huang SX, Xu Y, Rajski SR, Wang Y, Peters N, et al. Identification and characterization of a novel estrogenic ligand actinopolymorphol A. Biochem Pharmacol 2010;80:1221–9.
[39] Powell E, Xu W. Intermolecular interactions identify ligand-selective activity of estrogen receptor a/b dimers. Proc Natl Acad Sci USA 2008;105: 19012–7.
[40] Silva E, Scholze M, Kortenkamp A. Activity of xenoestrogens at nanomolar concentrations in the E-Screen assay. Environ Health Perspect 2007;115: 91–7.
[41] Zhang JH, Chung TD, Oldenburg KR. A simple statistical parameter for use in evaluation and validation of high throughput screening assays. J Biomol Screen 1999;4:67–73.

OPEN ACCESS Freely available online

PLoS one

Identification of Estrogen Receptor Dimer Selective Ligands Reveals Growth-Inhibitory Effects on Cells That Co-Express ERα and ERβ

Emily Powell[1], Erin Shanle[1], Ashley Brinkman[1], Jun Li[1¤], Sunduz Keles[2], Kari B. Wisinski[3], Wei Huang[4], Wei Xu[1]*

1 McArdle Laboratory for Cancer Research, University of Wisconsin–Madison, Madison, Wisconsin, United States of America, **2** Departments of Statistics and of Biostatistics and Medical Informatics, University of Wisconsin–Madison, Madison, Wisconsin, United States of America, **3** UW Carbone Cancer Center, University of Wisconsin School of Medicine and Public Health, University of Wisconsin–Madison, Madison, Wisconsin, United States of America, **4** Department of Pathology and Laboratory Medicine, University of Wisconsin–Madison, Madison, Wisconsin, United States of America

Abstract

Estrogens play essential roles in the progression of mammary and prostatic diseases. The transcriptional effects of estrogens are transduced by two estrogen receptors, ERα and ERβ, which elicit opposing roles in regulating proliferation: ERα is proliferative while ERβ is anti-proliferative. Exogenous expression of ERβ in ERα-positive cancer cell lines inhibits cell proliferation in response to estrogen and reduces xenografted tumor growth *in vivo*, suggesting that ERβ might oppose ERα's proliferative effects via formation of ERα/β heterodimers. Despite biochemical and cellular evidence of ERα/β heterodimer formation in cells co-expressing both receptors, the biological roles of the ERα/β heterodimer remain to be elucidated. Here we report the identification of two phytoestrogens that selectively activate ERα/β heterodimers at specific concentrations using a cell-based, two-step high throughput small molecule screen for ER transcriptional activity and ER dimer selectivity. Using ERα/β heterodimer-selective ligands at defined concentrations, we demonstrate that ERα/β heterodimers are growth inhibitory in breast and prostate cells which co-express the two ER isoforms. Furthermore, using Automated Quantitative Analysis (AQUA) to examine nuclear expression of ERα and ERβ in human breast tissue microarrays, we demonstrate that ERα and ERβ are co-expressed in the same cells in breast tumors. The co-expression of ERα and ERβ in the same cells supports the possibility of ERα/β heterodimer formation at physio- and pathological conditions, further suggesting that targeting ERα/β heterodimers might be a novel therapeutic approach to the treatment of cancers which co-express ERα and ERβ.

Citation: Powell E, Shanle E, Brinkman A, Li J, Keles S, et al. (2012) Identification of Estrogen Receptor Dimer Selective Ligands Reveals Growth-Inhibitory Effects on Cells That Co-Express ERα and ERβ. PLoS ONE 7(2): e30993. doi:10.1371/journal.pone.0030993

Editor: Susan Kovats, Oklahoma Medical Research Foundation, United States of America

Received August 31, 2011; **Accepted** December 28, 2011; **Published** February 7, 2012

Funding: This work is supported by National Institutes of Health grants R01125387, T32ES007015, T32 CA009135 and in part by NIH/NCI P30CA014520 - University of Wisconsin Comprehensive Cancer Center Support. The funders had no role in study design, data collection and analysis, decision to publish, or preparation of the manuscript.

Competing Interests: The authors have declared that no competing interests exist.

* E-mail: wxu@oncology.wisc.edu

¤ Current address: Cancer center, Shandong Provincial Hospital, Jinan, Shandong, China

Introduction

Estrogens exert their biological effects via interaction with two estrogen receptors (ERs), ERα and ERβ [1,2]. ERs regulate key physiological functions in the reproductive tract, breast, prostate, bone, brain and the cardiovascular system [1,2]. In some organs, ERα and ERβ are expressed at similar levels but in different cell types [3]. For example, in the prostate, ERα is predominately expressed in stroma while ERβ is expressed in the epithelium. Both receptors are expressed in normal mammary epithelial cells [4]. Studies with ERα knockout mice (αERKO) demonstrate that ERα is essential for ductal formation and mammary gland development [5]. Although ERβ knockout mice (βERKO) generate mild mammary phenotypes, Ki-67 expression is increased in luminal mammary epithelial cells of βERKO mice [6], suggesting that ERβ may be important for terminal differentiation of mammary epithelial cells. ERα and ERβ are also involved in growth and differentiation of the prostate gland and progression of prostate disease [7,8]. A recent study showed that stromal ERα promotes prostatic carcinogenesis [9]. Moreover, hyperplasia was observed in the prostates of βERKO mice [10] and ERβ expression was silenced in a subset of malignant human breast and prostate cancers [11,12], suggesting that ERβ plays protective roles in these diseases.

The classic mechanism through which the ERs modulate gene expression is a cascade of events: ligand binding to ERα or ERβ induces receptor dimerization, either as homodimers (ERα/ERα or ERβ/ERβ) or heterodimers (ERα/ERβ), translocation of dimers to the nucleus, and recognition of Estrogen Response Elements (EREs) on DNA. The target genes activated by these events, and hence the physiological responses, depend on the dimer pair activated by the ligand. Indeed, several studies have shown that ERα and ERβ exhibit opposing roles in cellular proliferation and apoptosis, with ERα inducing the transcription of pro-proliferative and anti-apoptotic target genes, and ERβ being anti-proliferative and pro-apoptotic [13,14,15]. In accordance

with this notion, target gene studies reveal that ERα and ERβ may have distinct biological functions; it is believed that ERα promotes cell growth, while ERβ inhibits it in breast and prostate cancer cells [11,14,16,17,18,19]. It has thus been deduced that the role of the ERα/α homodimer is to accelerate cellular proliferation, thus lending to carcinogenesis and tumor progression, while conversely the transcriptional activation from ERβ/β homodimers is thought to be protective against hormone-dependent diseases including breast and prostate cancers [13,14,15].

ERβ has well known growth modulatory activity in ERα-positive breast cancer cells. Compared with tumors expressing ERα alone, the co-expression of ERβ has been correlated with a more favorable prognosis [20] and decreased biological aggressiveness [11,21,22,23,24]. Moreover, ERβ has been shown to modulate the proliferative actions of estrogens when co-expressed with ERα [13,19,25,26] and can be considered an endogenous partial dominant negative receptor [27,28]. ERβ is thought to counteract the stimulatory effects of ERα through heterodimerization of the two receptors [29,30]. Indeed, these heterodimers have been shown to form and maintain function [31], and they have been suggested to be responsible for the activation of target genes which are distinct from those induced by either homodimer [32,33]. The co-expression of ERβ with ERα results in reduced ERα-mediated proliferation and invasion of breast cancer cells [11,16,17,18,19], at least in part due to ERβ's inhibition of ERα selective target gene expression. Furthermore, in the ERα/ERβ-positive mouse mammary epithelial cell line HC11, ERα drives cellular proliferation whereas ERβ contributes to growth inhibition and apoptosis in response to 17β-estradiol; (E2); the loss of ERβ in this cell line results in cellular transformation [14]. Thus, the ERα:ERβ ratio determines whether E2 will induce cellular proliferation. Despite the fact that the ERα/β heterodimer has been proposed to have a biological role that is unique from that of either homodimer, the biological function of these heterodimers *in vivo* has until now remained elusive, at least in part due to the heterogeneous population of dimers existent upon the co-expression of ERα and ERβ and the lack of heterodimer-specific compounds to elucidate their functions.

To circumvent this issue, the identification of ERα/β heterodimer-selective ligands that activate the transcriptional effects of ERα/β heterodimers, but not that of either homodimer, were sought in order to shed light upon the transcriptional outcomes and biological roles of these heterodimers. To this end, a multi-step high throughput small molecule screen for ER transcriptional activation and dimer selectivity was developed (Figure 1). This screening resulted in the identification of two phytoestrogens that are transcriptionally active and ERα/β heterodimer-selective at specific concentrations. These compounds were rigorously characterized for their biological activity in cell-based assays (Figure 1). The results of these studies suggest that the ERα/β heterodimer exerts growth inhibitory effects in breast and prostate epithelial cells. These compounds may serve not only as tools for deciphering the biological functions of the ERα/β heterodimer, but also potentially as a means for therapeutically targeting ERα/β heterodimers in hormone-dependent diseases including breast and prostate cancers.

Results

Characterization of Lead Compounds Cosmosiin and Angolensin Using Bioluminescence Resonance Energy Transfer (BRET) and Reporter Assays

We developed two-step high throughput screening (HTS) for identification of ER dimer-selective ligands (unpublished). The primary screening and counter-screening in the presence of the antagonist ICI 182,780 (Fulvestrant) for ER-specific transcriptional activity was performed in T47D-KBLuc as described in the Methods section. ER dimer selectivity of the primary hits was assessed in secondary HTS BRET assays as described in the Methods section and in [34]. Several compounds with dimer selectivity were identified after performing two-step HTS on >5200 compounds at the UWCCC Small Molecule Screening Facility (unpublished results). Two phytoestrogens, cosmosiin (apigenin-7-glucoside) and angolensin (R) (Fig. 2), were identified in HTS as ER dimer selective ligands. Angolensin exists in two enantiomeric forms; only the R form was identified and used in this study and is thus abbreviated as angolensin hereafter. To determine if they bind the same ligand binding pocket as 17β-estradiol and to measure their binding affinity to recombinant ERs, we employed *in vitro* Fluorescence Polarization (FP) competition binding assays [35]. The IC_{50} values for cosmosiin binding to ERα and ERβ were 15.9 μM and 3.3 μM, respectively (Fig. 2A). The IC_{50} values for angolensin binding to ERα and ERβ were 2.2 μM and 4.7 μM, respectively (Fig. 2B).

The ER dimer selectivity was validated in BRET and reporter assays in ER-negative HEK293 cells as described [35]. While cosmosiin exhibits preference for inducing both ERβ/β homodimers and ERα/β heterodimers (Fig. 3A), angolensin exhibits ERα/β heterodimer selectivity (Fig. 3B). Neither compound shows preference for inducing ERα/α homodimers. Because the lower limit of detection for these compounds was 1 μM, concentrations lower than 1 μM are not shown in this figure, although they were tested in a range from 1 nM to 10 μM; below 1 μM, the BRET ratios were the same as vehicle-treated. Furthermore, the ability of these lead compounds to induce the transcriptional activity of ERα alone, ERβ alone, or ERα in combination with ERβ was tested at a range of concentrations using the HEK293 ERE-luciferase reporter assays (Fig. 3C and 3D). Although these reporter assays do not directly examine ERα/β heterodimerization, the condition in which ERα and ERβ are cotransfected can be compared with each receptor transfected alone.

As shown in Figure 3B, BRET assays reveal that angolensin is capable of efficiently inducing the *formation* of ERα/β heterodimers at 1 μM and 10 μM, while not inducing ERα/α or ERβ/β homodimers. ERα/β heterodimerization appears to be favored in the presence of angolensin , and in the condition in which ERα and ERβ are co-transfected for luciferase reporter assays, the highest fold induction of transcriptional activity relative to DMSO vehicle is observed (Fig. 3D). Thus, angolensin (R) appears to be an ERα/β heterodimer-selective ligand at 10 μM. Cosmosiin appears to be less selective in terms of its ability to induce ERα/β heterodimers, as ERβ/β homodimers are also induced in BRET assays; however, ERα/α homodimers are not induced by cosmosiin (Fig. 3A). Cosmosiin at 1 μM appears to transcriptionally activate ERβ/β homodimers and ERα/β heterodimers (Fig. 3C). At 10 μM cosmosiin, while ERα/α and ERβ/β homodimers were slightly activated, co-transfecting ERβ with ERα exhibited much stronger transcriptional activity (Fig. 3C). Thus, cosmosiin appears to be ERβ/β homodimer- and ERα/β heterodimer-selective at 1 μM.

The transcriptional activity of ERα/α homodimers treated with 10 μM cosmosiin is despite the finding that the BRET assay does not show statistically significant ERα/α homodimerization (Fig. 3A). The most likely explanation for this discrepancy is differences in sensitivity between BRET and the luciferase reporter assays. These BRET assays and luciferase reporter assays are performed under different conditions and measure different signal outputs: BRET captures a single moment in time in which ERα

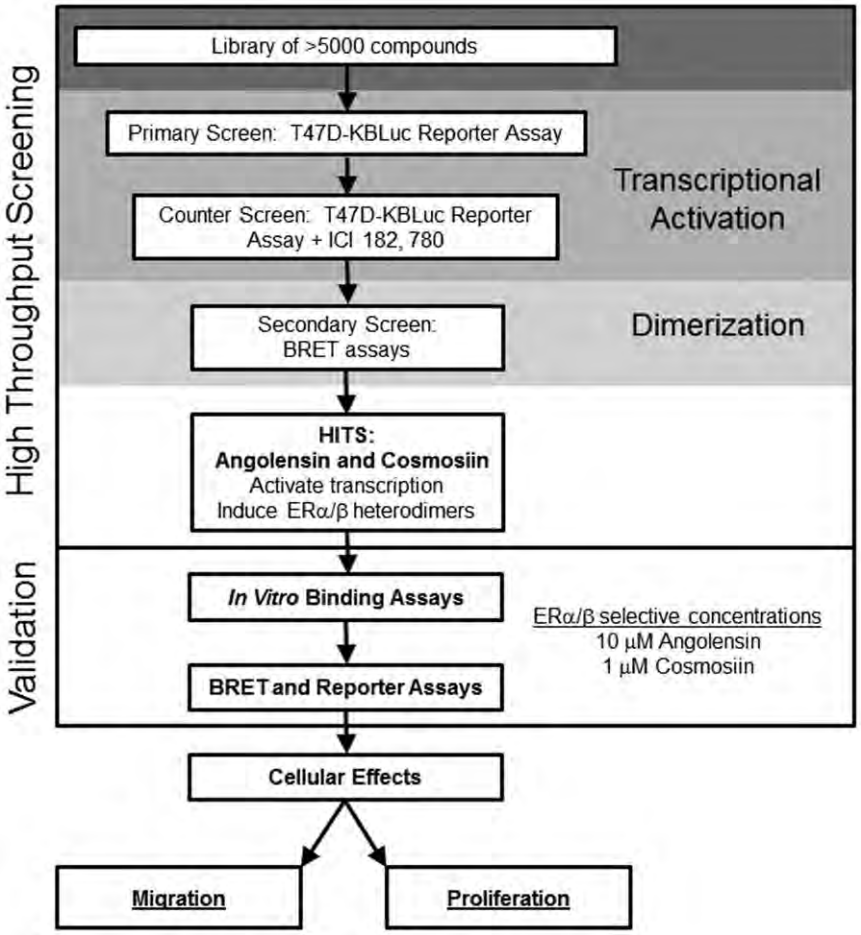

Figure 1. Flow scheme of high throughput screening and characterization of compounds with selectivity for ERα/ERβ heterodimers. A library of >5200 small molecules was screened ER transcriptional activity using T47D-KBLuc cells. Molecules with transcriptional activity were then screened for ERα/α, ERα/β, or ER β/β dimerization potential using BRET assays. Two phytoestrogens, angolensin and cosmosiin, were identified as ER dimer selective ligands. These molecules were validated using *in vitro* binding assays and BRET and ERE-luciferase reporter assays. Heterodimer selective concentrations were identified as 10 μM angolensin and 1 μM cosmosiin. The cellular effects of these two heterodimer-selective concentrations were characterized using cell migration and proliferation assays.
doi:10.1371/journal.pone.0030993.g001

and ERβ may or may not be dimerized. This moment in time was observed after 1 hour incubation with ligand. Conversely, the luciferase reporter assay measures an accumulation of transcriptional output signal (the transcribed luciferase protein) over 18–24 hours. Consequently, the dimerization ratios obtained via the BRET assay do not always completely agree with the transcriptional profiles obtained in the luciferase reporter assays for a given ligand. Therefore, it is important to consider the direct dimerization of ERα and ERβ in conjunction with the transcriptional output of these diverse dimer pairs.

Selection and generation of cell lines expressing different amounts of ERα and ERβ

In order to characterize the cellular effects of cosmosiin and angolensin, we surveyed a variety of breast and prostate cell lines for co-expression of ERα and ERβ. As shown in Fig. 4, the non-tumorigenic mammary epithelial cell HC11 and prostate cancer cell line PC3 were found to express both receptors (Lanes 1 and 2) as reported by others [14,36]; in contrast, DU-145 expresses only ERβ [36] (lane 6) and MDA-MB-231 is negative for both ERα and ERβ (lane 5). To delineate the functions of ERα/β heterodimers, we knocked down ERα and ERβ transcript levels in PC3 cells by means of stable transfection with specific shRNA plasmids targeting ERα and ERβ, respectively. Western blotting results showed that ERα is selectively silenced in PC3-shERα cells and ERβ is selectively silenced in PC3-shERβ cells (Fig. 4A, lanes 3 and 4). The silencing of one ER did not influence the expression of the other. All of these characterized cell lines were subsequently used for determination of compounds' cellular effects.

Cosmosiin and angolensin inhibit cell motility and migration but not apoptosis in PC3

In order to examine the influences of these ERα/β heterodimer-activating compounds on cell migration, wound healing assays were employed using migratory PC3 cells. This assay gives a qualitative measure of a compound's ability to inhibit cell migration. For these assays, 1 μM cosmosiin and 10 μM angolensin were utilized because these are the concentrations at which ERα/β heterodimers are most highly selectively induced by each respective compound. As shown in Figure 5A, the vehicle DMSO (0.1%) was unable to inhibit the migration of PC3 cells in scratch wound healing assays: cells can be seen infiltrating the wound 24 hours after scraping, and the wounds are completely filled 72 hours after scraping. Conversely, both 10 μM angolensin

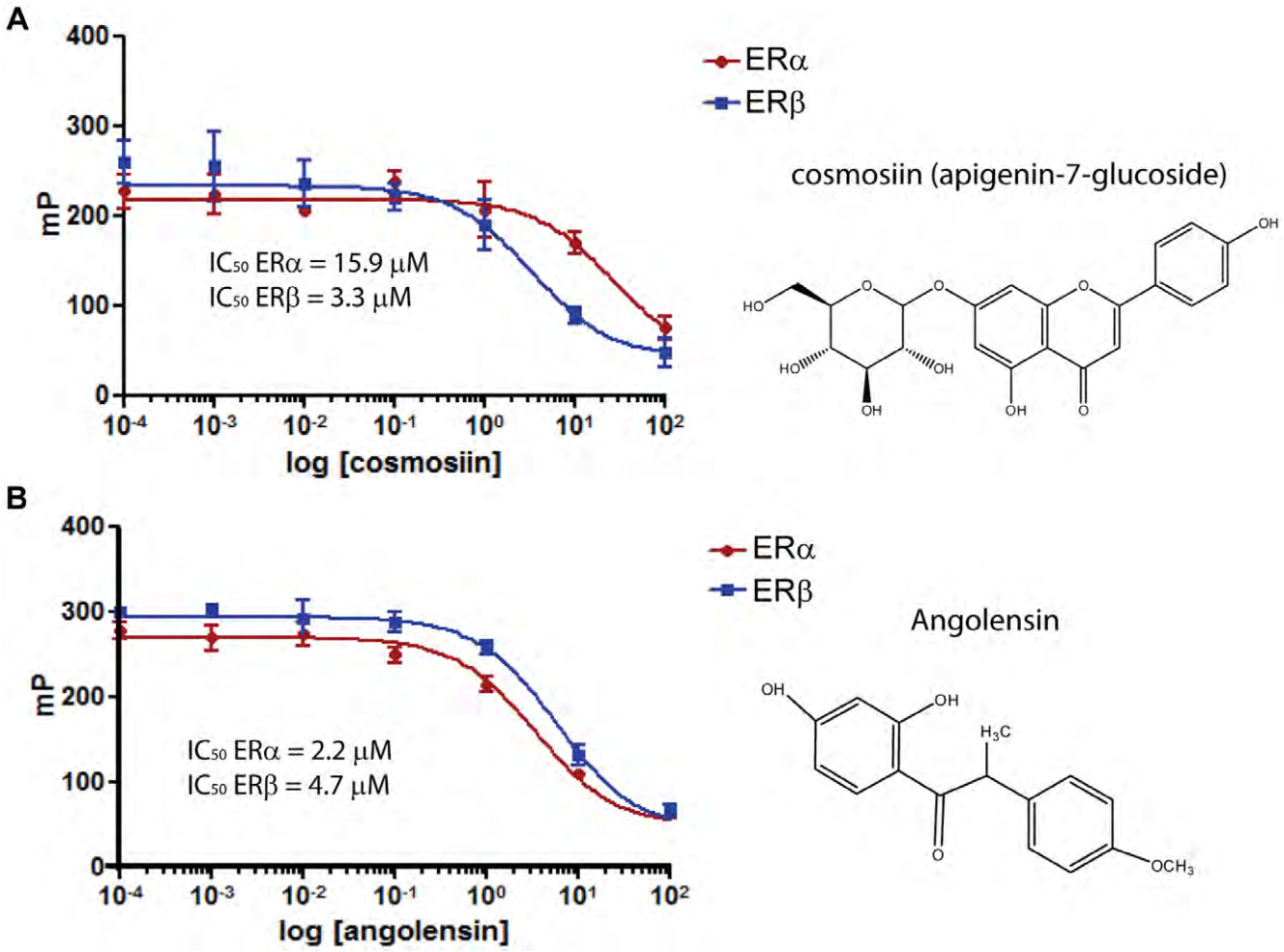

Figure 2. Fluorescence polarization competition binding assays for ERα and ERβ. Cosmosiin (A) and angolensin (B) bind to recombinant ERα and ERβ with μM affinities.
doi:10.1371/journal.pone.0030993.g002

and 1 μM cosmosiin are able to inhibit the ability of PC3 cells to infiltrate the wounds, indicating that these compounds can hinder cell motility.

To quantitatively measure the ability of cosmosiin and angolensin to inhibit cell migration, transwell assays were employed. Figure 5C shows that 10 μM angolensin can inhibit the ability of PC3 cells to migrate through the pore, and this inhibition of migration is ablated by the ER antagonist ICI 182,780. 1 μM angolensin, a concentration at which ERα/β heterodimers are not transcriptionally active (Fig. 3D), has a negligible effect on cell migration. Both 1 μM and 10 μM cosmosiin can inhibit cell migration through the pore, and this inhibition of migration is ablated by ICI 182,780 (Fig. 5B). These results are recapitulated when the transwell is coated with matrigel (data not shown), indicating that in addition to dampening the ability of PC3 cells to migrate, these compounds are able to dampen the ability of PC3 cells to invade.

The abilities of these lead compounds to influence apoptosis in PC3 cells were next evaluated using caspase 3/7 assays. PC3 cells were incubated with the indicated concentrations of DMSO vehicle (0.1%), the indicated concentrations of cosmosiin or angolensin (Fig. S1A and S1B), or the positive control cisplatin (10 μg/mL) for 24, 48, and 72 hours. Cisplatin did not activate the caspases 3/7 pathway at 24 hours and 48 hours (data not shown); only at 72 hours was a weak induction of the caspases 3/7 observed (Fig. S1). At no time point did these compounds reveal any activation of the caspase 3/7 pathway. Thus, it appears that cosmosiin and angolensin are not strong inducers of apoptosis, at least through the caspase 3/7 pathway.

Determination of the growth effects of compounds in PC3, PC3-shERα, PC3-shERβ cells

To determine if these compounds also inhibit cell proliferation in addition to migration, MTT assays were employed. This assay measures mitochondrial activity when yellow MTT (3-(4,5-Dimethylthiazol-2-yl)-2,5-diphenyltetrazolium bromide) is reduced to its purple formazan metabolic product [37]. Thus, the ability of a cell to metabolize MTT to formazan is correlated to its metabolic activity and cellular growth. To show that PC3 cells express functional ERs and that E2's cellular effects are ER-dependent, we compared E2's growth effects in PC3, PC3-shERα, PC3-shERβ cell lines. As shown in other ERα and ERβ co-expressing cell lines [14], E2 exhibits no effects in proliferation of PC3 (Fig. S2A). However, when ERβ expression was blocked, E2 induced proliferation (Fig. S2C) and E2's proliferative effects were completely abrogated by the pure ER antagonist ICI 182,780 and the ERα selective antagonist MPP dihydrochloride (Fig. S2C, *middle* and *right* panels). This result recapitulates the previous finding in HC11 mammary epithelial cells that ERα drives

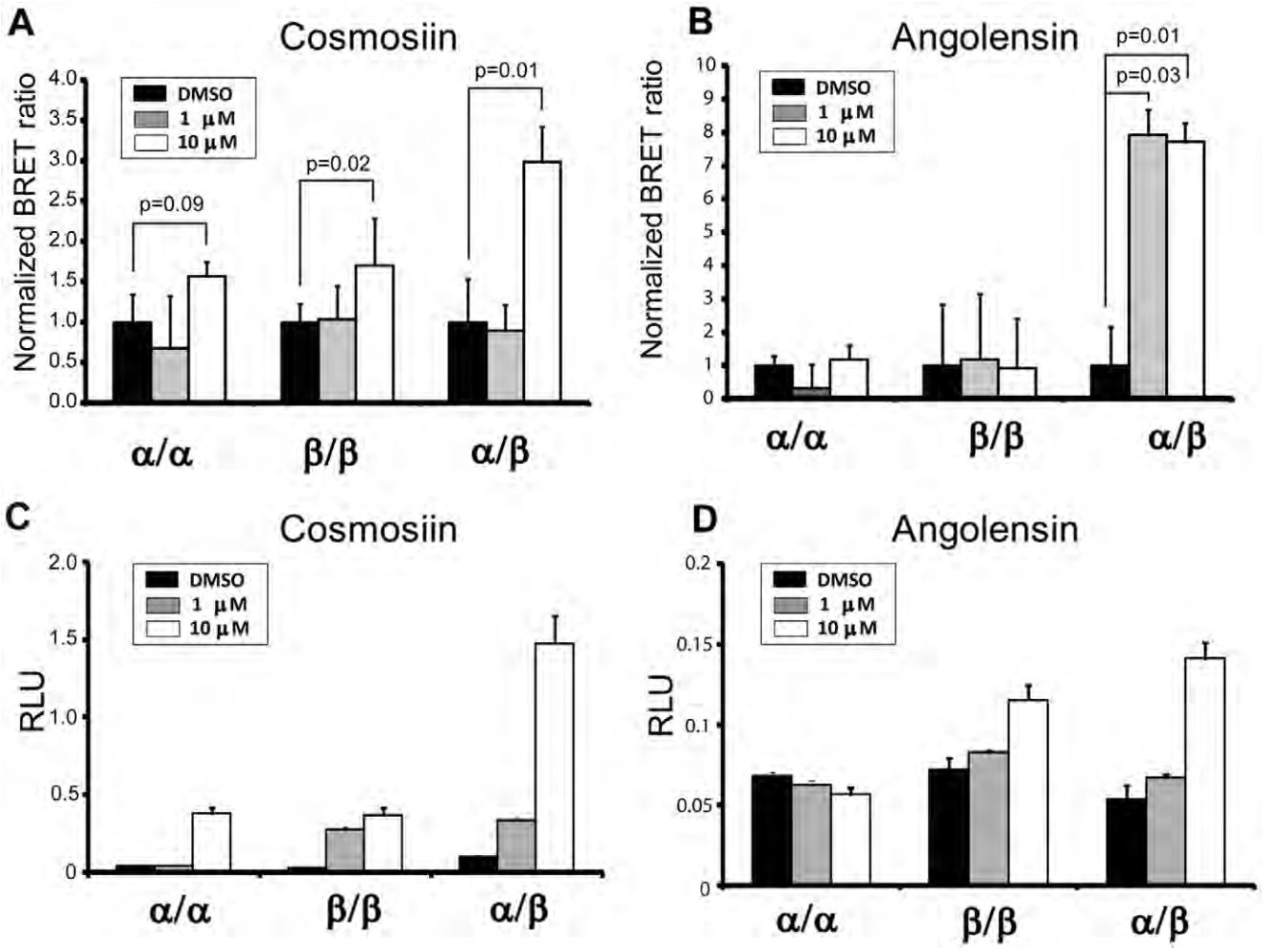

Figure 3. The dimer selectivity for cosmosiin and angolensin was demonstrated in dose-response BRET assays (A and B) and reporter assays (C and D) in HEK293 cells. ER dimer-specific BRET assays were performed over a range of compound concentrations of cosmosiin (A) and angolensin (B). HEK293T ERE-luciferase transcriptional assays reveal each compound's ability to transcriptionally activate various dimer pairs (C and D). ERα alone, ERβ alone, or ERα+ERβ was transfected along with an ERE-luciferase element in order to test the ability of cosmosiin (C) and angolensin (D) to transcriptionally activate these various ER dimer pairs. RLU, relative luciferase units. Error bars represent standard deviations from the mean of triplicate samples. In BRET (A), p values indicate all pairs with statistical significance by the Student's T-Test.
doi:10.1371/journal.pone.0030993.g003

proliferation in response to E2 [14]. It appears that silencing ERβ in PC3 cells causes the cells to respond to E2 with increased proliferation, similar to breast cancer cells [19,28]. In contrast to HC11 where ERβ is growth inhibitory, knockdown of ERα did not result in E2-dependent growth inhibition (Fig. S2B). The discrepancy might be due to cell line specific effects.

The cellular effects of cosmosiin and angolensin were determined in PC3, PC3-shERα or PC3-shERβ cells at concentrations that display ER selectivity. As shown in Figure 6, both 1 μM and 10 μM cosmosiin (Fig. 6A) and 10 μM angolensin (Fig. 6B) were able to inhibit the growth of PC3 cells compared to the vehicle DMSO. The inhibition of growth due to 10 μM angolensin was ablated by the antagonists ICI 182,780, indicating that this response is ER-specific. The inhibition of growth by 1 μM cosmosiin was also ER-specific. However, the inhibition of growth by 10 μM cosmosiin was not ablated by the antagonist, indicating that this response is not ER-specific in PC3 cells and is likely due to off-target effects or non-genomic ER signaling. Cell counting and viability assays with Trypan blue staining ruled out the possibility of general cytotoxicity due to these compounds (Fig. S3A, S3B).

In PC3-shERα cells, ERβ is the only functional ER present; thus, ERβ/β homodimers are the only ER dimers capable of forming and activating transcription. The growth inhibition observed by 1 μM cosmosiin (Fig. 6C) and 10 μM angolensin (Fig. 6D) in the parent PC3 cells is ablated with the loss of ERα in PC3-shERα cells. The addition of the ER antagonist ICI 182,780 had no effect on this cell line in the presence of 1 μM cosmosiin and 10 μM angolensin compared to these ligands alone. However, 10 μM cosmosiin was still able to inhibit the growth of these PC3-shERα cells in both the absence and presence of the ER antagonist ICI 182,780 (Fig. 6C). Thus, 10 μM cosmosiin is confirmed to have off-target, ER non-specific influences on growth regulation.

In PC3-shERβ cells, ERα is the only functional ER present; thus, ERα/α homodimers are the only ER dimers capable of forming and activating transcription. As shown in Figure 6F, angolensin has a negligible effect in this cell line, and treatment with the ER antagonist ICI 182,780 completely ablates any growth effects observed in the presence of this compound. This finding is consistent with angolensin's high degree of ERα/β heterodimer selectivity. However, contrary to observations in PC3

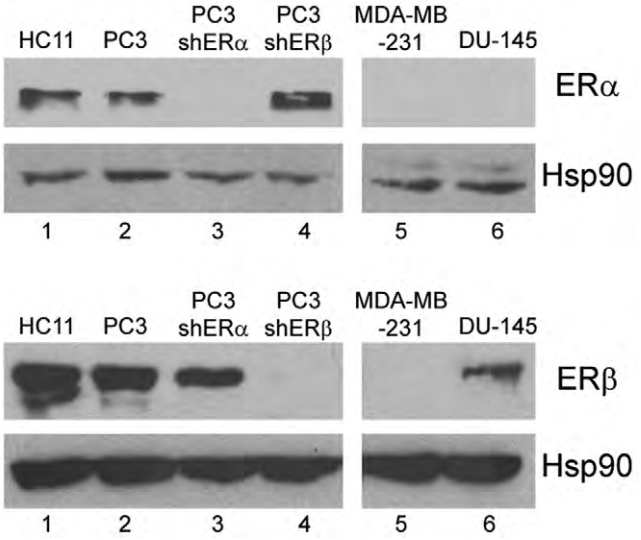

Figure 4. Determination of relative expression levels of ERα and ERβ in various cell lines. Western blotting analyses of ERα and ERβ expression in HC11 (lane 1), PC3 (lane 2), PC3shERα (lane 3), PC3shERβ (lane 4), MDA-MB-231 (lane 5), and DU145 (lane 6).
doi:10.1371/journal.pone.0030993.g004

cells and PC3shERα cells, cosmosiin increases the growth of PC3-shERβ cells at both 1 μM and 10 μM (Fig. 6E). The transcriptional activation of ERα/α homodimers is induced with 10 μM cosmosiin in HEK293 ERE-luciferase assays (Fig. 3C), which is in keeping with its ability to increase the growth of PC3-shERβ cells at this concentration. However, the increase in growth due to 1 μM cosmosiin is not predicted by the HEK293 ERE-luciferase assay (Fig. 3C). These data were confirmed with cell counting and viability assays with Trypan blue staining (data not shown). These growth increases in PC3-shERβ cells due to 1 μM cosmosiin are ablated by the antagonist ICI 182,780 (Fig. 6E), suggesting that these growth increases are due to ERα/α homodimers. Intriguingly, treatment with these antagonists in the presence of 10 μM cosmosiin not only ablates the growth increases observed at this concentration, but actually results in decreased growth (Fig. 6E). This inhibited growth in PC3-shERβ cells when ERα is antagonized may be explained by the off-target effects mediated by this compound: when ERα is the only ER present, it is not damped by heterodimerization with ERβ and is instead able to bind cosmosiin to increase cellular growth; however, when ERα is antagonized in this cell line, cosmosiin is free to mediate its off-target growth inhibitory effects, resulting in decreased growth.

The ERα/β heterodimers were found to be growth inhibitory using PC3 derived cell lines and ERα/β heterodimer-selective ligands at concentrations determined to be heterodimer-selective. The effects of ERα/β heterodimer-selective ligands in PC3 cells suggest that 1 μM cosmosiin and 10 μM angolensin are responsible for mediating the physiological responses of ERα/β heterodimers on a cellular level since loss of either ERα or ERβ abrogates growth inhibition at these concentrations (Fig. 6C–F). 10 μM cosmosiin mediates growth inhibitory effects via ERβ/β homodimerization and off-target effects when ERα is lost, and both concentrations of cosmosiin increase growth via ERα homodimers when ERβ is lost. Therefore, the expression levels of ERs appear to be important to the physiological outcome of these ligands at cellular levels.

The growth effects of cosmosiin and angolensin on additional cell lines with differing ERα:ERβ expression ratios

The differing cellular effects in PC3, PC3-shERα, and PC3-shERβ suggest that the ratio of ERα:ERβ may be a determinant for the ability of these dimer-selective ligands to act in a proliferative or anti-proliferative manner. To address this, growth and viability assays in several cell lines with differing expression levels of ERα and ERβ were compared. HC11 is a normal mouse mammary cell line that expresses both ERα and ERβ (Fig. 4A and [14]). As shown in Fig. S3, cosmosiin and angolensin are both able to inhibit the growth of this cell line. Specifically, 1 μM angolensin, a concentration at which ERα/β heterodimers are not predicted to be activated (Figures 3B, D) has no effect on the growth of this cell line, whereas 10 μM angolensin inhibits HC11's growth by ~10% compared to the vehicle DMSO (Fig. S3D), and this inhibition is ablated by the antagonist ICI 182,780, which suggests that this inhibition is ER-specific. Cosmosiin is also able to inhibit the growth of HC11 cells at 1 μM and 10 μM (Fig. S3C). The ~15% inhibition of growth resulting from 1 μM cosmosiin treatment is ablated by the antagonist ICI 182,780, indicating that this response is ER-specific. 10 μM cosmosiin inhibits the growth of HC11 cells by ~25% compared to the vehicle DMSO, and this response is not completely ablated by the antagonist ICI 182,780, indicating that the inhibition of proliferation by 10 μM cosmosiin is not ER-specific in agreement with earlier findings (Fig. 6A and 6D). Cell counting and viability assays with Trypan blue staining confirmed these findings of growth inhibition and indicated that they were not due to general cytotoxicity (Fig. S3A and S3B). The growth inhibitory effects of 1 μM cosmosiin and 10 μM angolensin in HC11 cells support the notion that ERα/β heterodimers are growth inhibitory. Furthermore, we examined the compounds' effects on ERα−/ERβ− cell line MDA-MB-231 and ERα−/ERβ+ DU-145. Neither compound has any effect on cell growth at all tested concentrations in MDA-MB-231 breast cancer cells (Fig. S4) nor DU-145 prostate cancer cells (Fig. S5). This result suggests that the growth effects exerted by compounds are ERα and ERβ-dependent in breast and prostate epithelial cells. This conclusion is supported by the findings that growth effects elicited by 1 μM cosmosiin and 10 μM angolensin could be completely antagonized by ER antagonist in PC3, PC3-shERα, and PC3-shERβ cells (Fig. 6).

Nuclear co-localization of ERα and ERβ in human breast tumor specimen

Our studies indicate that cosmosiin and angolensin could be therapeutically useful for inhibiting the growth of breast cancer cells that co-express ERα and ERβ. Although previous studies have shown 60% of ERα-positive breast tumors express ERβ [11,21], in order for ERα/β heterodimerization to occur, ERα and ERβ must be co-expressed in the same cell. To investigate the co-expression of ERα and ERβ in breast tumor samples, we analyzed a breast cancer tissue microarray (TMA) using the quantitative immunofluorescence AQUA® technology (HistoRx) that allows the quantitative measurement of proteins of interest within subcellular location of tissue samples by calculation of an AQUA® score. Such precision is not possible with conventional testing methods, such as standard immunohistochemistry (IHC). This TMA was purchased from US Biomax (BR2082) and contained 32 cases of metastatic carcinoma, 68 cases of invasive ductal carcinoma, 22 cases of invasive lobular carcinoma, 22 cases of intraductal carcinoma, 4 cases each of squamous cell carcinoma and lobular carcinoma in situ, 8 cases of fibroadenoma, 16 cases each of hyperplasia and inflammation, 10 cases of cancer adjacent

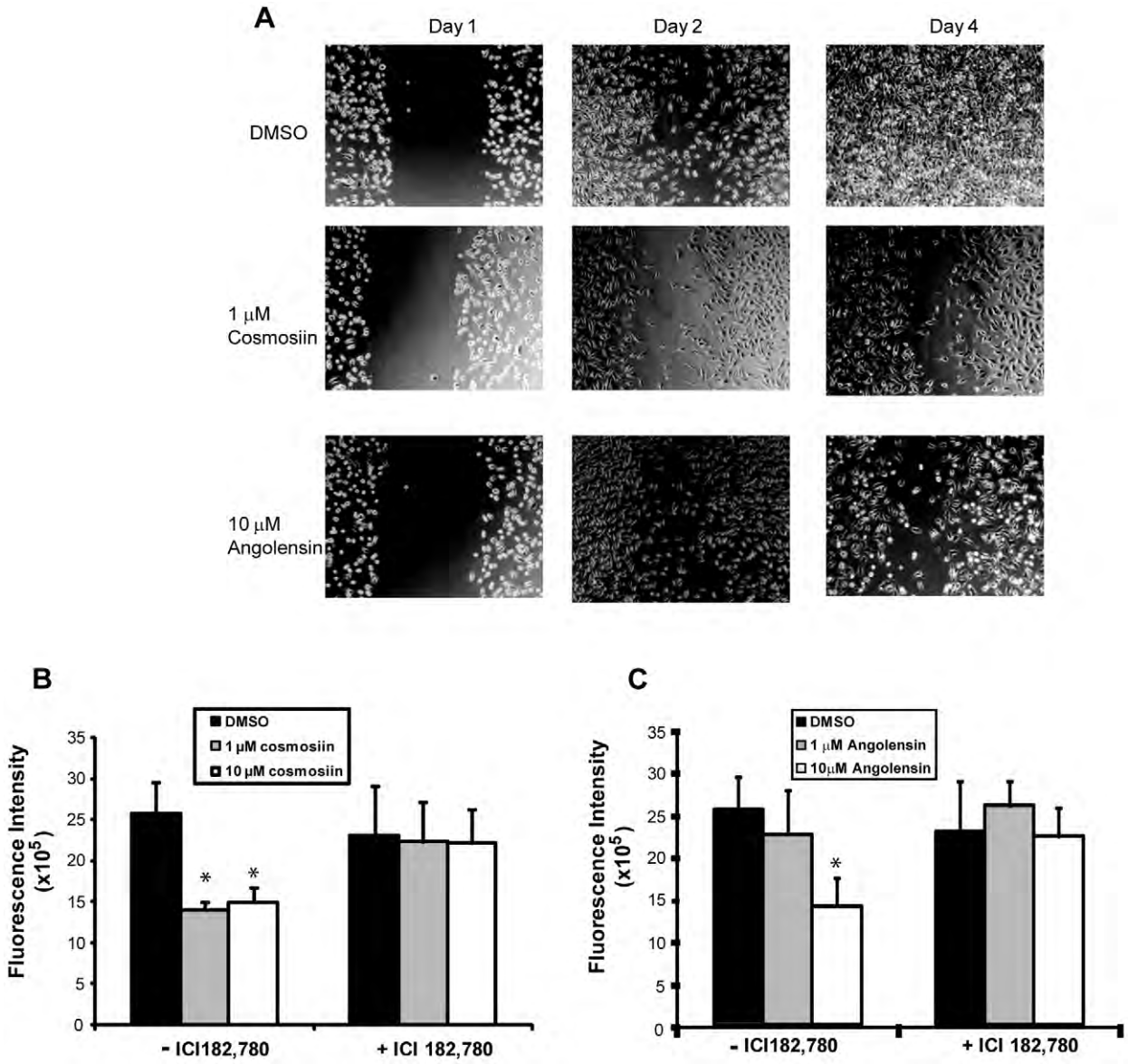

Figure 5. Cosmosiin and angolensin inhibit PC3 cell motility and migration. (A) Wound healing assays showing the effect of 1 μM cosmosiin and 10 μM angolensin on ERα,β-positive PC3 cells. Vehicle (DMSO) treatment resulted in cell motility to fill the wound (*top panels*) that was inhibited by 1 μM cosmosiin (*middle panels*) and 10 μM angolensin (*bottom panels*). (B) Transwell migration assays measured the ability of cosmosiin (B) and angolensin (C) to inhibit cellular migration of PC3 cells toward a chemoattractant. Cosmosiin (B) and angolensin (C) decreased the ability of PC3 cells to migrate through the pore, and this decreased ability was ablated by the antagonist ICI 182,780 at 100 nM.
doi:10.1371/journal.pone.0030993.g005

normal breast tissue (NAT) and 6 cases of normal tissue. A total of 208 cores were analyzed for nuclear ERα and ERβ intensity with DAPI and β-actin staining as references. As shown in Fig. 7A, the ERα/ERβ ratio increases throughout the stages of carcinogenesis and progression. Pairwise analysis with two-sample t-tests of benign tissue versus hyperplasia (p-value = 0.0039) and versus carcinoma (in situ, inflammation, metastatic, and malignant cases with p-values 0.0092, 0.0035, 0.0042, respectively) indicate that this ratio is significantly higher in cases of hyperplasia and carcinoma compared to benign tissue. Figure 7B shows that ERα and ERβ colocalize within the nucleus of the same cell in tissue samples. Overlaying the high resolution images (Fig. 7B, *right*) for ERα staining with those for ERβ staining shows that ERα and ERβ co-localize to the same spots within the same nucleus, rendering the possibility that ERα/β heterodimerization is feasible in these tissues.

Discussion

While the roles of ERα and ERβ in hormone-dependent diseases such as breast and prostate cancers are becoming increasingly elucidated, with ERα having a proliferative and ERβ having an anti-proliferative role, the mechanism by which these two receptors interact with each other in both normal and diseased states has remained elusive. Because the co-expression of ERβ along with ERα dampens the proliferative action of ERα, direct interaction of ERα and ERβ is thought to convey growth inhibitory effects, and the ERα/β heterodimer has been proposed to activate target genes mediating these anti-proliferative effects [38,39]. However, the heterogeneous population of dimer pairs present when ERα and ERβ are co-expressed and the lack of full length heterodimerized ER structures prevent a clear understanding of their biological function.

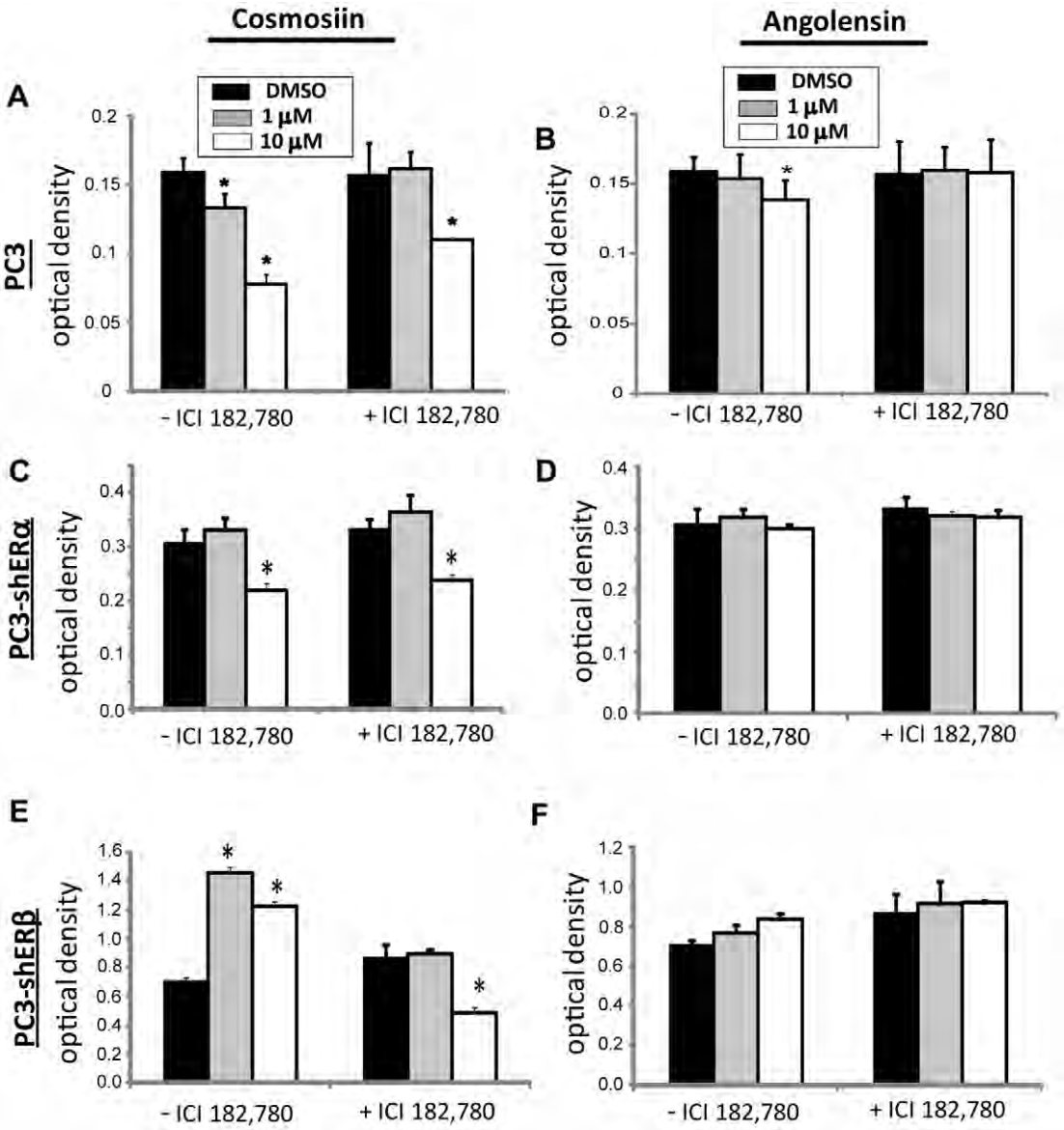

Figure 6. ER dimer-selective compounds influence cell growth in an ER-dependent and dose-dependent manner. Cosmosiin (A) and angolensin (B) decrease the growth of PC3 prostate cancer cells in a dose-dependent manner. These decreases are ER-specific for 1 μM cosmosiin and 10 μM angolensin, since the growth decreases are ablated by the ER antagonist ICI 182,780. These ER-specific effects by 1 μM cosmosiin (C) and 10 μM angolensin (D) are lost with the silencing of ERα in PC3-shERα cells, while ER non-specific effects due to 10 μM cosmosiin are retained. Silencing ERβ in PC3-shERβ results in cosmosiin-dependent increases in cell growth (E) that are ablated in the presence of the antagonist, and furthermore, when ERs are antagonized, ER non-specific growth inhibition in PC3-shERβ is retained. Angolensin has no statistically significant effects in PC3-shERβ (F). Error bars represent standard deviations from the mean of triplicate samples. * indicates statistical significance by the Student's T-Test.
doi:10.1371/journal.pone.0030993.g006

Thus, in order to shed light upon the biological action of these ERα/β heterodimers, we sought to identify small molecule ligands capable of specifically inducing heterodimers while not inducing ERα/α homodimers or ERβ/β homodimers with the rationale that these ligands could be used to decipher the biological action of ERα/β heterodimers.

The BRET technology developed in our lab [34,35] allowed the examination of each ER dimer pair (ERα/α homodimers, ERβ/β homodimers, and ERα/β heterodimers) in isolation. This segregation was especially essential in the case of the ERα/β heterodimer, as the co-expression of ERα and ERβ leads to the formation of all three dimer forms and prevents separation of the action of each individual dimer pair as they function in concert *in vivo*. However, the BRET assay allows the examination of ERα/β without observing homodimer formation. Specifically, we have previously shown that two phytoestrogens, genistein and liquiritigenin, preferentially induce different ER dimers [34]. Liquiritigenin selectively induced formation of ERβ/β homodimers and ERα/β heterodimers but not ERα/α homodimers at 1 μM [34], which provides proof-of-principle that small molecule compounds which preferentially induce ERα/β heterodimers over ERα/α homodimers do indeed exist. We had further shown that BRET assays can be optimized for HTS [35]. The goal of secondary HTS BRET screening in this study was to find a compound with similar characteristics to liquiritigenin but with greater ERα/β heterodimer selectivity. If a library compound was able to induce ERα/β

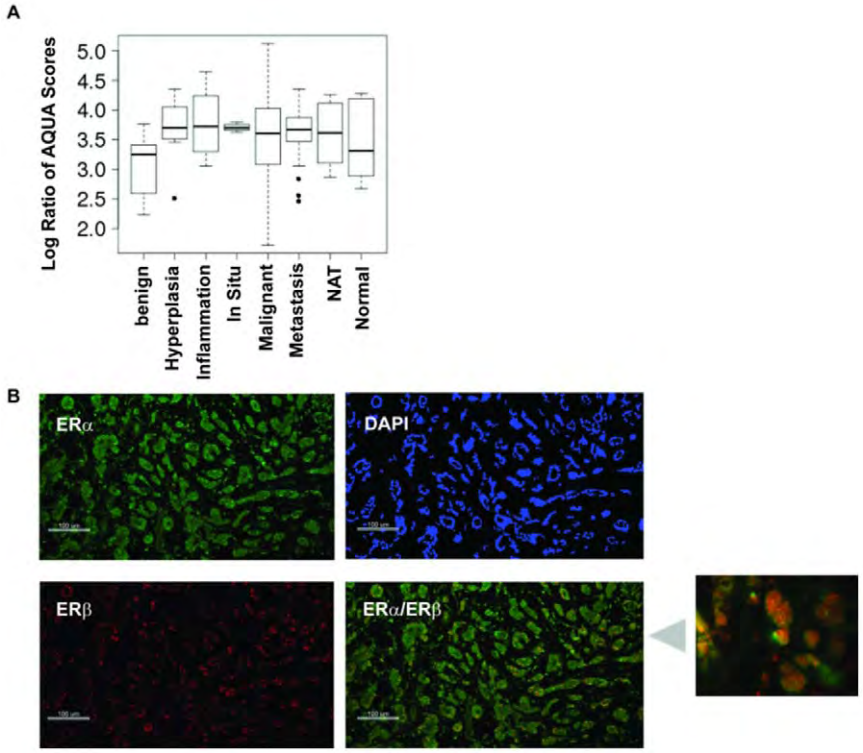

Figure 7. Automated quantitative measurement of ERα and ERβ expression in breast cancer tissue microarrays. (A) Tissue microarray analysis with the AQUA® technology shows that the ERα:ERβ ratio increases from benign samples throughout various stages of malignancy. Pairwise two-sample t-tests between the benign and malignant samples showed a statistically significant difference (p-values<0,01). (B) AQUA® analysis indicates that ERα and ERβ colocalize to the nucleus within the same cell in human breast tumors. Figures are shown at 200× magnification, and scale bars are present in the lower left corners of each image. The blow-up picture is an amplified section of AQUA staining showing co-localization of ERα and ERβ to the nucleus. * indicates statistical significance by the Student's T-Test. NAT = cancer adjacent normal breast tissue.
doi:10.1371/journal.pone.0030993.g007

heterodimerization while not inducing ER homodimerization, the ligand could be used in biological systems to determine the function of these heterodimers with minimal interference from either homodimer.

Two lead compounds were successfully identified in BRET screening. The two lead compounds are flavonoids, a group of potentially chemoprotective compounds widely distributed in fruit, vegetables, and beverages of plant origin including tea and wine, and have similar structures that consist of two phenolic benzene rings linked to a heterocyclic pyre or pyrone [40]. Isoflavones represent an important group of phytoestrogens and are found mainly in plants belonging to the Leguminosae family. Angolensin (*Trifolium pretense*, 2′,4′-dihydroxy-4″-methoxy-α-methyldeoxybenzoin, 1-(2,4-dihydroxyphenyl)-2-(4-methoxyphenyl)propan-1-one; CAS 642-39-7), is an isoflavone that was first isolated from the wood of *Pterocarpus angolensis* and later from the wood and bark of *Pterocarpus indicus*. Angolensin is a metabolite of Biochanin A and formononetin, which are present in red clover [41,42]. Dietary supplements manufactured from red clover are widely marketed to provide beneficial health effects of isoflavones without dietary changes. Specifically, red clover supplements are often consumed for the purported alleviation of post-menopausal symptoms. Cosmosiin (apigenin 7-O-beta-glucoside; apigenin-7-D-glucoside; apigenin-7-O-beta-D-glucopyranoside; apigenin-7-glucoside; cosmetin, Cosmosiine, Apigetrin,5-hydroxy-2-(4-hydroxyphenyl)-7-[(2S,3R,4S,5S,6R)-3,4,5-trihydroxy-6-(hydroxymethyl)oxan-2-yl]oxychromen-4-one; CAS 578-74-5) is a flavonoid present in chamomile flowers which are used pharmaceutically and cosmetically for their anti-spasmodic, anti-inflammatory and antimicrobial properties and also as a natural hair dye and fragrance. Cosmosiin has also been isolated from *Veratrum grandiflorum* (white hellebore) and *Kummerowia striata* (Korean clover). Cosmosiin has been shown to exhibit anti-inflammatory properties [43] and has been shown to exhibit HIV antiviral properties [44], although it has not received FDA approval for these purposes. The direct binding of angolensin and cosmosiin to the E2-binding pocket of ERs are observed (Fig. 2). To our knowledge, this is the first demonstration of cosmosiin as an estrogenic compound. Furthermore, we validated ERα/β-heterodimer specificity using BRET and reporter assays and showed that 1 μM cosmosiin and 10 μM angolensin are specific to ERα/β-heterodimers (Fig. 3).

Using ERα/β-heterodimer selective compounds at specific concentrations, we are able to show that the ERα/β-heterodimer is growth inhibitory. These compounds inhibit cell proliferation in HC11 and PC3 cells which co-express ERα and ERβ. Inhibition of cell growth (Fig. 6) and migration (Fig. 5) due to 1 μM cosmosiin and 10 μM angolensin is ablated with treatment of ICI 182,780 or the silencing of either ERα or ERβ in PC3-shERα and PC3-shERβ, respectively. These compounds, however, did not have an effect on ER-negative MDA-MB-231 and ERα-negative/ERβ-positive DU-145 cells, further supporting that the growth inhibitory effects observed with these compounds were dependent on expression of both ERα and ERβ. While these compounds appear to have little or no effect on ERα/α homodimerization and transcriptional activation in HEK293 BRET and ERE-luciferase assays employing exogenous ERs (Fig. 3), treatment of breast and prostate cancer cells expressing ERα at a much higher level than ERβ (PC3-shERβ) results in ERα-dependent growth increases

(Fig. 6E). This result is in agreement with the common theme that ERα is a major growth driver, and it also implicates the dependence of these compounds' growth effects on the relative expression ratio of ERα:ERβ, as these compounds ablate growth increases in PC3 and HC11, in which ERα and ERβ expression levels are relatively similar and heterodimerization may be favored [31]. Taken together, these data suggest that the ratio of ERα:ERβ in the same tumor cells is extremely important for physiological effects of these compounds. While the data presented herein provide initial evidence for a growth-inhibitory function of the ERα/β heterodimer, identification of higher affinity compounds with greater ERα/β heterodimer selectivity will be needed to validate our findings since both compounds are weak agonists, and cosmosiin at 10 μM appears to have off-target effects.

Compounds exhibiting ERα/β heterodimer-selectivity may have therapeutic or preventive efficacy in hormone-dependent diseases. A recent study shows that the tamoxifen metabolite endoxifen is capable of degrading ERα [45], stabilizing ERβ, and inducing ERα/β heterodimerization in a concentration dependent manner [46]. Tamoxifen is a widely-utilized FDA-approved breast cancer treatment and prevention drug. This finding suggests that tamoxifen's cancer preventive effects may be mediated by stimulation of ERα/β heterodimer formation. The possibility is supported by the fact that both ERs are expressed in normal mammary epithelial cells [4]. Similarly, naturally-occurring estrogen-like compounds such as phytoestrogens, a group of plant-derived compounds with estrogenic and/or antiestrogenic activities hold promise for action as preventive or therapeutic ER-regulators via their abilities to mediate estrogenic responses tissue-specifically. Indeed, consumption of soy phytoestrogens has been correlated with decreased breast cancer risk [47], although these data remain somewhat controversial [48]. Furthermore, consumption of genistein [49], resveratrol [50], and soy [51] has been inversely correlated with prostate cancer risk. Although these compounds may stimulate the proliferative action of ERα when ERβ is lost in tumors, they may have preventative effects under normal physiological conditions when both ERs are expressed.

Furthermore, our examination of nuclear co-localization of ERα and ERβ within the same tumor cell using the AQUA® technology (Fig. 7) support that ERα/β heterodimerization could potentially occur within tumor cells. Prior to these studies, the co-localization of ERα and ERβ within the same cell had not been examined. The punctate staining pattern suggests that ERα and ERβ are co-localized on DNA, and therefore may be transcriptionally active in these cells as ERα/β heterodimers. Furthermore, AQUA® analysis showed that the ERα:ERβ ratio is higher in malignant states compared to benign tissue samples, in agreement with the finding that ERβ levels often decrease in malignant breast cancers [52]. The growth inhibitory effects of ERα/β heterodimers might due to their activation of different target genes from their respective homodimers. Recently, global ChIP-Seq analyses of ERα and ERβ target genes show that perfectly or imperfectly palindromic EREs are preferential binding sites for ERα/β heterodimers as compared to ERα/α or ERβ/β homodimers which are more flexible in DNA recognition [53]. This is consistent with other reports that ERα/β heterodimers might regulate distinct genes [32,33]. The ERα/β heterodimer-selective ligands identified in this study will allow identification of heterodimer target genes in cells co-expressing ERα and ERβ (e.g. PC3). While our findings implicate the ERα/β heterodimer as a putative preventative and therapeutic target for hormone-responsive cancers, this example highlights the imminent need to decipher the role these heterodimers in breast and prostate cancers.

In conclusion, these data provide a proof-of-principle that ERα/β heterodimer-selective ligands can inhibit cell growth and migration in ERα/ERβ-positive cells such as PC3 and HC11 when ERα and ERβ are expressed at similar levels. We also found that the compounds' growth effects depend on the relative expression levels of ERα and ERβ. Upon knockdown of ERβ in PC3 cells, cosmosiin increases PC3 cell growth in an ERα-dependent manner. Thus, more heterodimer selective ligands need to be identified to clarify whether the heterodimer-selective ligands become growth stimulatory when ERβ expression is lost in human tumors. Although more studies are needed to demonstrate the ERα/β heterodimer as a therapeutic target, the concept of inducing ERβ to pair with ERα, thus antagonizing ERα's proliferative function, is distinct from existing breast cancer therapeutic strategies of targeting ERα alone. We also suggest that the relative ERα and ERβ expression levels in patient tumors should be carefully evaluated to better understand the ER-targeted drugs' therapeutic performance, as many of these drugs have not been evaluated for their dimer selectivity, and ERβ expression in patient tumors is not routinely evaluated.

Materials and Methods

High Throughput Screening Methods

All primary and secondary screens were performed at the University of Wisconsin Carbone Cancer Center (UWCCC) Keck Small Molecule Screening Facility (SMSF). Ten thousand T47D-KBLuc cells [54] were seeded into 384-well plates and allowed to attach overnight. The next day, 0.5 μl of 1 mM compound was added to a final concentration of 10 μM using an automated robotic system (Beckman Biomek FX). 10 nM E2 and 1% (0.5 μl) DMSO were used as positive and negative controls, respectively. Cells were incubated with compound for 18 hrs at 37°C in 5% CO_2 in a cell culture incubator. On day 3, media were removed, and 25 μl lysis buffer (Promega, cat# E2661) was added to each well using the robot. Cells were allowed to lyse for 10 min with constant agitation, and lysis was confirmed by microscopically viewing a clear-bottom 384-well plate maintained in parallel under identical conditions. 25 μl luciferase substrate (Promega, Cat# E2620) was then added, mixed for 30 seconds, and luciferase emission was immediately detected on a Tecan Safire 2 plate reader at 0.1 seconds per well. Counter-screening was performed in a similar fashion in the presence and absence of the ER antagonist ICI 182,780. Secondary Bioluminescence Resonance Energy Transfer (BRET) screening was performed in transiently transfected HEK293 cells (ATCC, CRL-1573). DNA encoding BRET fusions were transfected as described in [34]. Following 24 hours of protein expression after transfection, cells were trypsinized and counted using a Nexcelcom Cellometer, and cell viability was determined to be >95% in each condition. Cells were seeded at 11,000 cells per well of 384-well white-walled white-bottom plates in 40 μL PBS. 0.2 μL of 1 mM library compound was then added to each well using the Biomek FX Robot such that the final concentration per well was 5 μM. Cell suspensions were incubated with library compounds for 1 hour in a dark cabinet at room temperature, at which point 10 μL of the Renilla Luciferase (RLuc) substrate coelenterazine h was added to a final concentration of 5 μM. Plates were then gently shaken on a plate shaker for 10 seconds at 300 rpm, and RLuc emission was read at 460 nm followed immediately by YFP emission at 535 nm at 0.1 second per wavelength read per well. Each RLuc and YFP emission measurement was taken consecutively per well before moving to the next well. Emission values were used to calculate the BRET ratio as described in [34]. Additional details for BRET screening were described in [35].

In vivo BRET assays to monitor ER dimer formation in living cells

HEK293 cells (ATCC, CRL-1573) were either transfected with a single BRET fusion plasmid (pCMX-ERα-RLuc or pCMX-RLuc-ERβ) or co-transfected with RLuc and YFP BRET fusions (pCMX-ERα-RLuc+pCMX-YFP-ERβ for ERα/ERβ heterodimers; pCMX-ERα-RLuc+pCMX-ERα-YFP for ERα homodimers; or pCMX-RLuc-ERβ+pCMX-YFP-ERβ for ERβ homodimers) [34]. "Empty" expression vector pCMX-pL2 was used to keep the total amount of transfected DNA constant. 24 hr post-transfection, cells were trypsinized, counted, and resuspended in PBS in quadruplicate at ~50,000 cells per well of a 96-well white-bottom microplate. Cells were incubated with ligands for 1 hour. Coelenterazine h (Promega, Madison, WI) was added in PBS at a final concentration of 5 μM, and 460 nm and 530 nm emission detection measurements were immediately taken at 0.1 second per wavelength read per well on a Perkin Elmer Victor 3-V plate reader.

Immunofluorescence Staining

Deparaffinization and heat induced epitope retrieval were performed simultaneously using the Lab Vision PT module (Thermo Fisher Scientific, Fremont, CA) with Lab Vision citrate buffer pH 8.0 at 98°C for 20 minutes. All staining was performed at room temperature using the Lab Vision 360 automated staining system. Endogenous peroxidase was blocked for 5 minutes with Peroxidazed-1 (Cat.No. PX968, Biocare Medical). Non-specific protein binding was eliminated via a 60 minute block with Biocare Medical Sniper, and non-specific avidin was blocked using Biocare Medical Avidin Biotin kit, incubating 15 minutes. DaVinci Green Antibody Diluent (Cat.No. PD900L, Biocare Medical) was used for antibody dilution. Breast TMA BR2082 containing 208 cores was purchased from US Biomax Inc. (http://www.biomax.us/tissue-arrays/Breast/BR2082). ERα was detected using ERα rabbit mAb SP1 (1:50, 1 hr) (Thermo Fisher) and visualized with goat anti-rabbit conjugated with Alexa Fluor 555 (Invitrogen) secondary antibody. ERβ was detected with mouse mAb 14C8 (Abcam,1:1600, 1 hr) and visualized with Alexa Fluor 647 conjugated Tyramide Signal Amplification system (Invitrogen), which included biotinylated goat anti-mouse immunoglobulin, streptavidin-horseradish peroxidase and Alexa Fluor 647-Tyramide. Breast epithelial nuclei were masked using ProLong Gold Antifade Reagent with DAPI mounting medium (Invitrogen).

Automated Image Acquisition

Automated image capture was performed by the HistoRx PM-2000 using the AQUAsition software package (New Haven, CT). High-resolution (2048_2048 pixel, 7.4 mm), 8-bit grayscale digital images are obtained for each area of interest resulting in 256 discrete intensity values per pixel of an acquired image [55]. The breast epithelial nuclear compartment was defined with DAPI (blue). The target markers (ERα and ERβ) were visualized with Alexa Fluor 555 (green) and 647 (red), respectively.

AQUA ® Score Generation

Since the distributions of the original AQUA® scores exhibited deviation from the normal distribution, we took the natural log transformation of the original scores and then performed two sample t-tests for pairwise comparisons among different samples. Results from these tests were consistent with a Wilcoxon rank sum test on the original scores. Images were evaluated before scoring. Histospots showing <5% tumor area, tissue folding, too much debris, and those that were out of focus were disqualified from scoring. Nuclear AQUA® scores for ERα and ERβ for each histospot were generated based on the unsupervised pixel-cased clustering algorithm for optimal image segmentation for use in the pixel-based locale assignment for compartmentalization of expression algorithm as described previously [56]. Pixels that could not accurately be assigned to a compartment were discarded. The data were saved and subsequently expressed as the average signal intensity per unit of compartment area. All the signals in each compartment were then added. The AQUA® score is expressed as target signal intensity divided by the compartment pixel area and is expressed on a scale of 0 to 33333 (AQUA_2.0, HistoRx). The resultant AQUA® score is continuous and directly proportional to the number of molecules per unit area.

Additional descriptions of cell culture, TMA and experimental procedures can be found in **Methods S1**.

Supporting Information

Figure S1 Caspase 3/7 apoptosis assays showed that cosmosiin and angolensin exhibited no apoptotic effect via caspases 3 or 7 in PC3 cells at 96 hours. Cosmosiin (A) and angolensin (B) modestly increase apoptosis through this pathway in PC3 cells to a statistically non-significant level compared to the strong apoptotic inducer cisplatin, which served as a positive control. Statistical analysis method: Students T-Tests. Error bars represent standard deviations from the mean of triplicate samples.
(TIF)

Figure S2 MTT assays showing the effect of 10 nM 17β-estradiol in ERα,β-positive PC3 cells and variants of these cells in which ERα has been silenced (PC3-shERα) or ERβ has been silenced (PC3-shERβ). E2 has no effect on the proliferation of PC3 cells (A) or PC3-shERα cells (B); however, the silencing of ERβ in this cell line allows E2 to increase cellular growth (C, left panel) by binding to ERα, since the presence of the antagonists ICI 182,780 (C, middle panel) and MPP Dihydrochloride (C, right panel) ablates this increase. Statistical analysis method: Students T-Test; * indicates $p<0.05$. Error bars represent standard deviations from the mean of triplicate samples.
(TIF)

Figure S3 Cosmosiin at 1 μM and angolensin at 10 μM inhibited the growth of ERα/ERβ positive HC11 cells in an ER-dependent manner. Cosmosiin (A) and angolensin (B) had no cytotoxic effects at all tested concentrations. The growth inhibitory effects of cosmosiin at 1 μM (C) and angolensin at 10 μM (D) were ablated by pure ER antagonist ICI 182,780, suggesting the growth inhibitory effects are ER-dependent. These decreases due to 10 μM cosmosiin are ER-independent since they are retained in the presence of the antagonist ICI 182,780 (C). Statistical analysis method: Students T-Test; * indicates $p<0.05$. Error bars represent standard deviations from the mean of triplicate samples.
(TIF)

Figure S4 Neither cosmosiin (A) nor angolensin (B) influenced the growth of ER-negative MDA-MB-231breast cancer cells. Error bars represent standard deviations from the mean of triplicate samples.
(TIF)

Figure S5 Neither cosmosiin (A) nor angolensin (B) influenced the growth of ERα-negative, ERβ-positive DU-145 prostate cancer cells. Error bars represent standard deviations from the mean of triplicate samples.
(TIF)

Methods S1 Supplemental Methods file.
(DOC)

Acknowledgments

We thank Thomas Pier of UW TRIP lab for immunohistochemistry assistance and Jiacai Wu for help with construction of PC3shERα and PC3shERβ cell lines and graphics. We thank Yidan Wang for technical support. We are grateful to Drs. Elaine Alarid and William Ricke for critical reading of the manuscript.

Author Contributions

Conceived and designed the experiments: EP ES AB. Performed the experiments: EP ES AB JL WH. Analyzed the data: EP ES WH SK KW WX. Contributed reagents/materials/analysis tools: WH JL. Wrote the paper: EP WX.

References

1. Heldring N, Pike A, Andersson S, Matthews J, Cheng G, et al. (2007) Estrogen receptors: how do they signal and what are their targets. Physiol Rev 87: 905–931.
2. Deroo BJ, Korach KS (2006) Estrogen receptors and human disease. J Clin Invest 116: 561–570.
3. Nilsson S, Gustafsson JA (2011) Estrogen receptors: therapies targeted to receptor subtypes. Clin Pharmacol Ther 89: 44–55.
4. Shoker BS, Jarvis C, Sibson DR, Walker C, Sloane JP (1999) Oestrogen receptor expression in the normal and pre-cancerous breast. J Pathol 188: 237–244.
5. Hewitt SC, Harrell JC, Korach KS (2005) Lessons in estrogen biology from knockout and transgenic animals. Annu Rev Physiol 67: 285–308.
6. Forster C, Makela S, Warri A, Kietz S, Becker D, et al. (2002) Involvement of estrogen receptor beta in terminal differentiation of mammary gland epithelium. Proc Natl Acad Sci U S A 99: 15578–15583.
7. McPherson SJ, Ellem SJ, Patchev V, Fritzemeier KH, Risbridger GP (2006) The role of Eralpha and ERbeta in the prostate: insights from genetic models and isoform-selective ligands. Ernst Schering Found Symp Proc. pp 131–147.
8. Imamov O, Morani A, Shim GJ, Omoto Y, Thulin-Andersson C, et al. (2004) Estrogen receptor beta regulates epithelial cellular differentiation in the mouse ventral prostate. Proc Natl Acad Sci U S A 101: 9375–9380.
9. Ricke WA, McPherson SJ, Bianco JJ, Cunha GR, Wang Y, et al. (2008) Prostatic hormonal carcinogenesis is mediated by in situ estrogen production and estrogen receptor alpha signaling. FASEB J 22: 1512–1520.
10. Krege JH, Hodgin JB, Couse JF, Enmark E, Warner M, et al. (1998) Generation and reproductive phenotypes of mice lacking estrogen receptor beta. Proc Natl Acad Sci U S A 95: 15677–15682.
11. Jarvinen TA, Pelto-Huikko M, Holli K, Isola J (2000) Estrogen receptor beta is coexpressed with ERalpha and PR and associated with nodal status, grade, and proliferation rate in breast cancer. Am J Pathol 156: 29–35.
12. Zhu X, Leav I, Leung YK, Wu M, Liu Q, et al. (2004) Dynamic regulation of estrogen receptor-beta expression by DNA methylation during prostate cancer development and metastasis. Am J Pathol 164: 2003–2012.
13. Chang EC, Frasor J, Komm B, Katzenellenbogen BS (2006) Impact of estrogen receptor beta on gene networks regulated by estrogen receptor alpha in breast cancer cells. Endocrinology 147: 4831–4842.
14. Helguero LA, Faulds MH, Gustafsson JA, Haldosen LA (2005) Estrogen receptors alfa (ERalpha) and beta (ERbeta) differentially regulate proliferation and apoptosis of the normal murine mammary epithelial cell line HC11. Oncogene 24: 6605–6616.
15. Pettersson K, Delaunay F, Gustafsson JA (2000) Estrogen receptor beta acts as a dominant regulator of estrogen signaling. Oncogene 19: 4970–4978.
16. Lazennec G, Bresson D, Lucas A, Chauveau C, Vignon F (2001) ER beta inhibits proliferation and invasion of breast cancer cells. Endocrinology 142: 4120–4130.
17. Murphy LC, Peng B, Lewis A, Davie JR, Leygue E, et al. (2005) Inducible upregulation of oestrogen receptor-beta1 affects oestrogen and tamoxifen responsiveness in MCF7 human breast cancer cells. J Mol Endocrinol 34: 553–566.
18. Rousseau C, Nichol JN, Pettersson F, Couture MC, Miller WH, Jr. (2004) ERbeta sensitizes breast cancer cells to retinoic acid: evidence of transcriptional crosstalk. Mol Cancer Res 2: 523–531.
19. Strom A, Hartman J, Foster JS, Kietz S, Wimalasena J, et al. (2004) Estrogen receptor beta inhibits 17beta-estradiol-stimulated proliferation of the breast cancer cell line T47D. Proc Natl Acad Sci U S A 101: 1566–1571.
20. Omoto Y, Inoue S, Ogawa S, Toyama T, Yamashita H, et al. (2001) Clinical value of the wild-type estrogen receptor beta expression in breast cancer. Cancer Lett 163: 207–212.
21. Skliris GP, Carder PJ, Lansdown MR, Speirs V (2001) Immunohistochemical detection of ERbeta in breast cancer: towards more detailed receptor profiling? Br J Cancer 84: 1095–1098.
22. Roger P, Sahla ME, Makela S, Gustafsson JA, Baldet P, et al. (2001) Decreased expression of estrogen receptor beta protein in proliferative preinvasive mammary tumors. Cancer Res 61: 2537–2541.
23. Iwao K, Miyoshi Y, Egawa C, Ikeda N, Tsukamoto F, et al. (2000) Quantitative analysis of estrogen receptor-alpha and -beta messenger RNA expression in breast carcinoma by real-time polymerase chain reaction. Cancer 89: 1732–1738.
24. Iwao K, Miyoshi Y, Egawa C, Ikeda N, Noguchi S (2000) Quantitative analysis of estrogen receptor-beta mRNA and its variants in human breast cancers. Int J Cancer 88: 733–736.
25. Paruthiyil S, Parmar H, Kerekatte V, Cunha GR, Firestone GL, et al. (2004) Estrogen receptor beta inhibits human breast cancer cell proliferation and tumor formation by causing a G2 cell cycle arrest. Cancer Res 64: 423–428.
26. Williams C, Edvardsson K, Lewandowski SA, Strom A, Gustafsson JA (2008) A genome-wide study of the repressive effects of estrogen receptor beta on estrogen receptor alpha signaling in breast cancer cells. Oncogene 27: 1019–1032.
27. Frasor J, Chang EC, Komm B, Lin CY, Vega VB, et al. (2006) Gene expression preferentially regulated by tamoxifen in breast cancer cells and correlations with clinical outcome. Cancer Res 66: 7334–7340.
28. Chang EC, Charn TH, Park SH, Helferich WG, Komm B, et al. (2008) Estrogen Receptors alpha and beta as determinants of gene expression: influence of ligand, dose, and chromatin binding. Mol Endocrinol 22: 1032–1043.
29. Saji S, Hirose M, Toi M (2005) Clinical significance of estrogen receptor beta in breast cancer. Cancer Chemother Pharmacol 56 Suppl 1: 21–26.
30. Lindberg MK, Moverare S, Skrtic S, Gao H, Dahlman-Wright K, et al. (2003) Estrogen receptor (ER)-beta reduces ERalpha-regulated gene transcription, supporting a "ying yang" relationship between ERalpha and ERbeta in mice. Mol Endocrinol 17: 203–208.
31. Cowley SM, Hoare S, Mosselman S, Parker MG (1997) Estrogen receptors alpha and beta form heterodimers on DNA. J Biol Chem 272: 19858–19862.
32. Pettersson K, Grandien K, Kuiper GG, Gustafsson JA (1997) Mouse estrogen receptor beta forms estrogen response element-binding heterodimers with estrogen receptor alpha. Mol Endocrinol 11: 1486–1496.
33. Tremblay GB, Tremblay A, Labrie F, Giguere V (1999) Dominant activity of activation function 1 (AF-1) and differential stoichiometric requirements for AF-1 and -2 in the estrogen receptor alpha-beta heterodimeric complex. Mol Cell Biol 19: 1919–1927.
34. Powell E, Xu W (2008) Intermolecular interactions identify ligand-selective activity of estrogen receptor alpha/beta dimers. Proc Natl Acad Sci U S A 105: 19012–19017.
35. Powell E, Huang SX, Xu Y, Rajski SR, Wang Y, et al. (2010) Identification and Characterization of a Novel Estrogenic Ligand Actinopolymorphol A. Biochem Pharmacol 80: 1221–1229.
36. Lau KM, LaSpina M, Long J, Ho SM (2000) Expression of estrogen receptor (ER)-alpha and ER-beta in normal and malignant prostatic epithelial cells: regulation by methylation and involvement in growth regulation. Cancer Res 60: 3175–3182.
37. Mosmann T (1983) Rapid colorimetric assay for cellular growth and survival: application to proliferation and cytotoxicity assays. J Immunol Methods 65: 55–63.
38. Monroe DG, Secreto FJ, Subramaniam M, Getz BJ, Khosla S, et al. (2005) Estrogen receptor alpha and beta heterodimers exert unique effects on estrogen- and tamoxifen-dependent gene expression in human U2OS osteosarcoma cells. Mol Endocrinol 19: 1555–1568.
39. Stossi F, Barnett DH, Frasor J, Komm B, Lyttle CR, et al. (2004) Transcriptional profiling of estrogen-regulated gene expression via estrogen receptor (ER) alpha or ERbeta in human osteosarcoma cells: distinct and common target genes for these receptors. Endocrinology 145: 3473–3486.
40. Aherne SA, O'Brien NM (2002) Dietary flavonols: chemistry, food content, and metabolism. Nutrition 18: 75–81.
41. Heinonen SM, Wahala K, Adlercreutz H (2004) Identification of urinary metabolites of the red clover isoflavones formononetin and biochanin A in human subjects. J Agric Food Chem 52: 6802–6809.
42. Pfitscher A, Reiter E, Jungbauer A (2008) Receptor binding and transactivation activities of red clover isoflavones and their metabolites. J Steroid Biochem Mol Biol 112: 87–94.
43. Fuchs J, Milbradt R (1993) Skin anti-inflammatory activity of apigenin-7-glucoside in rats. Arzneimittelforschung 43: 370–372.
44. Wang HK, Xia Y, Yang ZY, Natschke SL, Lee KH (1998) Recent advances in the discovery and development of flavonoids and their analogues as antitumor and anti-HIV agents. Adv Exp Med Biol 439: 191–225.
45. Wu X, Hawse JR, Subramaniam M, Goetz MP, Ingle JN, et al. (2009) The tamoxifen metabolite, endoxifen, is a potent antiestrogen that targets estrogen receptor alpha for degradation in breast cancer cells. Cancer Res 69: 1722–1727.
46. Wu X, Subramaniam M, Grygo SB, Sun Z, Negron V, et al. (2011) Estrogen receptor-beta sensitizes breast cancer cells to the anti-estrogenic actions of endoxifen. Breast Cancer Res 13: R27.
47. Peeters PH, Keinan-Boker L, van der Schouw YT, Grobbee DE (2003) Phytoestrogens and breast cancer risk. Review of the epidemiological evidence. Breast Cancer Res Treat 77: 171–183.
48. Ju YH, Allred KF, Allred CD, Helferich WG (2006) Genistein stimulates growth of human breast cancer cells in a novel, postmenopausal animal model, with low plasma estradiol concentrations. Carcinogenesis 27: 1292–1299.
49. Mentor-Marcel R, Lamartiniere CA, Eltoum IA, Greenberg NM, Elgavish A (2005) Dietary genistein improves survival and reduces expression of osteopontin

in the prostate of transgenic mice with prostatic adenocarcinoma (TRAMP). J Nutr 135: 989–995.
50. Jones SB, DePrimo SE, Whitfield ML, Brooks JD (2005) Resveratrol-induced gene expression profiles in human prostate cancer cells. Cancer Epidemiol Biomarkers Prev 14: 596–604.
51. Lee MM, Gomez SL, Chang JS, Wey M, Wang RT, et al. (2003) Soy and isoflavone consumption in relation to prostate cancer risk in China. Cancer Epidemiol Biomarkers Prev 12: 665–668.
52. Sugiura H, Toyama T, Hara Y, Zhang Z, Kobayashi S, et al. (2007) Expression of estrogen receptor beta wild-type and its variant ERbetacx/beta2 is correlated with better prognosis in breast cancer. Jpn J Clin Oncol 37: 820–828.
53. Grober OM, Mutarelli M, Giurato G, Ravo M, Cicatiello L, et al. (2011) Global analysis of estrogen receptor beta binding to breast cancer cell genome reveals an extensive interplay with estrogen receptor alpha for target gene regulation. BMC Genomics 12: 36.
54. Wilson VS, Bobseine K, Gray LE, Jr. (2004) Development and characterization of a cell line that stably expresses an estrogen-responsive luciferase reporter for the detection of estrogen receptor agonist and antagonists. Toxicol Sci 81: 69–77.
55. Warren M, Twohig M, Pier T, Eickhoff J, Lin CY, et al. (2009) Protein expression of matriptase and its cognate inhibitor HAI-1 in human prostate cancer: a tissue microarray and automated quantitative analysis. Appl Immunohistochem Mol Morphol 17: 23–30.
56. Gustavson MD, Bourke-Martin B, Reilly DM, Cregger M, Williams C, et al. (2009) Development of an unsupervised pixel-based clustering algorithm for compartmentalization of immunohistochemical expression using Automated QUantitative Analysis. Appl Immunohistochem Mol Morphol 17: 329–337.

Histone H3R17me2a mark recruits human RNA Polymerase-Associated Factor 1 Complex to activate transcription

Jiacai Wu and Wei Xu[1]

McArdle Laboratory for Cancer Research, University of Wisconsin, Madison, WI 53706

Edited by Pierre Chambon, Institut de Génétique et de Biologie Moléculaire et Cellulaire (Centre National de la Recherche Scientifique Unité Mixte de Recherche 7104; Institut National de la Santé et de la Recherche Médicale U596; Université de Strasbourg; College de France), Illkirch-Cedex, France, and approved February 27, 2012 (received for review September 13, 2011)

The histone coactivator-associated arginine methyltransferase 1 (CARM1) is a coactivator for a number of transcription factors, including nuclear receptors. Although CARM1 and its asymmetrically deposited dimethylation at histone H3 arginine 17 (H3R17me2a) are associated with transcription activation, the mechanism by which CARM1 activates transcription remains unclear. Using an unbiased biochemical approach, we discovered that the transcription elongation-associated PAF1 complex (PAF1c) directly interacts with H3R17me2a. PAF1c binds to histone H3 tails harboring dimethylation at R17 in CARM1-methylated histone octamers. Knockdown of either PAF1c subunits or CARM1 affected transcription of CARM1-regulated, estrogen-responsive genes. Furthermore, either CARM1 knockdown or CARM1 enzyme-deficient mutant knockin resulted in decreased H3R17me2a accompanied by the reduction of PAF1c occupancy at the proximal promoter estrogen-responsive elements. In contrast, PAF1c knockdown elicited no effects on H3R17me2a but reduced the H3K4me3 level at estrogen-responsive elements. These observations suggest that, apart from PAF1c's established roles in directing histone modifications, PAF1c acts as an arginine methyl histone effector that is recruited to promoters and activates a subset of genes, including targets of estrogen signaling.

estrogen receptor-α | histone arginine methylation | PRMT

Coactivator-associated arginine methyltransferase 1 (CARM1), also known as PRMT4, is the first protein arginine methyltransferase identified as a coactivator for steroid receptors (1). It was later found to be a coactivator for a variety of transcription factors and is a multifunctional protein engaged in a variety of cellular processes, including gene expression, coupling of transcription with mRNA splicing, regulation of protein stability, and functioning in embryonic development (2). Loss of CARM1 in the mouse embryo leads to abrogation of the estrogen response and reduced expression of some estrogen receptor-α (ERα) target genes (3). Recently, CARM1 was shown to be a unique coactivator of ERα that can simultaneously block cell proliferation and induce differentiation through global regulation of ERα-regulated genes in breast cancer cells (4). The methyltransferase activity of CARM1 is required for its ability to regulate transcription of pS2 (TFF1), a standard ERα target gene (5). Moreover, the enzyme-dead CARM1 knockin mice have defects similar to those seen in their knockout counterparts (6). These observations suggest that the enzymatic activity of CARM1 is indispensable for the majority of CARM1's in vivo functions. Several putative mechanisms have been proposed to explain CARM1 activator function, including histone H3 methylation at arginine 17 (R17), methylation of other key transcription coactivators, and recruitment of chromatin remodeling factors. However, it is unclear which mechanisms drive CARM1 transcription activation function.

CARM1 was originally characterized as a histone arginine methyltransferase because of its ability to dimethylate arginines on histone H3. Subsequent biochemical analyses showed that histone H3 can be modified at R2, R17, and R26 (7). A recent study showed that asymmetrically dimethylated histone H3 at R2 (H3R2me2a) was mainly deposited by PRMT6 (8). ChIP analysis identified elevated levels of H3R17me2a at the estrogen-responsive pS2 promoter (5). Furthermore, kinetic ChIP analysis revealed that CARM1 was recruited in a cyclic manner, occurring at 40-min intervals upon treatment with 17β-estradiol (E2), and recruitment of CARM1 correlated with an increase in the H3R17me2a mark (9). These studies suggest that H3R17me2a likely accounts for CARM1's coactivator function in transcriptional regulation. Because many protein domains have been characterized to specifically bind to modified histone marks, effector molecules may exist that read H3R17me2a marks to mediate transcriptional activation. In support of this hypothesis, a recent study identified one effector protein, TDRD3, as a "reader" for H3R17me2a and H4R3me2a using a protein domain microarray approach (10). TDRD3 contains a tudor domain that is typical for mediating methyl-specific binding. Furthermore, TDRD3 functions as a coactivator in estrogen-responsive elements (ERE)-luciferase reporter assays and endogenous TDRD3 was detectable at the pS2 promoter in ChIP assays (10). Despite these observations, it is unclear how TDRD3 promotes transcriptional activation.

To further elucidate the mechanism by which CARM1 enzymatic activity and H3R17me2a mediate transcription activation, we took an unbiased biochemical approach to identify effector proteins that directly interact with the H3R17me2a mark using peptide pull-down assays from HeLa nuclear extract. We unexpectedly identified the transcription elongation-associated PAF1 complex (PAF1c) in direct association with H3R17me2a and found this association is required for complete activation of CARM1-regulated ERα target genes. Furthermore, PAF1c was detected at EREs, and its occupancy was abrogated by either knockdown of CARM1 or introduction of a CARM1 enzyme-deficient mutant, which was accompanied by the attenuation of H3R17me2a. This study presents a unique mechanism by which H3R17me2a functions to recruit PAF1c to facilitate transcription activation and encrypt a means for PAF1c's recruitment to the promoters of target genes.

Results

Identification of Human PAF1c as a Binding Partner for the Histone H3 Tail Containing the Asymmetrically Dimethylated Arginine 17. To identify proteins that recognize asymmetrically dimethylated arginine 17 at histone H3 (H3R17me2a), we took an unbiased biochemical approach using biotinylated histone tail pull-down from HeLa nuclear extract, according to previously published methods

Author contributions: J.W. and W.X. designed research; J.W. and W.X. performed research; J.W. contributed new reagents/analytic tools; J.W. and W.X. analyzed data; and J.W. and W.X. wrote the paper.

The authors declare no conflict of interest.

This article is a PNAS Direct Submission.

[1]To whom correspondence should be addressed. E-mail: wxu@oncology.wisc.edu.

This article contains supporting information online at www.pnas.org/lookup/suppl/doi:10.1073/pnas.1114905109/-/DCSupplemental.

(11–13). Two histone H3 N-terminal tail peptides encompassing amino acids 1–20, with or without asymmetrically dimethylated R17 (H3R17me2a), were used for pull-down assays. Equal amounts of biotinylated peptides preimmobilized on streptavidin magnetic beads were incubated with HeLa nuclear extract followed by acid elution (12). Eluted proteins were immediately neutralized, loaded on SDS/PAGE, and silver-stained. Fig. 1*A* showed that three bands were specifically associated with H3R17me2a tail compared with the nonmodified H3 tail. This experiment was repeated on a large scale, and the bands were Coomassie-stained, excised, and analyzed by MALDI-TOF MS. Three bands were identified as hCtr9, hCdc73, and hSki8, all of which belong to the same multisubunit PAF1c. The matched peptides sequences are shown in Fig. S1. The PAF1c was originally identified in yeast as a RNA polymerase II (RNAPII)-associated complex mediating transcription elongation (14). The human PAF1c (hPAF1c) has been shown to be involved in multiple steps in transcription, including control of H2B ubiquitination and H3K4me3, transcription initiation and elongation, and pre-mRNA processing (15). Because hPAF1c is composed of five subunits (hCtr9, hLeo1, hPaf1, hCdc73, and hSki8), we speculated that the whole complex (including two missing subunits, hLeo1 and hPaf1) bound to the H3R17me2a tail. Their absence in silver staining (Fig. 1*A*) could be because of inefficient elution or poor staining by silver. The antibodies for individual subunits were used to detect their presence in eluted fractions from 3 biotinylated peptide pull-downs. The results showed that although all PAF1c subunits are strongly detected in H3R17me2a tail pull-down, much weaker PAF1c binding was detected with the nonmodified H3 tail, and no binding was detected with negative control peptide pull-downs (Fig. 1*B*).

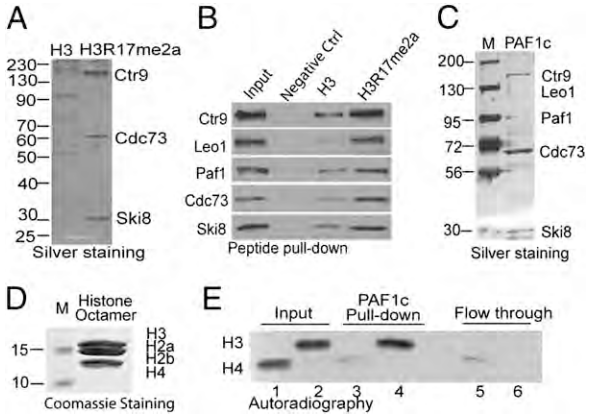

Fig. 1. The RNAPII-associated PAF1c displays binding specificity to asymmetrically dimethylated histone H3R17me2a. (*A*) Immobilized histone H3 tail (amino acids 1–20, *Left*) and the identical peptide carrying asymmetric dimethylated arginine 17 (*Right*) were used to identify specific effectors for the H3R17me2a mark in HeLa cell nuclear extract. Three proteins were specifically pulled down with H3R17me2a and later identified to be hCtr9, hCdc73, and hSki8 by in-gel digestion and mass spectrometry analyses. (*B*) Western blots showed that biotinylated H3R17me2a peptide selectively pull down PAF1c subunits, including Ctr9, Leo1, Paf1, Cdc73, and Ski8. (*C*) The PAF1c was affinity-purified from HEK293-Flag-Cdc73 cells and silver-stained. (*D*) Coomassie staining of the reconstituted histone octamers. (*E*) PAF1c preferentially interacts with CARM1 methylated histone octamers, which were reconstituted from bacterially expressed histone H3, H2A, H2B, and H4. Reconstituted histone octamers were in vitro methylated by CARM1 or PRMT1 in the presence of ^{3}H-AdoMet and incubated with PAF1c immobilized on anti-Flag resin. Equal volume of input, bound, and flow-through of PRMT1-methylated ^{3}H-histone H4R3me2 (lanes 1, 3, and 5) and CARM1-methylated ^{3}H-histone H3R17me2 (lanes 2, 4, and 6) were loaded. Autoradiography shows that more CARM1-methylated ^{3}H-histone H3R17me2 was found bound to PAF1c on the beads compared with PRMT1-methylated ^{3}H-histone H4R3me2.

To identify the PAF1c subunit responsible for direct interaction with the histone H3R17me2a tail, individual PAF1c subunits were recombinantly expressed as Flag-tagged proteins in Sf9 insect cells and purified (Fig. S2*A*). Purified subunits were individually used for pull-down assays. Western blots showed that Paf1 subunit elicited the strongest binding, whereas all other subunits displayed either weak (Cdc73) or negligible binding to histone H3 tails (Fig. S2*B*). This result suggested that the Paf1 subunit is the main component in PAF1c that interacts with the histone H3 tail. The observation that Paf1 unexpectedly binds to both nonmodified and H3R17me2a tails indicates that other subunits in the complex may contribute to the specificity of Paf1.

The recently identified H3R17me2a effector molecule TDRD3 was also found to interact with H4R3me2a, a site modified by PRMT1 on histone H4 (10). To investigate if PAF1c interacts with the PRMT1-modified histone mark, we reconstituted histone octamers from bacterially expressed core histones (Fig. 1*D*) and in vitro methylated histone octamers by PRMT1 in the presence of ^{3}H-AdoMet for binding assays. Similarly, histone octamers were methylated by CARM1 as a positive control. The in vitro methylation of reconstituted histone octamers by PRMTs generated ^{3}H-labeled octamers uniquely carrying either asymmetric dimethylation of R17 on histone H3 (H3R17me2a) mediated by CARM1 or asymmetric dimethylation of R3 on histone H4 (H4R3me2a) mediated by PRMT1. PAF1c was purified from Flag-Cdc73 stably-expressing HEK293 cells, as shown by silver staining (Fig. 1*C*), and preimmobilized on anti-Flag M2 resin. Equal amounts of preimmobilized PAF1c were incubated with ^{3}H-H3R17me2a or ^{3}H-H4R3me2a histone octamers in parallel. The input, flow-through, and bead-bound samples were resolved on SDS-PAGE, and the dried gel was exposed to an X-ray film to detect ^{3}H-labeled methylated octamers in each fraction. The autoradiography showed that the efficiency of octamer methylation by CARM1 and PRMT1 were similar, as indicated by the input samples containing equivalent radioactivity (Fig. 1*E*, compare lane 1 with lane 2). However, PAF1c strongly interacted with the ^{3}H-H3R17me2a histone octamers methylated by CARM1 (Fig. 1*E*, compare lane 4 with lane 3). Consistently, more PRMT1-methylated ^{3}H-H4R3me2a histone octamers were detected in the flow-through (Fig. 1*E*, compare lane 5 with lane 6). Our results demonstrated that, unlike TDRD3, PAF1c preferentially binds to CARM1-methylated histone octamers over those methylated by PRMT1. Moreover, PAF1c not only interacts with histone H3 tail peptides but also histone octamers carrying asymmetric dimethylation at R17 of histone H3.

Estrogen-Enhanced Cooccupancy of PAF1c and H3R17me2a at EREs of ERα Target Genes. Given that H3R17me2a peptide selectively binds to PAF1c in vitro, we next examined if PAF1c is recruited to ERα target genes that harbor the H3R17me2a mark in vivo. pS2, PTGES, and IGFBP4 genes were selected for ChIP analyses because they were previously shown as CARM1-regulated ER target genes (1, 16) and contain defined EREs. In agreement with past studies, H3R17me2a was enriched at EREs of selected genes upon 17β-estradiol (E2) treatment (Fig. 2 *A*, *E*, and *I*). Notably, Paf1 (Fig. 2 *B*, *F*, and *J*) and Cdc73 (Fig. 2 *C*, *G*, and *K*) occupancies at EREs were also enhanced by E2 treatment. To validate the specificity of Cdc73 antibody used in ChIP experiments, a MCF7-tet-on-shCdc73 cell line was constructed and used for ChIP assays using anti-Cdc73 antibody (Fig. 2*M*). E2-induced recruitment of Cdc73 to EREs was found decreased after knockdown of Cdc73 in MCF7 cells (Fig. 2*N*). Taken together, these results suggest that intact PAF1c is recruited to EREs in an E2-enhanced manner, and the recruitment of PAF1c is accompanied by the increase of H3R17me2a mark.

Recruitment of hPAF1c to EREs Is CARM1-Dependent. To determine if PAF1c is recruited to EREs via recognition of H3R17me2a

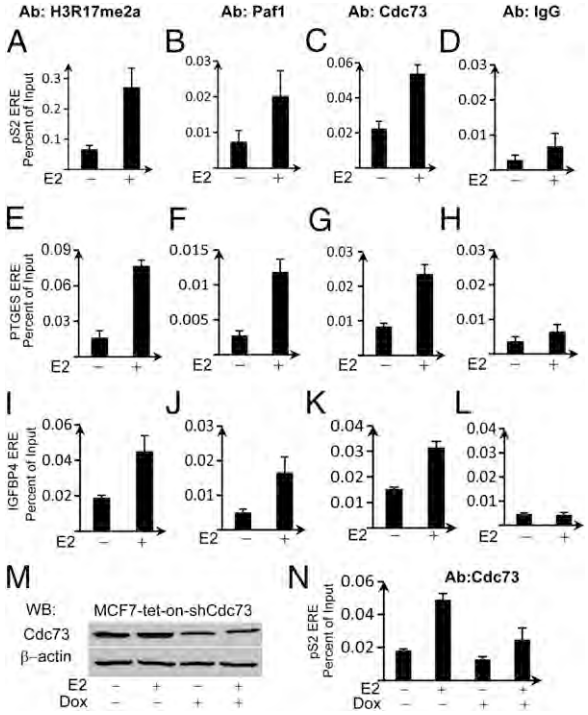

Fig. 2. E2 induces cooccupancy of PAF1c and H3R17me2a at the EREs of several ERα-target genes: pS2, PTGES, and IGFBP4. Cells were treated with or without E2 for 45 min followed by ChIP and quantitative PCR assays using the indicated antibodies. PAF1c occupancy at the ERE regions (*B, F*, and *J* for Paf1; *C, G*, and *K* for Cdc73) of ERα target genes coincides with the presence of the H3R17me2a mark (*A, E*, and *I*). (*D, H*, and *L*) IgG control for pS2, PTGES, and IGFBP4 ERE regions. (*M*) MCF7-tet-on-shCdc73 cell line was generated and knockdown efficiency of Cdc73 was shown in Western blots. (*N*) Cdc73 occupancy at pS2 ERE region was decreased after knockdown of Cdc73 in MCF7-tet-on-shCdc73 cells. Error bars represent SD (n = 3).

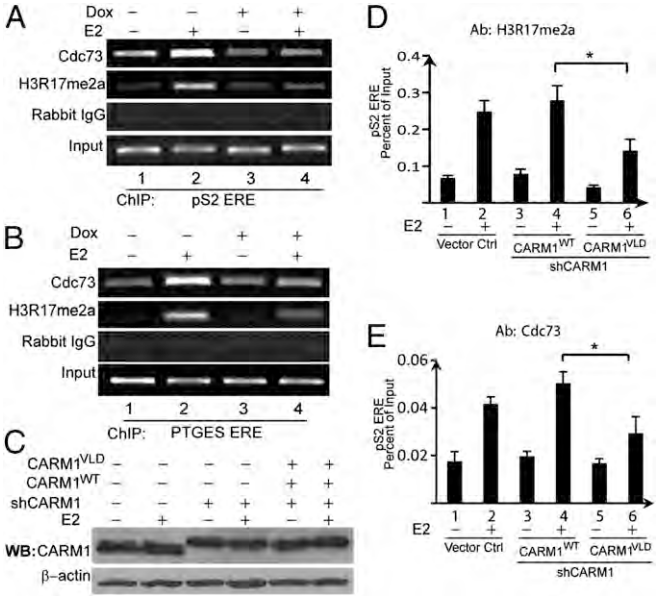

Fig. 3. The recruitment of PAF1c to proximal promoter EREs of ERα target genes is CARM1- and H3R17me2a-dependent. MCF7-tet-on-shCARM1 cells were pretreated with or without 0.5 μg/mL Dox for 4 d before E2 or vehicle treatment for 45 min. The occupancy of PAF1c subunit Cdc73 at EREs of pS2 (*A*) and PTGES (*B*) was analyzed using ChIP assays. When CARM1 is knocked down with Dox treatment, E2 stimulated H3R17me2a and PAF1c occupancy at EREs of pS2 and PTGES were greatly reduced (compare lane 4 with lane 2). (*C*) Western blots showed the expression levels of $CARM1^{WT}$ and $CARM1^{VLD}$ were comparable to the endogenous CARM1 in MCF7 cells when endogenous CARM1 was efficiently silenced. (*D* and *E*) ChIP analyses showed that expression of the enzyme-defective $CARM1^{VLD}$ mutant was insufficient to restore H3R17me2a level (*D*, $*P < 0.01$) and recruit PAF1c to pS2 ERE (*E*, $*P < 0.01$). In contrast, $CARM1^{WT}$ can fully rescue the function of endogenous CARM1 (histograms 3 and 4). Error bars represent SD (n = 3).

mark, we used a CARM1 inducible knockdown cell line (4) for ChIP assays because CARM1 is the only reported enzyme to create H3R17me2a mark. MCF7-tet-on-shCARM1 cells were treated with DMSO, E2, doxycycline (Dox), or Dox+E2 and subjected to ChIP assays. E2 treatment induced H3R17me2a accumulation at the ERE of pS2, whereas E2-induced H3R17me2a level was greatly reduced when CARM1 was knocked down by Dox treatment (Fig. 3*A*, compare lane 2 with lane 4). A similar observation was made with the PTGES gene under identical treatment conditions (Fig. 3*B*). These results confirm that CARM1 is responsible for writing the H3R17me2a mark in response to E2. Using this cell-line model, we found that Cdc73 E2-induced occupancy at the EREs of pS2 or PTGES was greatly abrogated after CARM1 knockdown (Fig. 3 *A* and *B*, compare lane 2 with lane 4). Because CARM1 has been implicated in transcription elongation and splicing processes, complete loss of CARM1 may indirectly affect transcription regardless of histone H3R17 dimethylation. To address this possibility, we replaced wild-type CARM1 with an enzyme-deficient CARM1 mutant by coinfecting MCF7 cells with lentiviruses encoding CARM1shRNA and Flag$CARM1^{VLD}$, a well-characterized CARM1 mutant defective for methyltransferase activity (1). As shown in Fig. 3*C*, endogenous CARM1 was successfully knocked down and the $CARM1^{VLD}$ mutant was expressed. As a control, we also restored wild-type CARM1 under the endogenous CARM1 knockdown background. ChIP assays were performed 5 d after viral infection and E2 or vehicle treatment of cells for 45 min. The results showed that E2-enhanced H3R17me2a level (Fig. 3*D*) and Cdc73 recruitment at ERE of pS2 (Fig. 3*E*) were significantly impaired in $CARM^{VLD}$ compared with $CARM1^{WT}$-expressing cells. These data suggest that PAF1c occupancy at EREs is CARM1-dependent, most likely mediated by the H3R17me2a mark.

PAF1c and CARM1 Coordinately Regulate a Common Set of ERα Target Genes. We had previously identified CARM1-regulated ERα target genes using microarrays (4). To establish the functional role of PAF1c in CARM1-regulated transcription, we attempted to knockdown PAF1c components and measure the effects on mRNA levels of CARM1-regulated ER targets. Knocking down Ctr9 was previously reported to affect expression of other PAF1c subunits in yeast and human cells (17, 18), and Ctr9 and Paf1 were shown as scaffold proteins for the formation of PAF1c (19). Therefore, we generated a Dox-inducible Ctr9 knockdown cell line, MCF7-tet-on-shCtr9, which allows transient knockdown of Ctr9 to minimize cellular toxicity associated with the loss of functional PAF1c. To examine if Ctr9 knockdown interferes with PAF1c integrity, MCF7-tet-on-shCtr9 cells were infected with lentiviral Flag-tagged Ski8 to immunoprecipitate PAF1c with anti-Flag affinity resin. This cell line was treated with Dox or vehicle for 5 d to knock down Ctr9, and then both whole-cell lysates and anti-Flag immunoprecipitated PAF1c were subjected to Western blots. In accompaniment with Ctr9 knockdown, the endogenous Paf1 level was significantly reduced in whole lysate (Fig. S3, lanes 1 and 2) as well as in Flag-Ski8 immunoprecipitated PAF1c (Fig. S3, lanes 3 and 4). Interestingly, despite no detectable loss of endogenous Leo1 expression, the presence of Leo1 in PAF1c was diminished, whereas Cdc73 level was moderately affected (Fig. S3). Our findings are in agreement with previous reports that Ctr9 plays a pivotal role in PAF1c assembly (19), and further indicate that Leo1 might

directly interact with Paf1 in PAF1c. Thus, the MCF7-tet-on-shCtr9 cell line is validated as a good model for elucidating the function of PAF1c in E2-dependent gene expression.

Because the MCF7-tet-on-shCARM1 cell line (4) was established from the same parental MCF7-tet-on clone as MCF7-tet-on-shCtr9, we compared expression of ERα target genes in both cell lines simultaneously. The Ctr9 and CARM1 knockdown efficiencies were confirmed by Western blots showing that 5 d of Dox treatment was sufficient to robustly decrease both protein levels by 90% (Fig. 4 *A* and *B*). To demonstrate that loss of CARM1 does not affect steady-state levels of any of the PAF1c subunits, we performed Western blots of PAF1c subunits in MCF7-tet-on-shCARM1 cell line. The results showed that PAF1c subunit levels were not altered by the loss of CARM1 (Fig. S4). The Ctr9 and CARM1 inducible knockdown cells were treated under four conditions and harvested for mRNA, followed by quantitative RT-PCR (qRT-PCR) analysis. pS2, PTGES, IGFBP4, EGR3, and MYC genes were selected for analyses because they were found to be CARM1-dependent E2 target genes (4). Fig. 4 showed that E2 induced expression of all these genes by more than twofold, and induction was inhibited over 50% by either Ctr9 or CARM1 knockdown (Fig. 4 *C*–*G*). Moreover, the trends for these ERα target genes in MCF7-tet-on-shCARM1 and MCF7-tet-on-shCtr9 cell lines under the four treatment conditions were similar (Fig. 4 *C*–*G*). These findings were further confirmed in MCF7 cells transiently transfected with siRNAs targeting Cdc73 or Paf1 subunits (Fig. S5). We also examined PAF1c dependency of three E2-induced, CARM1 nonregulated genes (4) by qRT-PCR in two inducible cell lines. Slc7a5 and Cyclin D1 were found not to be regulated by either CARM1 or PAF1c (Fig. S6 *A* and *B*), whereas TGF-α was found to be regulated by PAF1c but not by CARM1 (Fig. S6*C*). These data imply that PAF1c shares both common and distinct sets of genes from those of CARM1. Collectively, our data strongly support that PAF1c and CARM1 coregulate at least a subset of genes in the estrogen pathway.

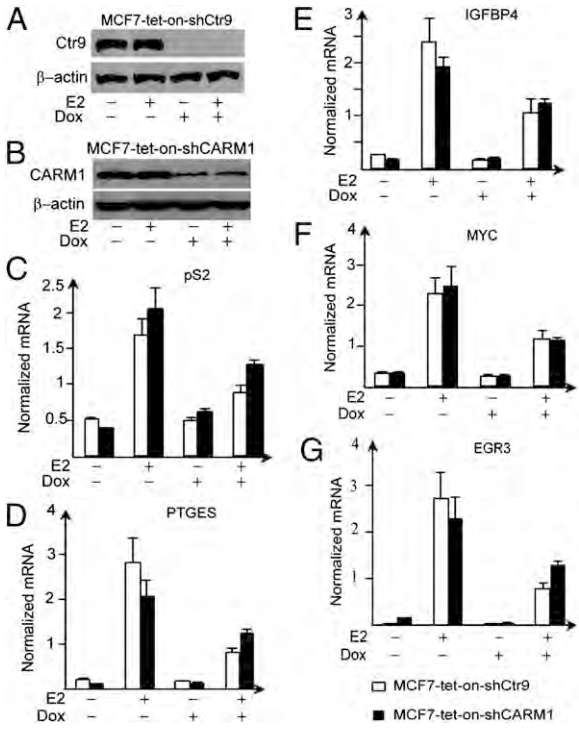

Fig. 4. Expression of several selected ERα target genes were similarly affected by knockdown of CARM1 or Ctr9. MCF-tet-on-shCtr9 and MCF7-tet-on-shCARM1 cell lines were treated with vehicle, E2 (5 h), Dox (5 d), or Dox (5 d) + E2 (5 h) in parallel. Endogenous Ctr9 (*A*) and CARM1 (*B*) were knocked down by 90% after 5 d of Dox treatment. The mRNA levels of pS2 (*C*), PTGES (*D*), IGFBP4 (*E*), MYC (*F*), and EGR3 (*G*) genes were analyzed by qRT-PCR in both cell lines after the indicated treatment. The attenuation of estrogen response was observed with all examined ER target genes in both Ctr9 and CARM1 knockdown cells after Dox induced silencing of Ctr9 or CARM1, respectively. Error bars represent SD (n = 3).

PAF1c Is Recruited to EREs of ERα Target Genes Downstream of the H3R17me2a Mark. We have shown that CARM1 knockdown affects H3R17me2a and occupancy of PAF1c at the EREs of ERα target genes, indicating that PAF1c binding is a downstream event of CARM1 and H3R17me2a. The MCF7-tet-on-shCtr9 cell line allows us to further dissect the consequence of PAF1c's association with H3R17me2a. We first comprehensively examined the association of PAF1c along the pS2 gene during E2-stimulated transcriptional activation. The distribution patterns of Cdc73, Paf1, RNAPII, C-terminal domain S2-phosphorylation (CTD S2-P), and H3R17me2a on the pS2 gene were determined by ChIP assays using primers amplifying different regions of the pS2 gene: −2,844 (upstream of transcription start site), −192 (promoter ERE), +879 (upstream coding region), +1,846 (downstream coding region). CTD S2-P was primarily found at the elongation region. In contrast, the H3R17me2a mark was only detected at the ERE but not the elongation region. Consistent with the established role of PAF1c as a RNAPII-associated elongation factor, Cdc73 and Paf1 were detected at both the promoter and coding regions coinciding with total RNAPII binding patterns (Fig. 5*A*). These data suggest that PAF1c is involved in transcriptional elongation of ERα target genes.

To delineate if H3R17me2a could serve as an upstream signal for recruitment of PAF1c, we measured H3R17me2a and H3K4me3 levels at the ERE of pS2 upon Ctr9 knockdown (Fig. 5 *B* and *C*). PAF1c was previously shown to recruit Set1, a histone lysine methyltransferase responsible for H3K4me3, and thus H3K4me3 is downstream of PAF1c and serves as a positive control to show the effects of Ctr9 knockdown on transcription. MCF7-tet-on-shCtr9 cells were pretreated with or without Dox for 5 d, then treated with 20 nM E2 or vehicle for 45 min before ChIP analyses followed by qRT-PCR. Fig. 5*B* shows that Ctr9 knockdown indeed reduced H3K4me3 at the proximal ERE of pS2, consistent with a previous report (20). In contrast, H3R17me2a level was not affected (Fig. 5*C*). Although H3R17me2a level at the ERE of pS2 was unchanged, pS2 transcription was inhibited by Ctr9 knockdown (Fig. 4*C*). This result suggests that although H3R17me2a is typically defined as a mark of transcriptional activation, this mark alone is insufficient to activate transcription without PAF1c. PAF1c was previously reported to mediate H3K4 trimethylation by recruitment of the mixed lineage leukemia (MLL) complex via direct interaction with Ash2L, a common subunit in MLL-1 and -2 complexes (21, 22). We thus speculate that H3R17me2a recruits PAF1c, which mediates downstream H3K4 trimethylation by interaction with the MLL complex in ER-mediated gene activation. Inducible knockdown of Ash2L cells were constructed by infecting MCF7 cells with pTRIPZ-Ash2LshRNA (Fig. 5*D*). Western blots results showed efficient knockdown of Ash2L by Dox treatment of MCF7-tet-on-shAsh2L cells for 6 d (Fig. 5*D*). As expected, ChIP assays showed that knockdown of Ash2L significantly decreased the level of H3K4me3 at the ERE of pS2 (Fig. 5*E*), whereas the level of H3R17me2a mark and occupancy of Cdc73 at ERE of pS2 were not significantly affected (Fig. 5 *F* and *G*). These results suggest that H3K4me3 is downstream event of H3R17me2a and PAF1c recruitment in ER-mediated gene activation.

Given that PAF1c and H3R17me2a occupancies at EREs were inhibited by CARM1 knockdown (Fig. 3 *D* and *E*), whereas Ctr9 knockdown did not affect H3R17me2a (Fig. 5*C*), our data support the sequential transcriptional activation model (Fig. S7)

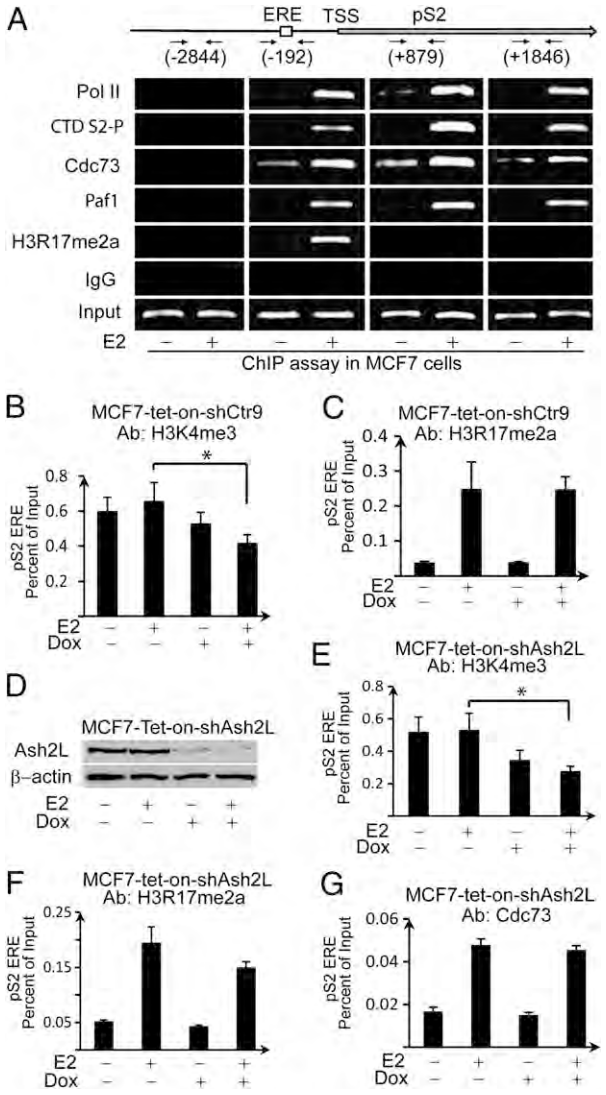

Fig. 5. Knockdown of Ctr9 did not alter the H3R17me2a level at the ERE of pS2; however, H3K4me3 level was reduced. (*A*) ChIP assays showed the occupancies of Cdc73, Paf1, total RNAPII, and CTD S2-phosphorylation at distal and proximal promoter and encoding regions of the pS2 gene. (*B* and *C*) Quantitative PCR of ChIP products showed that knockdown Ctr9 did not affect H3R17me2a level at the ERE region of the pS2 gene (*C*); however, H3K4me3 level at the ERE was significantly decreased (*B*, $*P < 0.02$). (*D*) Ash2L is effectively knocked down after 6-d Dox treatment in MCF7-tet-on-shAsh2L cells. (*E–G*) ChIP quantitative PCR results showed knockdown of Ash2L decreased H3K4me3 level at the ERE of pS2 (*E*, $*P < 0.002$), but had negligible effect on H3R17me2a level (*F*) and recruitment of Cdc73 (*G*). Error bars represent SD ($n = 3$).

in which CARM1 deposits H3R17me2a at the ERE, leading to the recruitment of PAF1c, which results in H3K4me3 deposition and transcriptional elongation via RNAPII.

Discussion

CARM1 and H3R17me2a are linked to transcription activation, yet little is known about how H3R17me2a signals transcription activation. Using an unbiased biochemical approach, here we report the identification of PAF1c as a unique transcription mediator of this active histone mark. We showed that PAF1c is an effector complex that binds to H3R17me2a peptide and histone octamers methylated by CARM1 (Fig. 1). The specificity of PAF1c was demonstrated by its inability to bind to H4R3me2a containing histone octamers modified by PRMT1 (Fig. 1*E*) (23). Nonetheless, our in vivo ChIP assays demonstrated that PAF1c was recruited to EREs of CARM1-regulated ERα target genes (Fig. 2), and the occupancy of PAF1c on the chromatin was dependent on CARM1 and the H3R17me2a mark (Fig. 3). In contrast, knockdown of PAF1c subunits did not alter the occupancy of CARM1 and H3R17me2a at EREs, whereas the known downstream H3K4me3 mark was attenuated (Fig. 5*B*). These results strongly suggest that PAF1c occupancy at EREs is mediated by H3R17me2a, which functions as an activation mark because of its ability to stimulate H3K4me3 through PAF1c recruitment.

PAF1c is known to participate in multiple steps of transcription, particularly in controlling histone methylation in later steps of transcriptional regulation. PAF1c is required for both H3K4me3 and H3K36me3 during transcription elongation via interaction with the histone H2B ubiquitination complex, the Set1 methyltransferase-containing COMPASS complex, and the Set 2 methylase (15, 20). Despite the established roles of PAF1c in directing histone modifications, it remains unclear how PAF1c is recruited to its target genes. In yeast, genes encoding Paf1 and Cdc73 are not essential, and their loss results in change of only a small subset of transcripts (14, 24). Similarly, only several hundred genes are affected, either positively or negatively, by the loss of PAF1c in Cdc73-depleted HeLa cells (25). Thus, the target-gene spectrum of metazoan PAF1c remains to be determined, and the roles of PAF1c in gene expression are speculated, at least in part, to be determined by the mechanism of PAF1c recruitment to specific promoters. Studies suggest that some transcription factors directly recruit PAF1c to their target genes. For example, Cdc73 directly binds β-catenin in both *Drosophila* and mammalian cells to activate transcription of genes in the Wnt pathway (26). Recently, the prototypical transcriptional activator GAL4-VP16 was shown to directly bind Paf1 and recruit PAF1c to the DNA template (27). Our finding that PAF1c regulates ERα target genes expands the role of PAF1c in regulating gene expression. Furthermore, we show that the recruitment of PAF1c to EREs depends on CARM1 and H3R17me2a, constituting a unique mechanism for PAF1c's recruitment to target genes. Moreover, the newly defined role of PAF1c as an arginine methyl-histone effector distinguishes PAF1c from its established role in controlling downstream histone ubiquitination and lysine methylation.

Although we demonstrated the functional connection between PAF1c and CARM1-mediated H3R17me2a in estrogen-stimulated transcription, PAF1c may activate other transcription factors regulated by CARM1 and functionally overlap with CARM1 in other biological processes. In support of this idea, PAF1c and CARM1 are known to regulate common target genes. One such gene, β-catenin, is a gene coregulated by PAF1c (26) and CARM1 (28). Additionally, both CARM1 and the PAF1c subunits are essential for mouse embryonic development and maintenance of ES cell pluripotency. CARM1-null mice die at birth and are smaller than their wild-type littermates (3). CARM1 and H3R17/R26me2 are associated with Oct4 and Sox2 promoters in ES cells; moreover, CARM1 is required for maintaining pluripotency of ES cells (29). Coincidently, Cdc73 null mice are embryonic-lethal (30). Microarray analysis of Cdc73 knockout mouse embryonic fibroblast cells demonstrated that PAF1c directly regulates many essential genes involved in cell growth and survival (30). Moreover, a recent genome-scale RNAi screen identified PAF1c as a regulator of Oct4 expression, demonstrating an important role for PAF1c in maintaining ES cell identity (20). Finally, both PAF1c and CARM1 are involved in transcriptional regulation at multiple levels. PAF1c functions in transcription initiation, elongation (15), mRNA 3′ end cleavage (25), polyadenylation of mRNA precursors (27), and small nucleolar RNA (snoRNA) 3′ end formation (31). In addition to transcriptional activation, CARM1 methylates splicing factors (32), modulates recognition

of 5′ splicing sites (33), and regulates the coupling of transcription and splicing (34). Furthermore, a recent report showed that RNAPII carboxyl-terminal domain is methylated by CARM1 (35). Mutating the CARM1 methylation site in RNAPII carboxyl-terminal domain affects snoRNA expression similar to the effect observed in CARM1$^{-/-}$ mouse embryonic fibroblast cells (35). Coincidently, 3′ end formation of mRNAs and snoRNAs are dependent on PAF1c (31). Collectively, PAF1c and CARM1 share overlapping genes and cellular processes, although the processes that require CARM1 methyltransferase activity and H3R17me2a for PAF1c function await elucidation.

Arginine methylation of histone tails correlates with either transcriptional activation or repression. The specific marks, as part of histone codes, are thought to promote or prevent the docking of key transcriptional effector molecules (36, 37). PAF1c subunits are nuclear proteins directly associated with RNAPII and can regulate multiple steps of transcription. Recently, TDRD3 was found to bind both the H3R17me2a and H4R3me2a marks (10). It is plausible that multiple effector proteins exist for the H3R17me2a mark that direct this mark to divergent biological processes. Future work should determine if these two H3R17me2a effectors directly interact and whether they regulate different CARM1-coupled biological processes in cell-type and tissue-specific manners. In conclusion, we identified PAF1c as an effector complex for H3R17me2a and linked its function to the regulation of estrogen-responsive genes. This study presents a unique mechanism by which the CARM1-catalyzed H3R17me2a mark is linked to transcriptional activation via recruitment of PAF1c (Fig. S7).

Materials and Methods

Cell Culture and Estrogen Treatment. MCF7 and HEK293 cells were maintained in DMEM supplemented with 10% (vol/vol) FBS. Three days before E2 treatment, the cells were transferred to phenol red-free DMEM containing 6xSFBS (six-time stripped FBS). The working concentration for E2 was 20 nM.

Peptide Pull-Down Assays. Peptide pull-down was performed according to previously published methods (12). For each assay, biotinylated peptide (1 μg) were immobilized on 200 μg streptavidin coated DynaBeads (Invitrogen). HeLa nuclear extract or purified recombinant proteins were incubated with the magnetic beads immobilized with indicated peptide for 2 h at 4 °C. The peptide interaction protein was detected by Western blot or silver staining.

Description on cell lines, antibodies, peptide pull-down, qRT-PCR, ChIP assay, transfection and in vitro methylation of histone octamer are available in *SI Materials and Methods*. All of the primers and oligo DNA are listed in Table S1.

ACKNOWLEDGMENTS. We thank Dr. Danny Reinberg for histone expression plasmids; Shaun V. Hernandez for technical support; Erin Shanle and Nancy Thompson for editing and comments; and Drs. Emery Bresnick and Shigeki Miyamoto for critical reading of the manuscript. This work was supported by National Institutes of Health Grant CA125387 (to W.X.), a Department of Defense Era of hope Scholar Award, Shaw Scientist Award from the Greater Milwaukee Foundation (to W.X.), and in part by NIH/NCI P30CA014520-University of Wisconsin Comprehensive Cancer Center Support.

1. Chen D, et al. (1999) Regulation of transcription by a protein methyltransferase. *Science* 284:2174–2177.
2. Kuhn P, Xu W (2009) Protein arginine methyltransferases: Nuclear receptor coregulators and beyond. *Prog Mol Biol Transl Sci* 87:299–342.
3. Yadav N, et al. (2003) Specific protein methylation defects and gene expression perturbations in coactivator-associated arginine methyltransferase 1-deficient mice. *Proc Natl Acad Sci USA* 100:6464–6468.
4. Al-Dhaheri M, et al. (2011) CARM1 is an important determinant of ERα-dependent breast cancer cell differentiation and proliferation in breast cancer cells. *Cancer Res* 71:2118–2128.
5. Ma H, et al. (2001) Hormone-dependent, CARM1-directed, arginine-specific methylation of histone H3 on a steroid-regulated promoter. *Curr Biol* 11:1981–1985.
6. Kim D, et al. (2010) Enzymatic activity is required for the in vivo functions of CARM1. *J Biol Chem* 285:1147–1152.
7. Schurter BT, et al. (2001) Methylation of histone H3 by coactivator-associated arginine methyltransferase 1. *Biochemistry* 40:5747–5756.
8. Guccione E, et al. (2007) Methylation of histone H3R2 by PRMT6 and H3K4 by an MLL complex are mutually exclusive. *Nature* 449:933–937.
9. Métivier R, et al. (2003) Estrogen receptor-alpha directs ordered, cyclical, and combinatorial recruitment of cofactors on a natural target promoter. *Cell* 115:751–763.
10. Yang Y, et al. (2010) TDRD3 is an effector molecule for arginine-methylated histone marks. *Mol Cell* 40:1016–1023.
11. Sims RJ, 3rd, Trojer P, Li G, Reinberg D (2006) Methods to identify and functionally analyze factors that specifically recognize histone lysine methylation. *Methods* 40: 331–338.
12. Wysocka J (2006) Identifying novel proteins recognizing histone modifications using peptide pull-down assay. *Methods* 40:339–343.
13. Xu W, et al. (2001) A transcriptional switch mediated by cofactor methylation. *Science* 294:2507–2511.
14. Shi X, et al. (1996) Paf1p, an RNA polymerase II-associated factor in *Saccharomyces cerevisiae*, may have both positive and negative roles in transcription. *Mol Cell Biol* 16:669–676.
15. Jaehning JA (2010) The Paf1 complex: platform or player in RNA polymerase II transcription? *Biochim Biophys Acta* 1799:379–388.
16. Bauer UM, Daujat S, Nielsen SJ, Nightingale K, Kouzarides T (2002) Methylation at arginine 17 of histone H3 is linked to gene activation. *EMBO Rep* 3:39–44.
17. Mueller CL, Porter SE, Hoffman MG, Jaehning JA (2004) The Paf1 complex has functions independent of actively transcribing RNA polymerase II. *Mol Cell* 14:447–456.
18. Zhu B, et al. (2005) The human PAF complex coordinates transcription with events downstream of RNA synthesis. *Genes Dev* 19:1668–1673.
19. Kim J, Guermah M, Roeder RG (2010) The human PAF1 complex acts in chromatin transcription elongation both independently and cooperatively with SII/TFIIS. *Cell* 140:491–503.
20. Ding L, et al. (2009) A genome-scale RNAi screen for Oct4 modulators defines a role of the Paf1 complex for embryonic stem cell identity. *Cell Stem Cell* 4:403–415.
21. Rozenblatt-Rosen O, et al. (2005) The parafibromin tumor suppressor protein is part of a human Paf1 complex. *Mol Cell Biol* 25:612–620.
22. Steward MM, et al. (2006) Molecular regulation of H3K4 trimethylation by ASH2L, a shared subunit of MLL complexes. *Nat Struct Mol Biol* 13:852–854.
23. Ruthenburg AJ, Li H, Patel DJ, Allis CD (2007) Multivalent engagement of chromatin modifications by linked binding modules. *Nat Rev Mol Cell Biol* 8:983–994.
24. Porter SE, Washburn TM, Chang M, Jaehning JA (2002) The yeast pafl-rNA polymerase II complex is required for full expression of a subset of cell cycle-regulated genes. *Eukaryot Cell* 1:830–842.
25. Rozenblatt-Rosen O, et al. (2009) The tumor suppressor Cdc73 functionally associates with CPSF and CstF 3′ mRNA processing factors. *Proc Natl Acad Sci USA* 106:755–760.
26. Mosimann C, Hausmann G, Basler K (2006) Parafibromin/Hyrax activates Wnt/Wg target gene transcription by direct association with beta-catenin/Armadillo. *Cell* 125: 327–341.
27. Nagaike T, et al. (2011) Transcriptional activators enhance polyadenylation of mRNA precursors. *Mol Cell* 41:409–418.
28. Ou CY, et al. (2011) A coactivator role of CARM1 in the dysregulation of β-catenin activity in colorectal cancer cell growth and gene expression. *Mol Cancer Res* 9: 660–670.
29. Wu Q, et al. (2009) CARM1 is required in embryonic stem cells to maintain pluripotency and resist differentiation. *Stem Cells* 27:2637–2645.
30. Wang P, et al. (2008) Parafibromin, a component of the human PAF complex, regulates growth factors and is required for embryonic development and survival in adult mice. *Mol Cell Biol* 28:2930–2940.
31. Sheldon KE, Mauger DM, Arndt KM (2005) A requirement for the *Saccharomyces cerevisiae* Paf1 complex in snoRNA 3′ end formation. *Mol Cell* 20:225–236.
32. Cheng D, Côté J, Shaaban S, Bedford MT (2007) The arginine methyltransferase CARM1 regulates the coupling of transcription and mRNA processing. *Mol Cell* 25: 71–83.
33. Ohkura N, Takahashi M, Yaguchi H, Nagamura Y, Tsukada T (2005) Coactivator-associated arginine methyltransferase 1, CARM1, affects pre-mRNA splicing in an isoform-specific manner. *J Biol Chem* 280:28927–28935.
34. Kuhn P, et al. (2011) Automethylation of CARM1 allows coupling of transcription and mRNA splicing. *Nucleic Acids Res* 39:2717–2726.
35. Sims RJ, 3rd, et al. (2011) The C-terminal domain of RNA polymerase II is modified by site-specific methylation. *Science* 332:99–103.
36. Di Lorenzo A, Bedford MT (2011) Histone arginine methylation. *FEBS Lett* 585: 2024–2031.
37. Smith E, Shilatifard A (2010) The chromatin signaling pathway: diverse mechanisms of recruitment of histone-modifying enzymes and varied biological outcomes. *Mol Cell* 40:689–701.